SHIP STRUCTURE COMMITTEE

The SHIP STRUCTURE COMMITTEE is constituted to prosecute a research program to improve the hull structures of ships and other marine structures by an extension of knowledge pertaining to design, materials, and methods of construction.

RADM J. D. Sipes, USCG, (Chairman)
Chief, Office of Marine Safety, Security and Environmental Protection
U. S. Coast Guard

Mr. H. T. Haller
Associate Administrator for Shipbuilding and Ship Operations
Maritime Administration

Mr. Alexander Malakhoff
Director, Structural Integrity Subgroup (SEA 55Y)
Naval Sea Systems Command

Mr. Thomas W. Allen
Engineering Officer (N7)
Military Sealift Command

Dr. Donald Liu
Senior Vice President
American Bureau of Shipping

CDR Michael K. Parmelee, USCG,
Secretary, Ship Structure Committee
U. S. Coast Guard

CONTRACTING OFFICER TECHNICAL REPRESENTATIVES

Mr. William J. Siekierka
SEA 55Y3
Naval Sea Systems Command

Mr. Greg D. Woods
SEA 55Y3
Naval Sea Systems Command

SHIP STRUCTURE SUBCOMMITTEE

The SHIP STRUCTURE SUBCOMMITTEE acts for the Ship Structure Committee on technical matters by providing technical coordination for determinating the goals and objectives of the program and by evaluating and interpreting the results in terms of structural design, construction, and operation.

AMERICAN BUREAU OF SHIPPING

Mr. Stephen G. Arntson (Chairman)
Mr. John F. Conlon
Mr. William Hanzalek
Mr. Philip G. Rynn

NAVAL SEA SYSTEMS COMMAND

Mr. Robert A. Sielski
Mr. Charles L. Null
Mr. W. Thomas Packard
Mr. Allen H. Engle

MILITARY SEALIFT COMMAND

Mr. Albert J. Attermeyer
Mr. Michael W. Touma
Mr. Jeffery E. Beach

U. S. COAST GUARD

CAPT T. E. Thompson
CAPT Donald S. Jensen
CDR Mark E. Noll

MARITIME ADMINISTRATION

Mr. Frederick Seibold
Mr. Norman O. Hammer
Mr. Chao H. Lin
Dr. Walter M. Maclean

SHIP STRUCTURE SUBCOMMITTEE LIAISON MEMBERS

U. S. COAST GUARD ACADEMY

LT Bruce Mustain

U. S. MERCHANT MARINE ACADEMY

Dr. C. B. Kim

U. S. NAVAL ACADEMY

Dr. Ramswar Bhattacharyya

STATE UNIVERSITY OF NEW YORK MARITIME COLLEGE

Dr. W. R. Porter

WELDING RESEARCH COUNCIL

Dr. Martin Prager

NATIONAL ACADEMY OF SCIENCES - MARINE BOARD

Mr. Alexander B. Stavovy

NATIONAL ACADEMY OF SCIENCES - COMMITTEE ON MARINE STRUCTURES

Mr. Stanley G. Stiansen

SOCIETY OF NAVAL ARCHITECTS AND MARINE ENGINEERS - HYDRODYNAMICS COMMITTEE

Dr. William Sandberg

AMERICAN IRON AND STEEL INSTITUTE

Mr. Alexander D. Wilson

Member Agencies:

United States Coast Guard
Naval Sea Systems Command
Maritime Administration
American Bureau of Shipping
Military Sealift Command

Ship Structure Committee

An Interagency Advisory Committee
Dedicated to the Improvement of Marine Structures

Address Correspondence to:

Secretary, Ship Structure Committee
U.S. Coast Guard (G-MTH)
2100 Second Street S.W.
Washington, D.C. 20593-0001
PH: (202) 267-0003
FAX: (202) 267-0025

December 3, 1990

SSC-355
SR-1317

RELATION OF INSPECTION FINDINGS TO FATIGUE RELIABILITY

Periodic inspections of marine structures are done to ensure continued structural integrity and operational safety. Limited information makes it very difficult to assess the reliability of inspection techniques when we consider the probability of detection (POD) of structural flaws. This report presents inspection procedures that are based on POD curves, component stress levels, and structural inspection and repair histories. The inspection intervals are aperiodic and are intended to maintain the reliability of marine structures at predetermined design levels. This report is an integral part of the Ship Structure Committee's development of probability based design procedures for marine structures.

J. D. SIPES
Rear Admiral, U.S. Coast Guard
Chairman, Ship Structure Committee

Technical Report Documentation Page

1. Report No.	2. Government Accession No.	3. Recipient's Catalog No.
SSC-355		

4. Title and Subtitle	5. Report Date
Relation of Inspection Findings to Fatigue Reliability	November 1989
	6. Performing Organization Code
	8. Performing Organization Report No. SR-1317
7. Author(s) M. Shinozuka	
9. Performing Organization Name and Address Modern Analysis Incorporated 825 Norgate Drive Ridgewood, NJ 07450	10. Work Unit No. (TRAIS) 11. Contract or Grant No. DTCG23-86-C-20057
12. Sponsoring Agency Name and Address Commandant U.S. Coast Guard 2100 Second Street, SW Washington, DC 20593	13. Type of Report and Period Covered Final Report 14. Sponsoring Agency Code G-M

15. Supplementary Notes

Sponsored by the Ship Structure Committee and its member agencies.

16. Abstract

The main objective of this work was to develop an aperiodic inspection procedure for marine structures so as to maintain their reliability at a predetermined design level throughout the design life. A summary of current inspection procedures for a variety of marine structures is provided. Limited information makes it very difficult to assess the reliability of inspection techniques. Probability of detection (POD) curves used in the aerospace industry for flaw detection were reviewed and provided a guide for establishing POD curves for the marine industry. Aperiodic inspection procedures based on Baysian upgrading and POD curves, component stress levels, and structural inspection and repair histories are developed. Validity and effectiveness of the Baysian analysis is demonstrated by numerical example. Current inspection procedures are generally incompatible with the probabilistic approach this work intends to develop.

17. Key Words	18. Distribution Statement
Inspection Technique Baysian Analysis Probability of Detection Curve Structural Inspection, Fatigue Reliability	Available from: Nat'l Technical Information Service Springfield, VA 22161 or Nat'l Technical Information Facility National Maritime Research Center Kings Point, NY 10024-1699

19. Security Classif. (of this report)	20. Security Classif. (of this page)	21. No. of Pages	22. Price
Unclassified	Unclassified		

Form DOT F 1700.7 (8-72) Reproduction of completed page authorized

METRIC CONVERSION FACTORS

Approximate Conversions to Metric Measures

Symbol	When You Know	Multiply by	To Find	Symbol
		LENGTH		
in	inches	*2.5	centimeters	cm
ft	feet	30	centimeters	cm
yd	yards	0.9	meters	m
mi	miles	1.6	kilometers	km
		AREA		
in^2	square inches	6.5	square centimeters	cm^2
ft^2	square feet	0.09	square meters	m^2
yd^2	square yards	0.8	square meters	m^2
mi^2	square miles	2.6	square kilometers	km^2
	acres	0.4	hectares	ha
		MASS (weight)		
oz	ounces	28	grams	g
lb	pounds	0.45	kilograms	kg
	short tons (2000 lb)	0.9	tonnes	t
		VOLUME		
tsp	teaspoons	5	milliliters	ml
Tbsp	tablespoons	15	milliliters	ml
fl oz	fluid ounces	30	milliliters	ml
c	cups	0.24	liters	l
pt	pints	0.47	liters	l
qt	quarts	0.95	liters	l
gal	gallons	3.8	liters	l
ft^3	cubic feet	0.03	cubic meters	m^3
yd^3	cubic yards	0.76	cubic meters	m^3
		TEMPERATURE (exact)		
°F	Fahrenheit temperature	5/9 (after subtracting 32)	Celsius temperature	°C

*1 in. = 2.54 cm (exactly). For other exact conversions and more detail tables see NBS Misc. Publ. 286, Units of Weight and Measures. Price $2.25 SD Catalog No. C13 10 286.

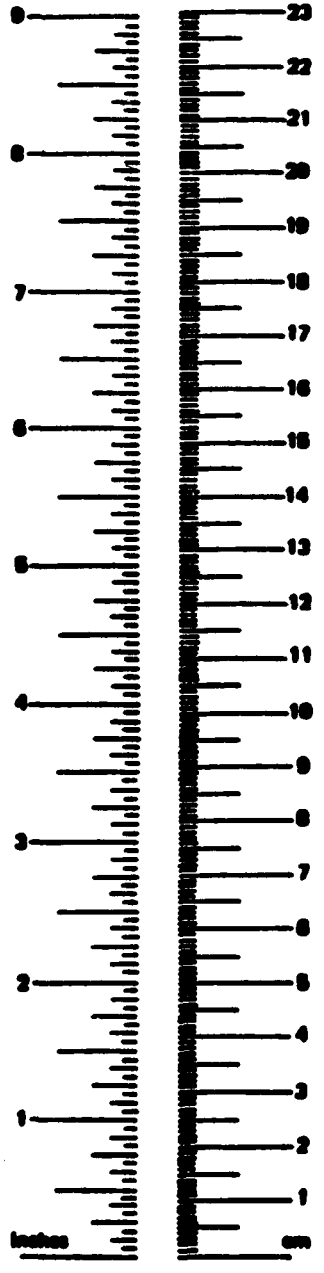

Approximate Conversions from Metric Measures

Symbol	When You Know	Multiply by	To Find	Symbol
		LENGTH		
mm	millimeters	0.04	inches	in
cm	centimeters	0.4	inches	in
m	meters	3.3	feet	ft
m	meters	1.1	yards	yd
km	kilometers	0.6	miles	mi
		AREA		
cm^2	square centimeters	0.16	square inches	in^2
m^2	square meters	1.2	square yards	yd^2
km^2	square kilometers	0.4	square miles	mi^2
ha	hectares (10,000 m^2)	2.5	acres	
		MASS (weight)		
g	grams	0.035	ounces	oz
kg	kilograms	2.2	pounds	lb
t	tonnes (1000 kg)	1.1	short tons	
		VOLUME		
ml	milliliters	0.03	fluid ounces	fl oz
l	liters	2.1	pints	pt
l	liters	1.06	quarts	qt
l	liters	0.26	gallons	gal
m^3	cubic meters	35	cubic feet	ft^3
m^3	cubic meters	1.3	cubic yards	yd^3
		TEMPERATURE (exact)		
°C	Celsius temperature	9/5 (then add 32)	Fahrenheit temperature	°F

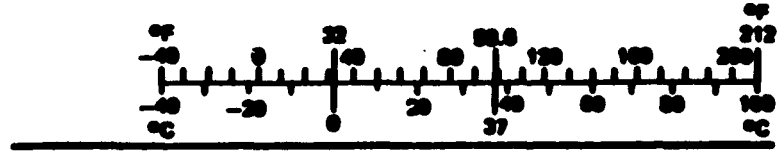

TABLE OF CONTENTS

EXECUTIVE SUMMARY

The main objective of this work is to develop a non-periodic inspection procedure for marine structures so as to maintain their reliability at a prespecified design level throughout their life. In the first chapter of this work, a summary of inspection procedures for a range of marine steel structures is provided. Specifically, inspection procedures for bulk carriers, fixed offshore structures and semi-submersible units are reviewed. This review shows that there is very little information available to assess the reliability of these inspection techniques. It is noted that only one reliable probability of detection (POD) curve was found. In view of the limited information available to assess the reliability of inspection procedures for marine steel structures, a review of POD curves used in the aerospace industry is presented in the second chapter. This review is done because it is believed that the shape of POD curves used in the aerospace industry can provide useful guidelines for assessing the reliability of flaw detection and at the same time, for establishing POD curves for marine structures. In this chapter, emphasis is given to the log odds model which is investigated extensively. Another very good model is the Weibull model which has been well studied in dealing with applications and found to be very reasonable for the POD function. Indeed, it is a special case of the Weibull model that is used as a POD curve in the third chapter. In the third and main chapter of this report, a non-periodic inspection procedure is developed based on Bayesian upgrading and taking into account the detailed record of the entire inspection history including repair or replacement records for each and every component of the structure. It is assumed that different components of the structure are subjected to different stress levels. In the research done in the past using Bayesian analysis, all the components of the structure were assumed to be subjected to the same stress level. This assumption was not realistic and therefore different stress levels are considered for different components of the structure. A numerical example is provided that verifies the validity and effectiveness of Bayesian analysis to determine appropriate inspection intervals for marine structures so as to maintain their reliability

at a prespecified design level throughout their life. The above-described main objective of this work is carried out in the third chapter.

The state-of-the-art in current inspection procedures of marine structures has been found to be generally incompatible with the probabilistic approach this work intends to develop. Hence, the first two chapters describing the results of the two tasks called for by the contract could not provide probabilistic information directly usable in Chapter 3. This fact has contributed to the appearance that the first three chapters of this report are somewhat unrelated, although they are all an integral part of this work.

Finally, further study is suggested in the following five areas:

a. In this work, the three parameters $\beta, c,$ and d introducing uncertainty to the time to crack initiation, fatigue crack propagation and probability of crack detection respectively, were considered to be uncorrelated. However, there is strong evidence that $\beta, c,$ and d are in reality correlated to each other. Therefore, the statistical correlation among $\beta, c,$ and d and the effect of this correlation on the obtained results require further study. Another aspect of future work concerning parameters $\beta, c,$ and d is to examine their sensitivity on the obtained results;

b. The effect of the form of certain POD curves on the reliability of marine structures throughout their service life requires further study. A comparison has to be made among several established POD curves in the aerospace industry, in order to assess their relative influence on the reliability of marine structures subjected to non-periodic inspections. In this way, more reliable POD curves can be established for marine structures;

c. The cost-effectiveness of the proposed method of non-periodic inspections based on Bayesian analysis requires further study. Specifically, a cost-benefit analysis can be performed taking into consideration the cost of the non-periodic inspection procedure and the increased level of reliability for the structure. These results have to be compared with the results of the cost-benefit analysis associated with the standard periodic inspection procedure;

d. The verification of the proposed methodology using actual data from inspections of marine

structures is one of the most important tasks of future work. This task can be accomplished by taking advantage of already completed inspections of marine structures to determine whether these structures actually maintained a prespecified reliability level throughout their life;

e. The failure rate expression after crack initiation should at least be validated by Monte Carlo simulation utilizing the crack propagation law and uncontrolled crack growth condition based on fracture mechanics theory under various random stress histories consistent with the stress intensity factor fluctuation considered.

SUMMARY

A summary of inspection procedures for a range of marine steel structures is provided in the first chapter of this work. Specifically, inspection procedures for bulk carriers, fixed offshore structures and semi-submersible units are reviewed. This review shows that there is very little information available to assess the reliability of these inspection techniques. It is noted that only one reliable probability of detection (POD) curve was found. In view of the limited information available to assess the reliability of inspection procedures for marine steel structures, a review of POD curves used in the aerospace industry is presented in the second chapter. This review is done because it is believed that the shape of POD curves used in the aerospace industry can provide useful guidelines for assessing the reliability of flaw detection and at the same time, for establishing POD curves for marine structures. In this chapter, emphasis is given to the log odds model which is investigated extensively. Another very good model is the Weibull model which has been well studied in dealing with applications and found to be very reasonable for the POD function. Indeed, it is a special case of the Weibull model that is used as a POD curve in the third chapter.

The third chapter constitutes the main part of this work whose basic objective is to develop a non-periodic inspection procedure for marine structures so as to maintain their reliability at a prespecified design level throughout their life. This procedure is based on Bayesian upgrading and takes into account the detailed record of the entire inspection history including repair or replacement records for each and every component of the structure. It is considered that different components of the structure are subjected to different stress levels. In the research done in the past using Bayesian analysis, all the components of the structure were assumed to be subjected to the same stress level. This assumption was not realistic and therefore different stress levels are considered for different components of the structure. Finally, a numerical example is provided that verifies the validity and effectiveness of Bayesian analysis to determine

appropriate inspection intervals for marine structures so as to maintain their reliability at a prespecified design level throughout their life.

I. REVIEW OF CURRENT INSPECTION PROCEDURES OF MARINE STRUCTURES

1.1 Introduction

This chapter presents results of work performed by Stewart Technology Associates (STA), subcontractor to Modern Analysis, Inc. on a project for the US Coast Guard.

This project deals with the reliability of marine structures, concentrating on fatigue damage and its detection during regular in-service inspection. The main thrust of the work performed by STA was to summarize inspection procedures for a range of marine steel structures and to provide summaries of inspection findings, in cooperation with classification societies. The work was directed towards the structural integrity of the main hull, or main structure, of each of the marine structure categories considered. Fatigue damage, as evidenced by surface cracks, was the principal type of damage to be considered resulting in a reduction in strengths.

STA visited the American Bureau of Shipping (then) in New York, and Det norske Veritas in Norway, in order to discuss the inspection procedures and results. Additionally, three visits were made to key individuals and organizations in London, as well as to Exxon in Houston. Telephone discussions with other companies also contributed to the general picture of industry experience and current practice presented in these earlier reports.

This report summarizes the key information presented in earlier reports and additionally presents some further key published information relating to the probability of detecting cracks underwater when marine structures are inspected. During the course of the work by STA, it became clear that the industry had very little information enabling any kind of assessment of the reliability of inspection techniques to be made. Consequently, STA was directed by Modern Analysis to try to obtain any available probability of detection (POD) information. Only one reliable POD curve was found, and this was in cooperation with DnV.

1.2 Summary of Inspection Procedures

1.2.1 Bulk Carriers

Both the American Bureau of Shipping (ABS) and Det norske Veritas (DnV) have rules that govern the inspection requirements for bulk carriers, including dry bulk and oil tankers. These requirements concentrate principally upon corrosion and thickness testing. All inspection for cracks is visual unless there is something unusual, and then it is up to the judgment of the individual surveyor. For tankers, particularly in the DnV rules, the inspection requirements are greater than for dry cargo vessels, but there is still no requirement for anything more than visual inspection to locate cracks. Thickness measurements are required at special periodic surveys. These special periodic surveys are typically at 2–1/2 or 4–year intervals. No guidance is given in these rules as to acceptable defect sizes if cracks are found. It is up to the judgment of the individual surveyor as to whether or not the cracks will be repaired.

All inspection normally takes place with ships in the dry. This is done by internal inspection of the ship's structure, either while the ship is floating or dry-docked. External inspection of the hull structure is normally done in dry dock. Both classification societies have some provision for underwater surveys, but both eventually require dry-docking after a number of years.

Neither classification society has adopted a philosophy for calculating the growth rate of defects that may develop in ship hull structures. This is principally because through-hull cracks are generally detected because of leakage into cargo or other normally dry spaces, and in the event of a through-hull crack, it is repaired immediately.

1.2.2 Fixed Offshore Structures

In 1986 a notice of proposed rule-making was published in the Federal Register. This proposed an inspection requirement for structures on the U.S. offshore continental shelf (OCS). The requirement was rather general, requiring that periodic inspection of such structures is performed to determine "the condition of the entire structure." An annual report from the operator is to be submitted to the MMS, "stating which platforms have been inspected in the preceding

12 months, the extent and area of inspection, and the type of inspection employed, i.e., visual, magnetic particle, ultrasonic testing." In the absence of existing requirements to inspect OCS structures, it is noted that operators perform their own inspections, sometimes within a carefully planned framework of life-cycle costing, but more frequently without an overall plan. Inspection procedures vary from simply checking periodically that the structure is still there (unmanned structures) to cleaning and NDT of critical joints, underwater, on a regular planned basis. It is true to say that the level of inspection of fixed structures in OCS waters is considerably lower than that undertaken for structures in the North Sea.

For structures in the North Sea, governmental requirements are more detailed, and inspection procedures are more rigorous and certainly cost a great deal of money. Every year a considerable amount of in-service inspection of offshore structures in North Sea waters is performed in order to ensure the safety of personnel and production. The Norwegians, in particular, have developed systematic methods based on probabilistic models and cost resource allocation for the inspection of structures in Norwegian waters.

DnV have produced rules addressing the questions of personnel qualifications, inspection procedures, and equipment capability. These rules also differentiate between three types of inspection:

Type I (Green):

General visual inspection to detect obvious damage. Prior cleaning of inspection items is not needed.

Type II (Blue):

Close visual inspections to detect hidden damage. Prior cleaning of inspection items is normally necessary.

Type III (Red):

Close visual inspection and testing (NDT or DT) to detect incipient or hidden damage. Prior cleaning of inspection items is required.

DnV cite two basic methods for planning an in-service inspection program, one based upon the design, fabrication, and installation (DFI) knowledge, and the other based upon the structure's condition records (SCR). DFI principally identifies areas where inspection should be concentrated, based upon calculation of the structure's predicted performance in the ocean environment, taking account of any deviations from the original design occurring during fabrication and installation. SCR is a system of continuous revision to take account of inspection findings in service, when it may be found in practice that deterioration of some areas occurs more rapidly than predicted with DFI as the inspection basis. DnV emphasize the bookkeeping aspects of inspection results, enabling trend analyses to be relatively easily undertaken. As with the ABS, they refer to an inspection program, specific to each installation; but the DnV rules give much guidance as to the form of such a program, while the ABS rules do not. DnV rules also offer guidance as to selection or areas, in general, for inspection and offer possible types and causes of defects that may be found.

One of the most useful pieces of information giving a picture of inspection findings for fixed steel structures in the Norwegian Sector of the North Sea was a table provided by DnV for piled steel structures they have inspected in the years 1975 to 1984. This table is reproduced below:

Table 1.1 PILED STEEL STRUCTURES

1975–1984

TOTAL NOS: 21

	Nos. of Platforms With Defects
WIRE SCAFING	18
DEFLECTED MEMBERS	11
DENTED MEMBERS	15

Table 1.1 (Continued) PILED STEEL STRUCTURES

1975–1984

TOTAL NOS: 21

MISSING, LOOSE, DEFECT ANODES	14
GENERAL CORROSION	2
PITTING CORROSION	20
BURN MARK	4
HEAVY MARINE GROWTH	13
SCOUR	1
DEBRIS	21
CONFIRMED CRACK	12
PROPAGATING CRACK	3

As can be seen from this table, in all these years of inspection on the 21 structures, only three propagating cracks were found (in major structural members, not secondary members such as conductor bay framing).

Figure 1.1 seems to represent the best POD information available in the industry at 1987, which indeed will be used in Chapter II where a method is developed to more rigorously estimate POD functions on a similar database.

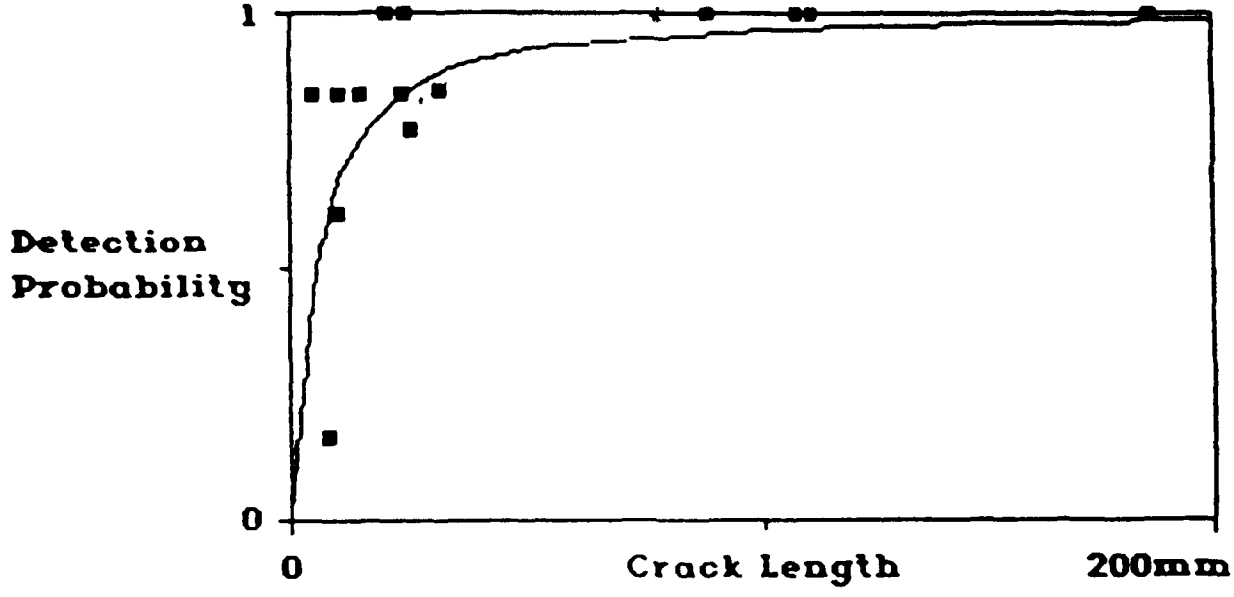

Figure 1.1 Example of Crack Detection Probabilities for Magnetic Particle Testing Under Water Based on Measurements by Moncaster. Included Are 200 Observations on 14 Cracks

Although very few propagating cracks had been found at that time on main structural members, there was a lot of information available about cracks found on conductor bay framing, particularly as a result of design errors in the 1970's. These design errors had omitted considering vertical wave force effects on the conductor bay framing. These vertical forces resulted in bounce action of the bay framing and often led to rapid fatigue failures. Although potentially dangerous in that risers would lose support, the overall structural integrity was not affected by loss of conductor bays.

1.2.3 Semi-Submersible Units

The ABS requirements for inspection of semi-submersibles in ABS class are given in the ABS Rules for Building and Classing Mobile Offshore Drilling Units. The minimum requirements, as

stated in the rules, are for annual and 4–yearly inspections (special periodic surveys). The rules also provide for continuous surveys, and this is becoming the most common practice in industry. Dry-docking is required every 2–1/2 years. Recently the ABS have emphasized the advantage of having an inspection manual for each rig. Reference 1.1 contains their suggestions for an inspection manual as presented at a February 1989 meeting of the Society of Naval Architects and Marine Engineers in Houston.

As noted in the original STA report, the growth or fatigue cracks in semi-submersible units has been the subject of much research in the offshore industry. Units operating in the Gulf of Mexico and other relatively calm water areas do not suffer the fatigue damage to which units operating in harsh environments are prone. Since the 1980 Alexander L. Kielland sinking in a storm in the North Sea, when 123 lives were lost, a great deal of attention has been centered upon detecting fatigue cracks and predicting the rate of growth of fatigue cracks in harsh environment semi-submersibles. DnV have evolved inspection procedures for semi's involving a monthly inspection of all critical joints for through-thickness cracks that can be internally detected by leakage into normally dry spaces. Their philosophy is that a close visual inspection of all critical joints will be undertaken, using MPI, every four to five years. However, they believe the time taken for a crack to propagate to through-thickness is around two to five years in the North Sea for typical semi-submersibles. Hence they have an intermediate survey every two and one-half years, or they have monthly inspection for leaks into normally dry areas. They estimate that the time for a through-thickness crack to propagate until member separation is typically several months. Additionally, they have now introduced a redundancy requirement such that rigs must be able to survive at least a one-year storm after the failure of any individual bracing or bracing connection.

It was clear from both DnV's experience with extraordinary surveys of rigs following the Alexander Kielland accident and from discussions with Exxon, who had been performing their own special surveys of rigs, that many cracks were missed during in-service inspections. Furthermore, these cracks had often been missed during several in-service inspections and were,

in fact, attributed to fabrication defects which had existed since the rig left the fabrication yards. Although this knowledge was common in industry, there was almost no quantification of the probability of cracks being missed during in-service inspections. It should also be noted that these cracks were missed on rigs which were being inspected in relatively good conditions, i.e., benign weather, above the water, without the need for special rigging.

1.3 New Information

Reference 1.2 is a paper presented at OMAE Europe 89' in March 1989 by Inge Lotsberg and Finn Kirkemo of DnV. This paper describes a systematic method of planning in-service inspection of steel offshore structures. The method centers upon a mathematical model for optimization of in-service inspection based upon reliability methods and resource allocation. Bayesian updating of reliability is included in the model. This paper includes the same probability of detection (POD) curve that was produced in the STA initial reports. It is assumed in the paper that inspection for fatigue cracks below water is performed using magnetic particle inspection (MPI). It is a POD curve for MPI that is produced in the paper. It is also noted in the paper that the probability of detecting a crack is a function of its surface length. Accounting for uncertainty in fatigue life predictions and reliability of the inspection method in the mathematical model, the fatigue reliability in the paper is updated according to Bayes rule. Inspection intervals can then be optimized while maintaining a prescribed minimum reliability level. Due to this updating of reliability, the inspection interval is increased as a function of service life. This result is based upon no crack being detected during inspection.

Another conclusion from the paper is that it is cost-efficient to base the inspection reliability on a crack depth equal to one-third of the thickness of the joint, due to a low repair cost for this crack depth compared to a crack depth completely through the thickness of the joint. This is because a crack depth of just one-third of the joint thickness can be repaired by grinding. The repair for a crack that has gone through the thickness of the joint requires underwater welding and is therefore enormously more expensive.

It is also noted that the authors of this paper assumed that an aspect ratio for crack depth to length of 0.15 is appropriate to the cracks and joints of offshore structures that the paper addresses. Their POD curves gives a 90–percent probability of detecting a 3–millimeter deep crack.

Reference 1.3 is another paper presented at the March OMAE conference. This paper is by Paul Frieze and Jacob Kam. Its title is "The Reliability Assessment of the Nondestructive Inspection of Offshore Tubular Structures." In this paper the authors note the historical aerospace inspection requirement to achieve a 90/95 success rate. That is, inspection should achieve 90–percent POD at the 95–percent level of confidence. These figures are derived assuming POD trial results can be statistically quantified by nomial distribution. This approach has been basically inherited by the offshore industry. However, in order to achieve this level of success, 28 cracks in a particular range are all required to be detected. If one is missed, 46 successful detections are necessary if the same level of success is to be realized. It has been noted recently that should success fall significantly below this level, the relevant statistical distribution may no longer be binomial but some unknown distribution.

The authors quantify POD success using a variety of geometrical definitions. These are as follows:

- Size ratio (or length ratio)
- Coverage ratio
- Overlap ratio

Size (length) ratio is defined as the ratio $\frac{LM}{LA}$, where LM and LA are the measured and the actual crack sizes (lengths), respectively. Values can range from zero to infinity. Zero indicates a miss, infinity a spurious indication, and unity a completely successful indication. With an average inspection technique, plots of frequency versus length ratio are shown in Fig. 1.2.

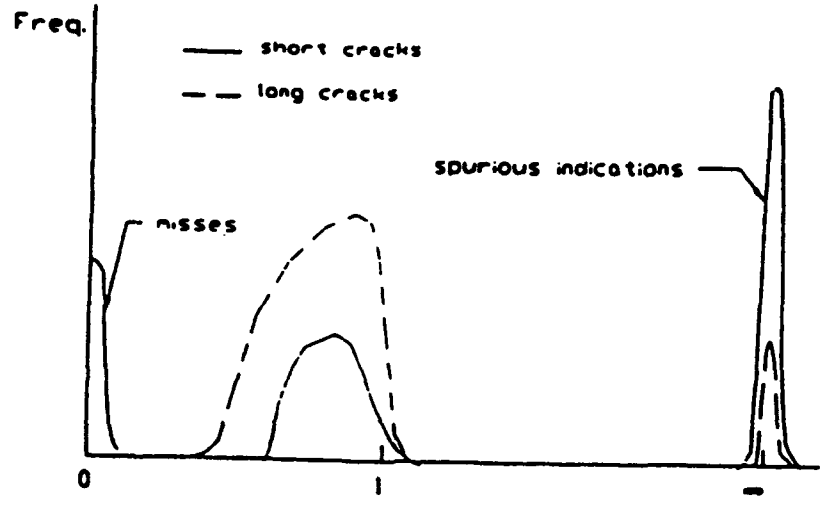

Fig. 1.2 Typical distributions of inspection results based on length ratio.

POD curves can then be generated for any "threshold" value of length ratio. These POD curves represent the area under the curves in Figure 1.2 to the right of the threshold level. Figure 1.3 illustrates POD curves for 0, 50 and 90 percent threshold levels. They all converge to 0 POD as crack length diminishes, as few techniques are successful in this range.

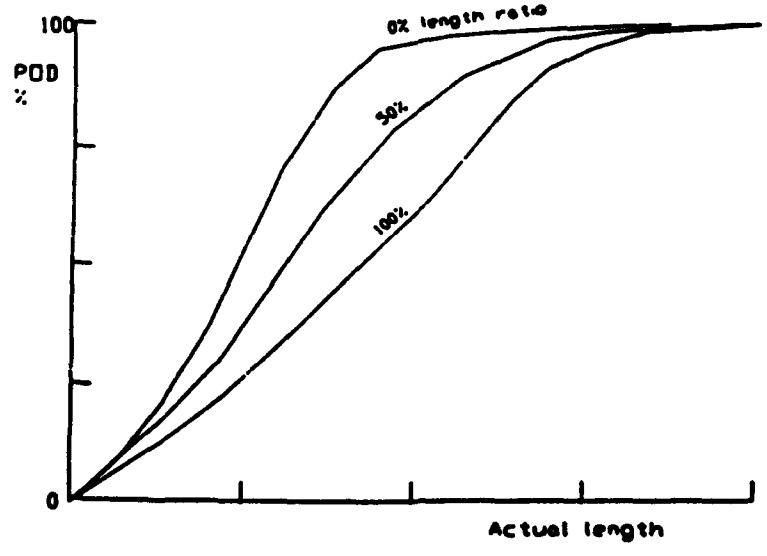

Fig. 1.3 Typical length ratio POD curves.

Unfortunately, the authors are constrained by confidentiality agreements with their clients and have not put numbers to the actual length axis of their POD curve. However, it should be noted that the general shape of the curve is similar to that produced by STA in their earlier reports.

The reader of this report is encouraged to refer to Ref. 1.3 to understand the authors' definitions of coverage ratio and overlap ratio. In the view of STA, both these definitions are helpful in understanding the significant differences between attempts to define POD curves for the offshore industry and POD curves that have historically been established in the aerospace industry.

Another important aspect of Ref. 1.3 is the cost information that it presents relating to underwater inspection and repair. A diving team often consists of eight to twelve divers/inspectors, which for nonsaturation diving currently costs some $7,000 per day. For a short run of two to three weeks, the total cost is nearly $140,000. Usually two shifts are used to make maximum use of the weather window. Full saturation diving is considerably more expensive. A diving support vessel costs around $50,000 per day. With mobilization costs, specialist equipment hire, and daily supplies, a modest full saturation inspection generates a minimum outlay in the region of $1.4 million. For year-round surveys of a large offshore field in the North Sea, an operator may have to spend as much as $24 million. The authors point out that there is presently no objective criterion to determine how successful the surveys are or what they have achieved for this enormous investment.

References 1.4 and 1.5 are two articles from Ocean Industry, March 1987. The first one by W.P. Stewart [1.4] includes the original POD curve presented in the initial STA report and reproduced here in Fig. 1.4.

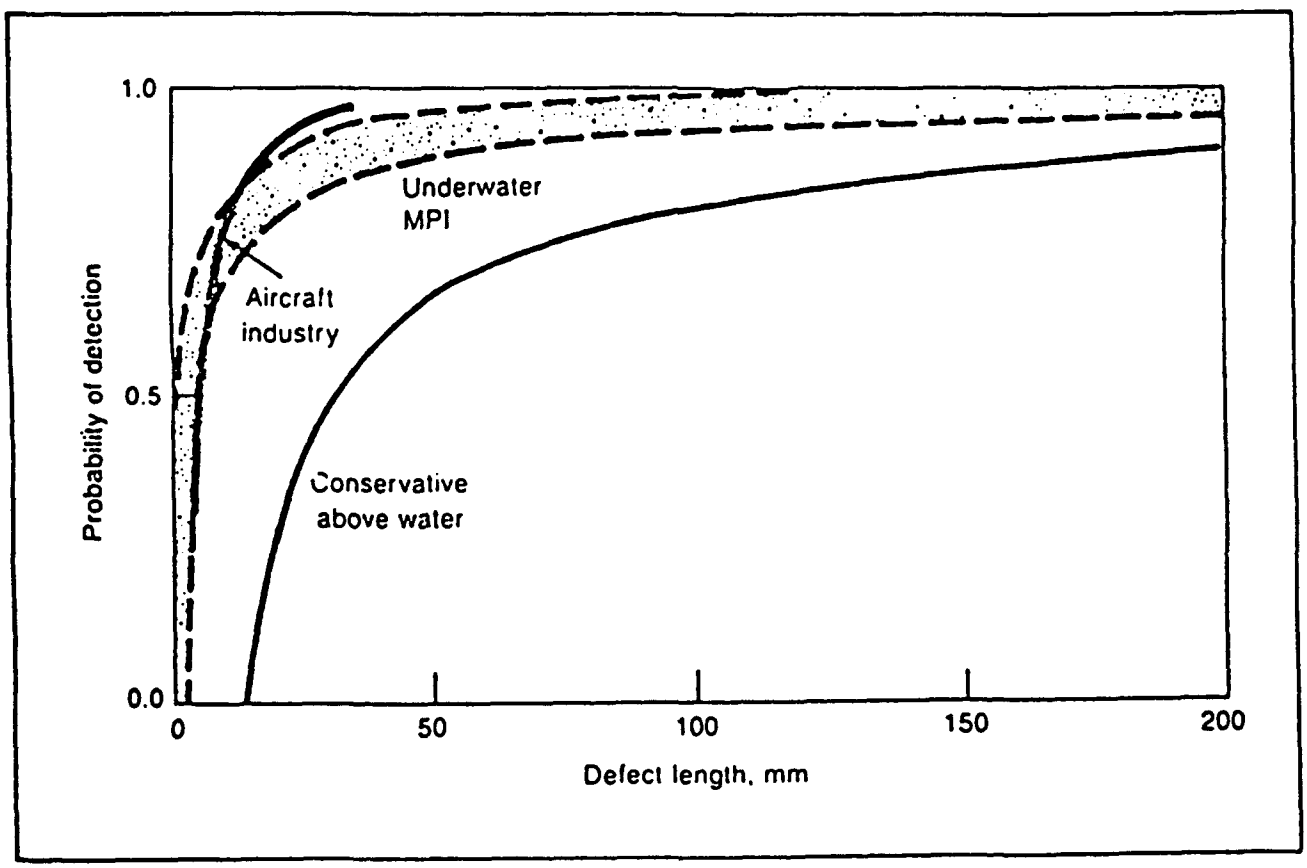

Fig. 1.4 Shaded area shows results from a UK DOE/Shell North Sea study where MPI was applied underwater to detect fatigue cracks. A 95% confidence band is shown for the probability-of-detection regression curve. A total of 34 defects was inspected, with 342 observations. The colored curve in the plot shows results from in-air inspection of aircraft structures; the mean value curve is shown from a series of 60 inspections of more than 20 defects, with over 2,000 observations. The lower black curve is a more conservative viewpoint of typical POD values commonly experienced for above-water inspection of rigs when MPI is used.

The second [1.5] is a paper by F.R. Frisbie on "Inspecting and Repairing Offshore Platforms Today." This paper gives some interesting cost information in Figure 1.5.

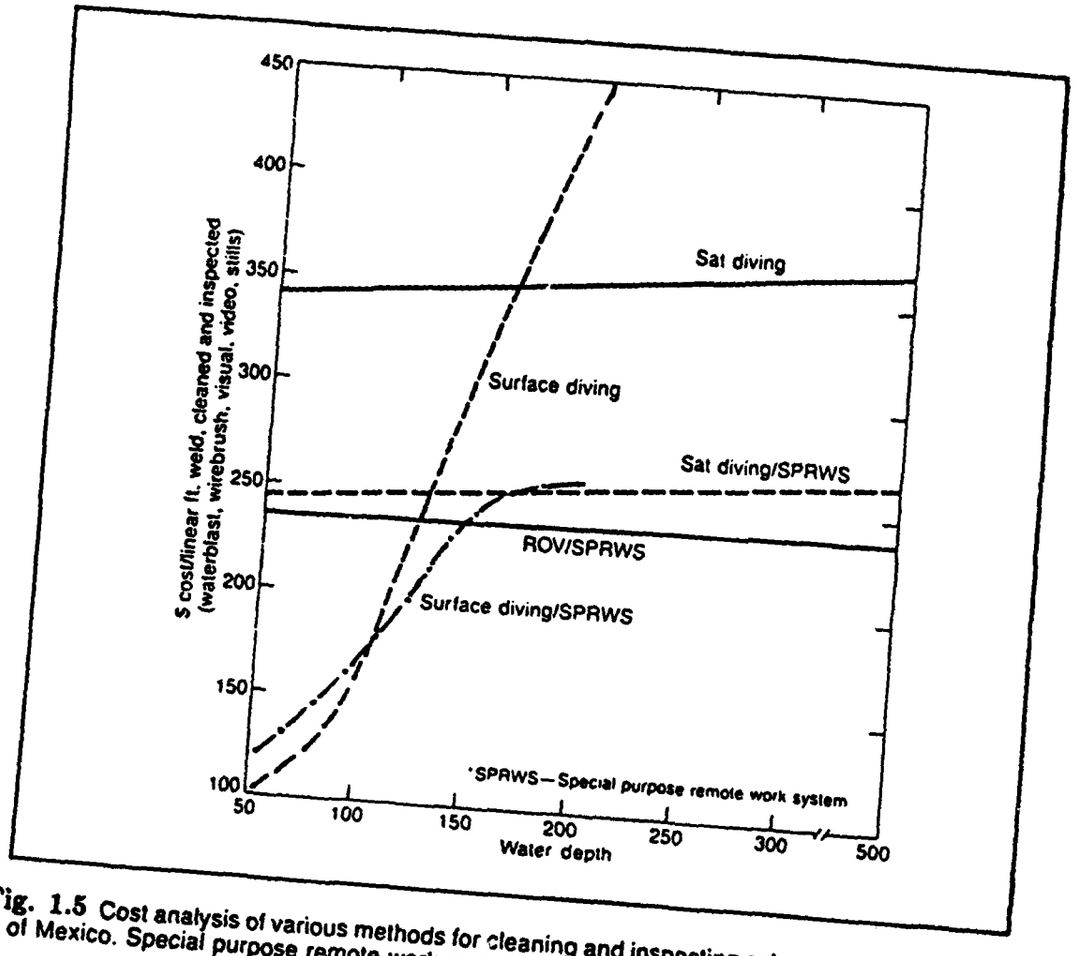

Fig. 1.5 Cost analysis of various methods for cleaning and inspecting subsea welds in the Gulf of Mexico. Special purpose remote work system used in this case was DYNACLAMP.

Reference 1.6, an OTC paper, "Developments of AIM (Assessment, Inspection, Maintenance) Programs for Fixed and Mobile Platforms," by Bea, Puskar, Smith and Spencer is included. While directly relevant to the objective of determining inspection reliability or to the objective of finding data for POD curves, this paper does give a general overview of the industry's assessment inspection and maintenance philosophy.

Reference 1.7 contains extracts from the "The Effectiveness of Underwater Nondestructive Testing — Summary Report of a Program of Tests." This is an Offshore Technology report

from the U.K. Department of Energy published in 1984. It is included since it was sent to Dr. Shinozuka at Modern Analysis by Mr. Ken Bitting from the U.S. Coast Guard R&D Center following a request from the SR-1317 Project Technical Committee members for any information on probability of detection data for underwater inspection systems. The information this document contains is of some interest in that it includes data using ultrasonic measurements and MPI measurements underwater. However, it principally shows some of the difficulties with correlating this type of data and the almost impossible task of using this type of data to develop POD curves.

1.4 Conclusions

In this chapter, a summary of inspection procedures for a range of marine steel structures was provided. Specifically, inspection procedures for bulk carriers, fixed offshore structures and semi-submersible units were reviewed. This review showed that there is very little information available to assess the reliability of these inspection techniques. It is noted that only one reliable probability of detection (POD) curve was found. In view of this limited information available to assess the reliability of inspection procedures for marine steel structures, a review of POD curves used in the aerospace industry will be presented in the following chapter. This review will be done because it is believed that the shape of POD curves used in the aerospace industry can provide useful guidelines for assessing the reliability of flaw detection and for establishing POD curves for marine structures.

REFERENCES

1.1 Bryant, Robert E. Jr. and Corcoran, G. Chris, *On-Site Surveys on Semi-Submersibles and Suggestions for Development of an Inspection Manual*, Texas Section, The Society of Naval Architects and Marine Engineers, February 24, 1989.

1.2 Lotsberg, I. and Kirkemo, F., *A Systematic Method for Planning In-Service Inspection of Steel Offshore Structures*, presented at OMAE Europe 89 – 8th International Conference on

Offshore Mechanics and Arctic Engineering, The Hague, The Netherlands, March 18–23, 1989.

1.3 Frieze, P.A. and Kam, J.C.P., *The Reliability Assessment of the Non-Destructive Inspection of Offshore Tubular Structures*, OMAE Europe 89 – 8th International Conference on Offshore Mechanics and Arctic Engineering, The Hague, The Netherlands, March 18–23, 1989.

1.4 Stewart, W.P., *Practical Aspects of Platform Inspection*, Ocean Industry, March 1987, pp. 54–56.

1.5 Frisbie, F.R., *Inspecting and Repairing Offshore Platforms Today*, Ocean Industry, March 1987, pp. 60–63.

1.6 Bea, R.G., Puskar, F.J., Smith, C. and Spencer, J.S., *Development of AIM (Assessment, Inspection, Maintenance) Programs for Fixed and Mobile Platforms*, Proceedings of the 20th Annual Offshore Technology Conference, Houston, Texas, May 2–5, 1988, pp. 193–205.

1.7 Techword Services, *The Effectiveness of Underwater Non-Destructive Testing - Summary Report of a Programme of Tests*, UK Dept. of Energy Offshore Technology Report No. 84 203, 1984.

II. RELIABILITY OF FLAW DETECTION

2.1 Introduction

In view of the limited information available to assess the reliability of inspection procedures for marine steel structures as concluded in the first chapter, a review of POD curves used in the aerospace industry is presented in this chapter. This review is done because it is believed that the shape of POD curves used in the aerospace industry can provide useful guidelines for assessing the reliability of flaw detection and for establishing POD curves for marine structures.

Current nondestructive inspection (NDI) systems are not capable of repeatedly producing correct indications when applied to flaws of the same length. The chance of detecting a given crack length depends on many factors, such as the location, orientation and shape of the flaw, materials, inspectors, inspection environments, etc. As a result, the probability of detection (POD) for all cracks of a given length has been used in the literature to define the capability of a particular NDI system in a given environment.

In aerospace applications, a nondestructive inspection limit, a_{NDE}, is chosen, which is a crack length that usually corresponds to a high detection probability and high confidence level. For instance, the damage tolerance specifications for aircraft structures require that the NDI system be capable of detecting a specified crack length, a_{NDE}, at a particular location with a 90% detection probability and 95% confidence level (see Ref. 2.1). The fracture mechanics propagation life, N_f, is the life for crack length a_{NDE} to propagate to the critical crack length a_c, under expected usage environments. The inspection interval, τ, is equal to N_f divided by a safety factor, S_f, i.e., $\tau = N_f/S_f$. In evaluating the structural reliability under scheduled inspection maintenance, however, the information of a_{NDE} is of little value and the uncertainty of the NDI system should be taken into account [2.2–2.5].

Flaw detection reliability is defined as the probability of detecting a flaw under pre-specified inspection conditions. This probability is a function of the crack length. Figure 2.1 shows a plot of inspection results for individual cracks emanating from fastener holes in a skin and stringer

wing assembly using eddy current surface scans [2.6–2.7]. The points represent the proportion of times individual flaws were detected versus the length of the flaw. This figure illustrates that although the detection probabilities of individual flaws generally increase with crack length, not all flaws of the same length have the same detection probability. This variability in detection probabilities at a crack length requires a consistent definition of the probability of detection (POD) as a function of crack length "a." The POD (a) function is defined as the proportion of flaws that will be detected as a function of crack length, i.e., the mean trend in detection probabilities as a function of crack length [2.6–2.7]. The solid curve in Fig. 2.1 is a POD function obtained from the inspection results (points) as will be described later.

It follows from Fig. 2.1, that an NDI system may result in two types of incorrect indications (i) failure to give a positive indication in the presence of a crack whose length is greater than a_{NDE}, referred to as a Type I error, and (ii) give a positive indication when the crack length is smaller than a_{NDE}, referred to as a Type II error. The Type I error allows components containing a crack length longer than a_{NDE} to remain in service, thus greatly increasing the potential safety hazard. For safety critical components, the Type I error is of primary concern. The Type II error rejects good components and, hence has an adverse effect on the cost of repair/replacement and life cycle cost. In applications such as retirement-for-cause (RFC) life management, however, both Type I and Type II errors are important, because the criterion used in RFC life management is the minimization of the life-cycle-cost (LCC) [2.8–2.9]. For a given NDI system with a single inspection, it is impossible to reduce the Type II error without increasing the Type I error and vice versa [2.10–2.12]. It is obvious that the ideal inspection capability of an NDI system is a unit step function. Figure 2.2 schematically shows an ideal and a realistic POD function. The ideal inspection system would detect all flaws larger than a_{NDE} and none smaller than a_{NDE} as indicated by a unit step function in Fig. 2.2, in which both Type I and Type II errors are zero. Unfortunately, such an ideal NDI system is far from reality. Technical approaches to reduce both types of errors using multiple inspection procedures were studied recently by Yang et al. [2.10–2.12].

Many factors influence the capability of an NDI system to identify flaws in a structure. These include (1) system factors which affect the ability of the system to consistently produce and interpret the information upon which flaw decisions are made, and (2) factors which are characteristics of the individual flaws being inspected. The net effect is uncertainty in the detection of flaws so that the process of quantifying the inspection capability of a particular system requires a careful NDI reliability demonstration program coupled with a probabilistically based analysis of the data. This section describes the reliability of flaw detection and the analysis of NDI reliability data following Refs. 2.6 and 2.7.

As described previously, the detection probability for a given crack length involves considerable statistical variability. The distribution of detection probabilities at a given crack length is illustrated in Fig. 2.3. The curve connecting the average values of the detection probabilities for all crack lengths is defined as the POD(a) function. Hence, the POD(a) function is a function which passes through the mean of detection probabilities at each crack length, i.e., a regression function. Consequently, many individual cracks will have detection probabilities below the POD(a) value.

2.2 POD Functional Form

The information on POD functions for NDI systems is needed in the reliability analysis of structures under scheduled inspection maintenance. It is also crucial for the determination of the inspection interval. To establish the POD function from experimental test results, a functional form should be assumed. The so-called log odds or log logistic model has been investigated extensively [2.6–2.7],

$$\text{POD}(a) = \left\{1 + \exp\left[-\frac{\pi}{3}\left(\frac{\ln a - \mu}{\sigma}\right)\right]\right\}^{-1} \tag{2.1a}$$

in which POD(a) is the probability of detecting crack size a, and μ and σ are parameters. Methods for estimating the parameters μ and σ from NDI reliability data is a major subject of this section.

Let $a_{0.5}$ be the median crack detection capability, i.e., the crack length associated with a 50% detection probability, $\text{POD}(a_{0.5}) = 0.5$. Then, it follows from Eq. 2.1a that

$$\mu = ln a_{0.5} \tag{2.1b}$$

Thus, the parameter μ represents the central location of the POD curve. The parameter σ is a measure of the flatness of the POD function, the larger the value of σ, the slower the POD function approaches one. The parameters μ and σ are referred to as the location and scale parameters, respectively.

Another POD function, referred to as the Weibull function, has also been used [2.2, 2.3, 2.10]:

$$\begin{aligned} \text{POD}(a) &= 0 && a < \epsilon \\ &= 1 - \exp\left[-\left(\frac{a-\epsilon}{\beta}\right)^{\alpha}\right] && a \geq \epsilon \end{aligned} \tag{2.2}$$

in which ϵ is the crack length below which a crack cannot be detected by the NDI system. Again, α and β are constants, representing the bandwidth and central location of the POD function, respectively.

As mentioned previously, the POD function is a unit step function at a_{NDE} for an ideal NDI system, i.e.,

$$\begin{aligned} \text{POD}(a) &= 0 && a < a_{NDE} \\ &= 1 && a > a_{NDE} \end{aligned} \tag{2.3}$$

Such an ideal POD function can be obtained from the Weibull function by setting $\epsilon = a_{NDE}$, $\beta \rightarrow 0$ and $\alpha \rightarrow \infty$. Hence the Weibull function given by Eq. 2.2 includes the ideal POD curve, Eq. 2.3, as a special case.

These and other POD functions have been proposed in the literature [e.g., 2.2–2.5, 2.13, 2.14]. Among these, the Weibull model and log odds model appear to be most viable for the analysis that is to be performed here. However, the Weibull model has been well studied in dealing with other applications. Therefore, only the log odds model has been investigated here extensively using available NDI reliability data [2.6,2.7] and it has been shown that the log odds model is also very reasonable for the POD function. In Chapter III, however, a special case of the Weibull model with $\alpha = 1$ and $\epsilon = 0$ will be used.

2.3 Statistical Estimation of POD Function

In order to establish the POD function for a particular NDI system associated with a particular structural detail under a particular inspection environment, NDI reliability demonstrations should be conducted. Data collected from NDI reliability demonstration programs consist of two categories: (i) data in which the inspection result (pass or fail) is recorded, and (ii) data in which the response signal $\hat{a}$ is recorded. Data in the first category may be divided into two types: (i) data in which a single inspection is made for each flaw, and (ii) data in which multiple inspections are made for each flaw. Analysis techniques for estimating POD functions are described in this section. Two techniques for analyzing NDI results recorded in the pass/fail form are presented first followed by estimation of POD functions from $\hat{a}$ versus a data.

2.3.1 Analysis of Pass/Fail Data

Traditionally, NDI reliability data has been collected as a crack length, a_i, along with an indication of whether or not the crack was found during a particular inspection. Crack lengths a_i, are determined through independent means such as replicates or tear-down inspections. During the inspections, the inspectors record whether each site or flaw passed or failed the inspection. Because most of the NDI reliability data currently available is in this pass/fail format, the analysis of pass/fail data is discussed first.

An NDI reliability demonstration experiment can be conducted in two ways: one inspection per flaw or multiple inspections per flaw. For data collected with a single inspection per flaw, all the observations are independent and the analysis is reasonably simple. Multiple inspections conducted on the same flaw will be correlated so that there are dependencies between observations when more than one inspection is made for each flaw. These two types of experimental data will be analyzed differently.

Two techniques can be used to analyze pass/fail data, depending on the type of data. A regression analysis can be used to estimate the parameters of the POD model when there are

multiple inspections for each flaw. For data with a single inspection per flaw, the maximum likelihood method provides good estimates of the POD model parameters.

The analyses described on the following are based on the log odds function given in Eq. 2.1a. A direct analysis of the model when expressed in the form given by Eq. 2.1a is very complicated. The analysis can be simplified by using the reparameterized model.

$$\text{POD}(a) = \frac{\exp(\alpha + \beta ln(a))}{1 + \exp(\alpha + \beta ln(a))} \tag{2.4}$$

The relationship between μ and σ of Eq. 2.1a and α and β of Eq. 2.4 is:

$$\mu = -\alpha/\beta \tag{2.5}$$

$$\sigma = \pi/\left(\beta\sqrt{3}\right) \tag{2.6}$$

For both the regression analysis and the maximum likelihood method, estimates of μ and σ can be calculated by substituting the appropriate estimates of α and β into the right-hand sides of Eqs. 2.5 and 2.6.

2.3.1.1 Regression Analysis

Regression analysis can be used for NDI reliability data in which (i) multiple inspections are performed for each flaw, and (ii) a single inspection is performed for each flaw but the data can be grouped conveniently into crack length intervals. The log odds transformation converts Eq. 2.4 to

$$ln\left[\frac{\text{POD}(a)}{1 - \text{POD}(a)}\right] = \alpha + \beta\, ln\, a \tag{2.7}$$

or

$$Y = \beta X + \alpha \tag{2.8}$$

in which $Y(a)$ and X are transformed variables

$$Y(a) = ln\left(\frac{\text{POD}(a)}{1 - \text{POD}(a)}\right) \tag{2.9}$$

and

$$X = ln\, a \tag{2.10}$$

Thus, the linear regression method can be used to estimate α and β.

Before performing linear regression on NDI reliability data, the data must be reduced to a set of n pairs, (a_i, p_i) where a_i is the crack length for the i-th pair and p_i is the proportion of times the flaw (or flaws) were detected. If the data contain multiple inspections of each flaw, a_i will be the length of a single flaw and p_i will be the proportion of time that the flaw was detected. If flaws are grouped into crack length intervals, a_i will be the midpoint of the i-th interval and p_i will be the proportion of flaws in the i-th interval that were detected.

Given the n pairs of (a_i, p_i) data points to be fit by the regression analysis, the transformations of Eqs. 2.9 and 2.10 are performed, resulting in a set of n (X_i, Y_i) pairs, i.e., $X_i = lna_i$ and $Y_i = ln\left[p_i/(1-p_i)\right]$.

Variables X and Y are then used in a linear regression analysis, Eq. 2.8, resulting in estimates of $\hat{\alpha}$ and $\hat{\beta}$ as

$$\hat{\beta} = \frac{\sum_{i=1}^{n} X_i Y_i - n\,\overline{X}\,\overline{Y}}{\sum_{i=1}^{n} X_i^2 - \frac{1}{n}\left(\sum_{i=1}^{n} X_i\right)^2} \tag{2.11}$$

$$\hat{\alpha} = \overline{Y} - \hat{\beta}\,\overline{X} \tag{2.12}$$

where

$$\overline{Y} = \frac{1}{n}\sum_{i=1}^{n} Y_i,\ \overline{X} = \frac{1}{n}\sum_{i=1}^{n} X_i \tag{2.13}$$

The estimated mean of Y as a function of a follows from Eqs. 2.8 and 2.10 as

$$\overline{Y}(a) = \hat{\alpha} + \hat{\beta}\, lna \tag{2.14}$$

The formula for a lower confidence bound on the mean of $Y(a)$ is given by

$$\overline{Y_L}(a) = \hat{\alpha} + \hat{\beta}\, lna - t_{(n-2),\gamma}(S)\sqrt{\frac{1}{n} + \frac{(lna - \overline{X})^2}{SSX}} \tag{2.15}$$

where γ = confidence coefficient (level), $t_{(n-2),\gamma}$ = γ-th percentile of t distribution with $n-2$ degrees of freedom.

$$S^2 = \frac{1}{n-2}\sum_{i=1}^{n}\left(Y_i - \hat{\alpha} - \hat{\beta}X_i\right)^2 \tag{2.16}$$

$$SSX = \sum_{i=1}^{n} X_i^2 - \frac{1}{n}\left(\sum_{i=1}^{n} X_i\right)^2 \tag{2.17}$$

The inverse transformation of Eq. 2.9 gives the estimate of POD (a) and its lower confidence bound, denoted by $POD_L(a)$, as follows

$$\text{POD}(a) = \frac{\exp\left(\overline{Y}(a)\right)}{1+\exp\left(\overline{Y}(a)\right)} \tag{2.18}$$

$$POD_L(a) = \frac{\exp\left(\overline{Y_L}(a)\right)}{1+\exp\left(\overline{Y_L}(a)\right)} \tag{2.19}$$

in which $\overline{Y}(a)$ and $\overline{Y_L}(a)$ are given by Eqs. 2.14 and 2.15, respectively.

When the observed proportion of detected cracks at a crack length is zero or one, i.e., $p_i = 0$ or $p_i = 1$, the transformation for $Y_i = ln\left[p_i/(1-p_i)\right]$ is undefined. There are several alternatives to circumvent this problem. One possibility is to use the mean estimate, $\overline{p}$, for the proportion, p_i, of detected cracks at a crack length.

$$\overline{p} = \left\{ \begin{array}{l} \dfrac{i}{n+1} \text{ if } i > \dfrac{n}{2} \\ \dfrac{1}{2} \text{ if } i = n/2 \\ \dfrac{i+1}{n+1} \text{ if } i < \dfrac{n}{2} \end{array} \right\} \tag{2.20}$$

Another possibility is to use the median estimate $\tilde{p}$:

$$\tilde{p} = \left\{ \begin{array}{l} \dfrac{i-0.3}{n+0.4} \text{ if } i > \dfrac{n}{2} \\ \dfrac{1}{2} \text{ if } i = n/2 \\ \dfrac{i+0.7}{n+0.4} \text{ if } i < \dfrac{n}{2} \end{array} \right\} \tag{2.21}$$

Consequently, it follows from Eqs. 2.5 and 2.6 that estimates of the location and scale parameters, μ and σ, for the log odds model given by Eq. 2.1a are given by

$$\hat{\mu} = -\hat{\alpha}/\hat{\beta} \tag{2.22}$$

$$\hat{\sigma} = \pi/\left(\hat{\beta}\sqrt{3}\right) \tag{2.23}$$

Inspection data for magnetic particle examinations applied under water for detection of fatigue cracks and artificial defects was obtained in graphical form as shown in Fig. 2.4. In this figure, each circle represents a data point with the area of the circle proportional to the number of observations for each crack. Unfortunately, the raw data set was not available. For illustrative purposes, the circles in Fig. 2.4 were read graphically without accounting for the size of the circles. The results were plotted in Fig. 2.5 as circles. Using the regression analysis presented above, the POD(a) function, i.e., the mean curve, is plotted as Curve 1 and the lower 95% confidence bound is plotted as Curve 2. The lower confidence bound, Curve 2, lies above many of the individual data points. Note that the confidence bound is a bound on the mean or POD(a) curve of the detection probabilities, not the population of detection probabilities.

2.3.1.2 Maximum Likelihood Estimates

In using the method of regression analysis, grouping of NDI observed data in each crack length interval is required, when the experiment involves a single inspection per flaw. In this fashion, data of (a_i, p_i) pairs can be obtained. Frequently, however, the crack length for NDI reliability data with a single inspection per flaw cannot be grouped conveniently. In this regard, the method of maximum likelihood can be used to estimate the parameters of the POD(a) model given by Eq. 2.1a. With such an approach, the parameters are estimated which maximize the probability of obtaining the observed data. Unlike the regression analysis, the maximum likelihood estimates do not require grouping of data with a single inspection per flaw. Instead, they are based directly on the observed outcome of 0 for a non-detection and 1 for a detection.

To find the maximum likelihood estimates of Eq. 2.4 from a sample of single inspections of n cracks, the following procedure adopted from Cox [2.15] can be used. The maximum likelihood estimates $\hat{\alpha}$ and $\hat{\beta}$ of α and β satisfy the simultaneous equations:

$$0 = \sum_{i=1}^{n} Z_i - \sum_{i=1}^{n} \frac{\exp\left(\hat{\alpha} + \hat{\beta} ln\,(a_i)\right)}{1 + \exp\left(\hat{\alpha} + \hat{\beta} ln\,(a_i)\right)} \tag{2.24}$$

$$0 = \sum_{i=1}^{n} Z_i ln\,(a_i) - \sum_{i=1}^{n} \frac{ln\,(a_i)\, exp\left(\hat{\alpha} + \hat{\beta} ln\,(a_i)\right)}{1 + \exp\left(\hat{\alpha} + \hat{\beta} ln\,(a_i)\right)} \tag{2.25}$$

in which the observed data set is denoted by (a_i, Z_i) where $Z_i = 1$ if the flaw is detected and 0 if it is not.

The variances and covariance of the estimates $\hat{\alpha}$ and $\hat{\beta}$ are

$$\text{Var}\,(\hat{\alpha}) = \sum_{i=1}^{n} \frac{\exp\,(\alpha + \beta ln\,(a_i))}{(1 + \exp\,(\alpha + \beta ln\,(a_i)))} \tag{2.26}$$

$$\text{Var}\left(\hat{\beta}\right) = \sum_{i=1}^{n} \frac{(ln\,(a_i))^2 \exp\,(\alpha + \beta ln\,(a_i))}{(1 + \exp\,(\alpha + \beta ln\,(a_i)))^2} \tag{2.27}$$

$$\text{Cov}\left(\hat{\alpha}, \hat{\beta}\right) = \sum_{i=1}^{n} \frac{ln\,(a_i) \exp\,(\alpha + \beta ln\,(a_i))}{(1 + \exp\,(\alpha + \beta ln\,(a_i)))^2} \tag{2.28}$$

Estimates of these variances and covariance are calculated by substituting the estimates $\hat{\alpha}$ and $\hat{\beta}$ in Eqs. 2.24 and 2.25 for α and β in Eqs. 2.26–2.28.

The maximum likelihood estimate of the POD function is calculated by substituting $\hat{\alpha}$ and $\hat{\beta}$ for α and β in Eq. 2.4. The change of variables must be made using the same transformation that was used in the regression analysis to obtain

$$ln\left[\frac{\text{POD}\,(a)}{1 - \text{POD}\,(a)}\right] = Y\,(a) = \hat{\alpha} + \hat{\beta} ln\,(a) \tag{2.29}$$

For very large sample sizes, estimates of the variances and covariance of $\hat{\alpha}$ and $\hat{\beta}$ can be used to calculate a lower confidence bound on $Y\,(a)$ as given by

$$Y_L\,(a) = \hat{\alpha} + \hat{\beta} ln\,(a) - z_\gamma \sqrt{S^2_{\hat{\alpha}} + 2ln\,(a) + S^2_{\hat{\alpha}\hat{\beta}} + (ln\,(a))^2\, S^2_{\hat{\beta}}} \tag{2.30}$$

where γ is the confidence level, z_γ satisfies $\Phi(z_\gamma) = \gamma$ with $\Phi()$ being the standard normal distribution function, $S^2_{\hat{\alpha}}$ is the estimate of $\text{Var}(\hat{\alpha})$ given by Eq. 2.26, $S^2_{\hat{\alpha}\hat{\beta}}$ is the estimate of $\text{Cov}\left(\hat{\alpha}, \hat{\beta}\right)$ given by Eq. 2.28, and $S^2_{\hat{\beta}}$ is the estimate of $\text{Var}\left(\hat{\beta}\right)$ given by Eq. 2.27.

Since the log odds transformation is monotonic, the inverse transformation of the confidence bound on $Y(a)$ will be the confidence bound on $\text{POD}(a)$. Specifically,

$$\text{POD}(a) = \frac{\exp(Y(a))}{1 + \exp(Y(a))} \tag{2.31}$$

$$POD_L(a) = \frac{\exp(Y_L(a))}{1 + \exp(Y_L(a))} \tag{2.32}$$

in which $Y(a)$ and $Y_L(a)$ are given by Eqs. 2.29 and 2.30, respectively.

Generally, maximum likelihood estimates are better than regression estimates that require the grouping of data for single inspection per flaw; however, if the number of flaws is very large (greater than 100) and the groupings do not result in many 0's and 1's for p_i's, the results of both analyses should be similar.

The equations for solving the maximum likelihood estimates $\hat{\alpha}$ and $\hat{\beta}$ given by Eqs. 2.24 and 2.25 are nonlinear. In solving simultaneous nonlinear equations, suitable initial estimates of $\hat{\alpha}$ and $\hat{\beta}$ are needed. It is possible that $\hat{\alpha}$ and $\hat{\beta}$ have more than one solution and the iteration procedures will converge to the solution closest to the initial estimates. As a result, the initial estimates of $\hat{\alpha}$ and $\hat{\beta}$ are important. In this connection, the moment method has been suggested in Ref. 2.7 to determine the initial estimates.

An example for the application of the method of maximum likelihood is given in Fig. 2.6. In this figure, the circles represent a set of hypothetical inspection data for a single inspection per flaw. Hence, the data is binary, i.e., one for detection and zero for nondetection. The $\text{POD}(a)$ curve is shown by Curve 1 and the 95% lower confidence bound is indicated by Curve 2.

2.3.2 Analysis of $\hat{a}$ Versus a Data

The POD is the measure of inspection uncertainty, not the cause. Causes of uncertainty should be defined in terms of the inspection process. Typical NDI systems apply a stimulus to a suspect area and record the signal that returns from the specimen. A positive flaw indication occurs if the signal is higher than a threshold value. The variability of the response signals comes from the following reasons:

1. Material variability results in unpredictable changes in the stimulus before it reaches the flaw and in the signal before it returns to the NDI system;
2. Variability in flaw geometry and orientation produces variability in the signal;
3. Calibration changes in the instruments from inspection to inspection reduces the predictability of the signal.

Since a flaw is detected if the response signal $\hat{a}$ is larger than the threshold, the POD(a) is the probability that the response signal $\hat{a}$ is greater than the threshold a_{th}. Furthermore, the variability of the response signal $\hat{a}$ depends on the inspection process. A typical plot for the response signal $\hat{a}$ versus crack length a is shown in Fig. 2.7. It is observed from Fig. 2.7 that the $\hat{a}$ values from a single flaw are typically grouped around a point that is shifted from the mean curve. This pattern of grouping indicates that there are two sources of variation in the response signal. One source is the variability in the mean $\hat{a}$ from flaw to flaw, and the other is the variability in $\hat{a}$ from inspection to inspection of the same flaw.

The causes of uncertainty can be grouped into two sources of variation: (1) the material properties, flaw location, geometry and orientation, and the pattern of residual stresses which are strictly associated with individual flaws and which do not change from inspection to inspection; (2) factors that change from inspection to inspection including human factors, such as transducer variability and calibration. Because of these two distinct sources of variation, the response signal has a compound distribution. First a flaw is picked at random along with its individual mean $\hat{a}$. Then the human factors and equipment factors come into play resulting in random deviation

from the flaw mean for an individual inspection. These are two distinct random processes with distinct random variables. As a result, the response signal $\hat{a}$ can be expressed as

$$\hat{a} = f(a) + c + e \tag{2.33}$$

where $f(a)$ represents the overall trend in $\hat{a}$ as a function of a, c represents the flaw to flaw variation, and e represents the variation from inspection to inspection of the same flaw. The function $f(a)$ is fixed while variables c and e are random with means of 0.

NDI uncertainty is attributed to random variation in the response signal or $\hat{a}$ value for an NDI system. The POD can be expressed as the probability that $\hat{a}$ is bigger than the detection threshold a_{th}. The analysis of $\hat{a}$ versus a data and estimation of the POD function will be described in the following.

Equation 2.33 provides the basic model for the analysis of $\hat{a}$ versus a data. The flaw-related and flaw-independent terms c and e are random variables with means equal to 0 and variances equal to s_c^2 and s_e^2, respectively. The mean and variance of $\hat{a}$ for a single inspection of a flaw of size a picked at random are:

$$\begin{aligned} E(\hat{a}/a) &= f(a) \\ \text{Var}(\hat{a} \mid a) &= s_c^2 + s_e^2 \end{aligned} \tag{2.34}$$

Methods for analyzing the inspection data $\hat{a}$ versus a, are based on a model of Eq. 2.33 available in the literature. However, the choice of a suitable method depends on the functional form of $f(a)$, Eq. 2.33 and the number of inspections per flaw. In general. it would be more convenient to choose a linear function for $f(a)$ through appropriate transformations of $\hat{a}$ and a. Suppose $\hat{a}$ and a are transformed into Y and X through:

$$Y = ln\hat{a},\ X = lna \tag{2.35}$$

and consider a linear function for $f(a)$, i.e., $f(a) = \alpha + \beta X$, so that Eq. 2.33 becomes:

$$Y = \alpha + \beta X + c + e \tag{2.36}$$

where α and β are parameters to be determined from NDI reliability data of $\hat{a}$ versus a. Note that α and β in Eq. 2.36 are new parameters different from those discussed previously, such as those appearing in Eqs. 2.4–2.6.

If the error variables c and e are assumed to have normal distributions with zero means, it follows from Eq. 2.36 that Y is a normal random variable with mean value of $\alpha + \beta X$ and standard deviation $S = \left(s_c^2 + s_e^2\right)^{1/2}$. Then, the POD function is given by:

$$\begin{aligned} \text{POD}(a) &= P(\hat{a} > a_{th}) = P\{ln(\hat{a}) > ln(a_{th})\} = P(Y > Y_{th}) \\ &= 1 - \Phi\left[\frac{Y_{th} - (\alpha + \beta X)}{S}\right] \end{aligned} \tag{2.37}$$

in which:

$$S = \sqrt{s_c^2 + s_e^2} \text{ and } Y_{th} = ln a_{th} \tag{2.38}$$

and $\Phi(x)$ is the standard normal distribution function. Using the symmetry properties of $\Phi(x)$, Eq. 2.37 becomes:

$$\text{POD}(a) = \Phi\left(\frac{X - \left(\frac{Y_{th} - \alpha}{\beta}\right)}{S/\beta}\right) \tag{2.39}$$

Equation 2.39 is a form of the lognormal distribution function with mean $\overline{\mu}$ and standard deviation $\overline{\sigma}$ of log crack length given by:

$$\overline{\mu} = (ln(a_{th}) - \alpha)/\beta \tag{2.40}$$

$$\overline{\alpha} = S/\beta \tag{2.41}$$

In the previous analysis, the log logistic function of Eq. 2.1a was used to model the POD function; however, the log logistic function is a close approximation to the lognormal distribution. The use of the lognormal distribution above (Eq. 2.39) instead of the log logistic distribution will therefore result in very similar estimates of the POD function.

Since Eq. 2.36 is linear, the method of linear regression described previously can be used conveniently to estimate the parameters α, β and S appearing in the POD(a) function of Eq.

2.39 as follows. The NDI reliability data is expressed in n $(\hat{a}_i, a_i)$ pairs. These n pairs of data are transformed into a set of n (Y_i, X_i) pairs through the transformation of Eq. 2.35, i.e., $Y_i = ln\hat{a}_i$ and $X_i = lna_i$. By use of linear regression analysis, formulas for estimates $\hat{\alpha}$, $\hat{\beta}$ and $\hat{S}$ for parameters α, β and S are identical to those given by Eqs. 2.11, 2.12 and 2.16, respectively. After estimating α, β and S from these equations, parameters $\overline{\mu}$ and $\overline{\sigma}$ can be computed from Eqs. 2.40 and 2.41 in which α, β and S are replaced by $\hat{\alpha}$, $\hat{\beta}$ and $\hat{S}$, respectively. Hence, the POD(a) function (Eq. 2.39) can be expressed as:

$$\text{POD}(a) = \Phi\left(\frac{lna - \overline{\mu}}{\overline{\sigma}}\right) \tag{2.42}$$

It is noted from Eqs. 2.39–2.42 that the POD(a) function depends on the specifying detection threshold a_{th}. The effects of the detection threshold a_{th} on POD(a) are described in the following. First, the median detection crack length increases with the detection threshold. Second, the slope of the POD(a) function decreases as the detection threshold increases.

A method described by Cheng and Iles [2.16] for calculating confidence bounds on the lognormal cumulative distribution can be adopted to calculate confidence bounds on the POD function given by Eq. 2.42. The formulas given by Cheng and Iles [2.16] for the γ percent lower confidence bound can be used as follows:

$$\text{POD}(a) = \Phi(z_L) \tag{2.43}$$

in which

$$z_L = \hat{z}\sqrt{\frac{\lambda}{n}\left(\frac{\hat{z}^2}{2} + \frac{(X - \overline{X})^2}{SSX} + 1\right)} \tag{2.44}$$

where

$$X = lna \text{ and } \overline{X} = \frac{1}{n}\sum_{i=1}^{n} lna_i \tag{2.45}$$

In Eq. 2.44, n is the sample size, λ is the γ – th percentile of a Chi-Square distribution with two-degrees-of-freedom, SSX is given by Eq. 2.17 and:

$$\hat{z} = \frac{X - \overline{\mu}}{\overline{\sigma}} \tag{2.46}$$

Theoretically speaking the $\hat{a}$ versus a data sets are superior to the pass/fail data sets, since $\hat{a}$ versus a data contains more statistical information regarding the uncertainties of an NDI system. With the current state of NDI technology for marine structures, extensive research effort is needed to obtain $\hat{a}$ versus a data.

2.4 Conclusions

A review of POD curves used in the aerospace industry was presented in this chapter. This review was done because it is believed that the shape of POD curves used in the aerospace industry can provide useful guidelines for assessing the reliability of flaw detection and for establishing POD curves for marine structures. Emphasis was given to the log odds model which was investigated extensively. Another very good model is the Weibull model which has been well studied in dealing with other applications and found to be very reasonable for the POD function. Indeed, it is a special case of the Weibull model that will be used as a POD curve in the third chapter that follows.

REFERENCES

2.1 Gallagher, J.P. et al., *USAF Damage Tolerant Design Handbook: Guidelines for the Analysis and Design of Damage Tolerant Aircraft Structures*, AFWAL-TR-82–3073, Air Force Wright Aeronautical Laboratories, Wright-Patterson Air Force Base, Ohio.

2.2 Yang, J-N. and Trapp, W.J., *Reliability Analysis of Fatigue-Sensitive Aircraft Structures Under Random Loading and Periodic Inspection*, Air Force Materials Laboratory Technical Report AFML-TR-74–2, Wright-Patterson Air Force Base, February 1974.

2.3 Yang, J-N. and Trapp, W.J., *Reliability Analysis of Aircraft Structures Under Random Loading and Periodic Inspection*, AIAA Journal, AIAA, Vol. 12, No. 12, 1974, pp. 1623–1630.

2.4 Yang, J-N. and Trapp, W.J., *Inspection Frequency Optimization for Aircraft Structures Based on Reliability Analysis*, Journal of Aircraft, AIAA, Vol. 12, No. 5, 1975, pp. 494–496.

2.5 Shinozuka, M., *Development of Reliability-Based Aircraft Safety Criteria: An Impact Analysis* Vol. I, AFFDL, Wright-Patterson AFB, Ohio, April 1976.

2.6 Berens, A.P. and Hovey, P.W., *Evaluation of NDE Reliability Characterization*, Air Force Wright Aeronautical Laboratories Technical Report AFWAL-TR-81–4160, Wright-Patterson Air Force Base, 1981.

2.7 Berens, A.P. and Hovey, P.W., *Flaw Detection Reliability Criteria, Vol. 1 – Method and Results*, Air Force Wright Aeronautical Laboratories Technical Report AFWAL-TR-84–4022, Wright-Patterson Air Force Base, 1984.

2.8 Yang, J-N. and Chen, S., *Fatigue Reliability of Gas Turbine Engine Components Under Scheduled Inspection Maintenance*, Journal of Aircraft, AIAA, Vol. 22, No. 5, 1985, pp. 415–422.

2.9 Yang, J-N. and Chen, S., *An Exploratory Study of Retirement-for-Cause for Gas Turbine Engine Components*, Journal of Propulsion and Power, AIAA, Vol. 2, No. 1, 1986, pp. 38–49.

2.10 Yang, J-N. and Donath, R.C., *Improving NDE Capability Through Multiple Inspections with Application to Gas Turbine Engine*, Air Force Wright Aeronautical Laboratories Technical Report AFWAL-TR-82–4111, Wright-Patterson Air Force Base, August 1982.

2.11 Yang, J-N. and Donath, R.C., *Improving NDE Reliability Through Multiple Inspections*, Review of Progress in Quantitative NDE, Eds. D.O. Thompson and D.E. Chimenti, Plenum Press, NY, Vol. 1, 1983, pp. 69–78.

2.12 Yang, J-N. and Donath, R.C., *Inspection Reliability of Components with Multiple Critical Locations*, Proceedings of the 14th Symposium on NDE, San Antonio, TX, April 19–21, 1983.

2.13 Packman, P.F., Klima, S.J., Davies, R.L., Malpani, J., Moyzis, J., Walker, W., Yee, B.G.W. and Johnson, D.P., *Reliability of Flaw Detection by Nondestructive Inspection*, ASM Metal Handbook, Vol. 11, 8th Edition, Metals Park, Ohio, 1976, pp. 214–224.

2.14 Yee, B.G.W., Chang, F.H., Coughman, J.C., Lemon, G.G. and Packman, P.F., *Assessment of*

NDE Reliability Data, NASA CR-134991, National Aeronautics and Space Administration, Lewis Research Center, Cleveland, Ohio, 1976.

2.15Cox, D.R., *The Analysis of Binary Data*, Methuen and Co., Ltd., London, 1970.

2.16Cheng, R.C.H. and Iles, T.C., *Confidence Bands for Cumulative Distribution Functions of Continuous Random Variables*, Technometrics, Vol. 25, No. 1, 1983, pp. 77–86.

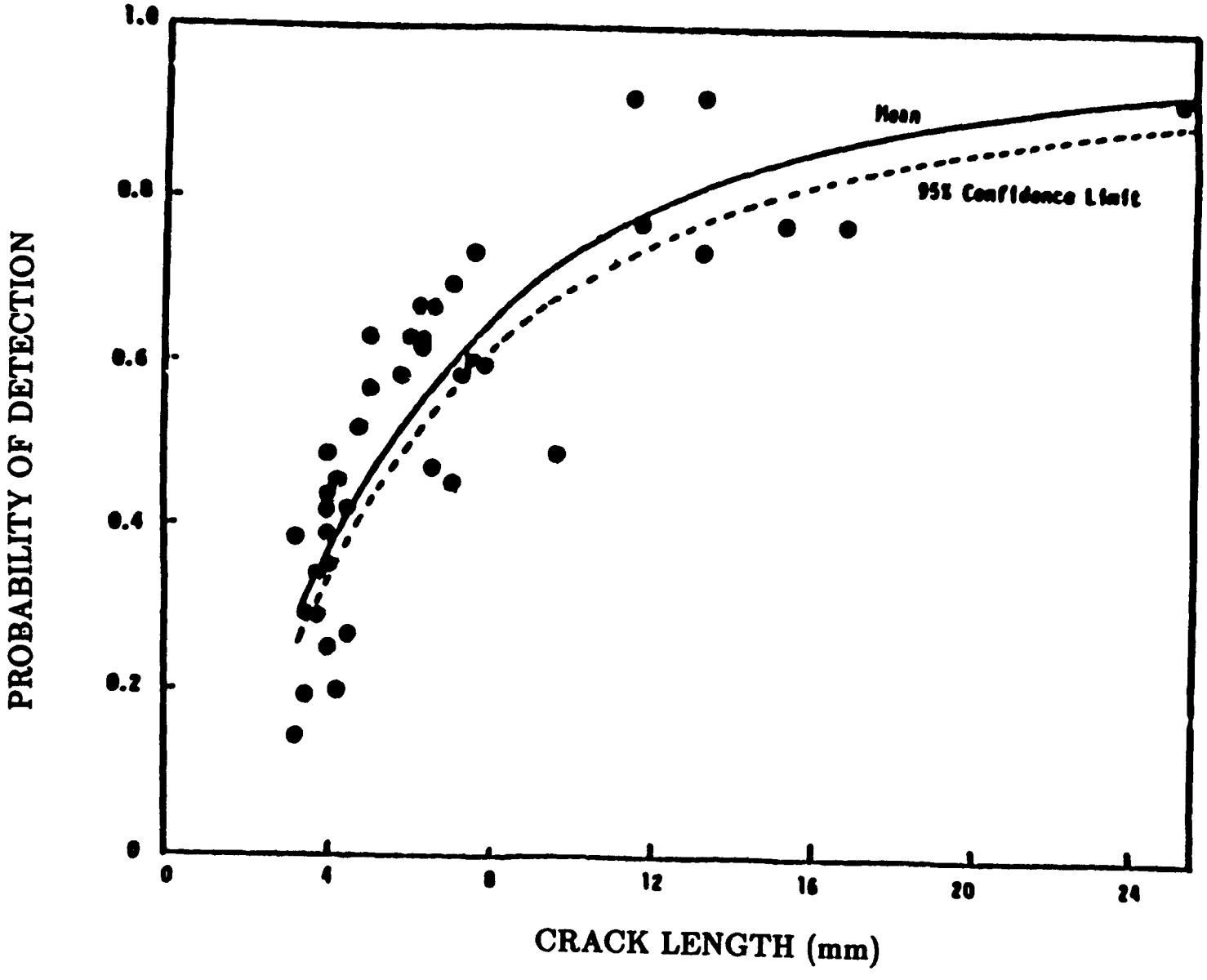

Fig. 2.1 Example Application of Log Odds-Regression Analysis.

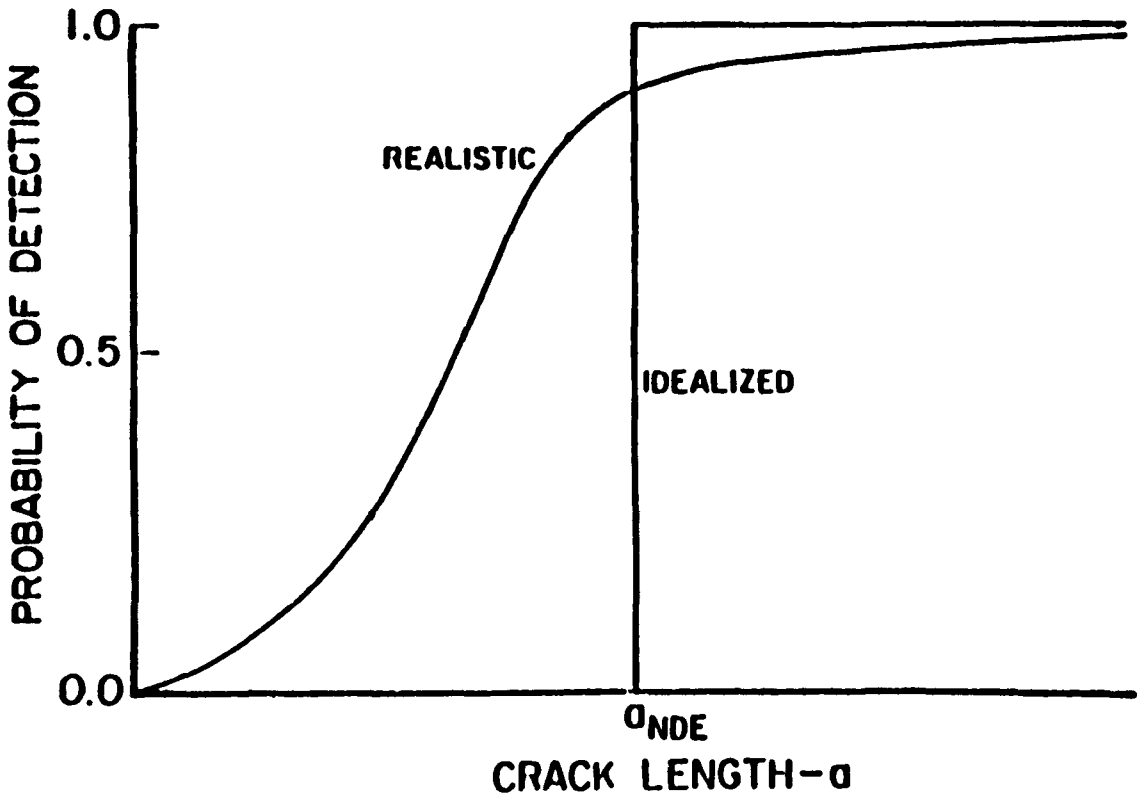

Fig. 2.2 Schematic of Probability of Detection Curves.

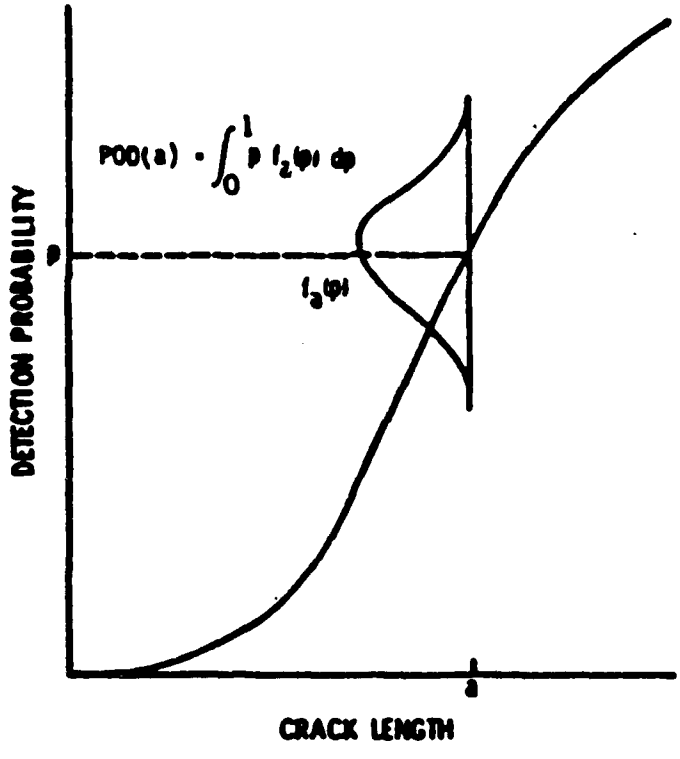

Fig. 2.3 Schematic of Probability Density Function of Crack Detection Probabilities at a Crack Length.

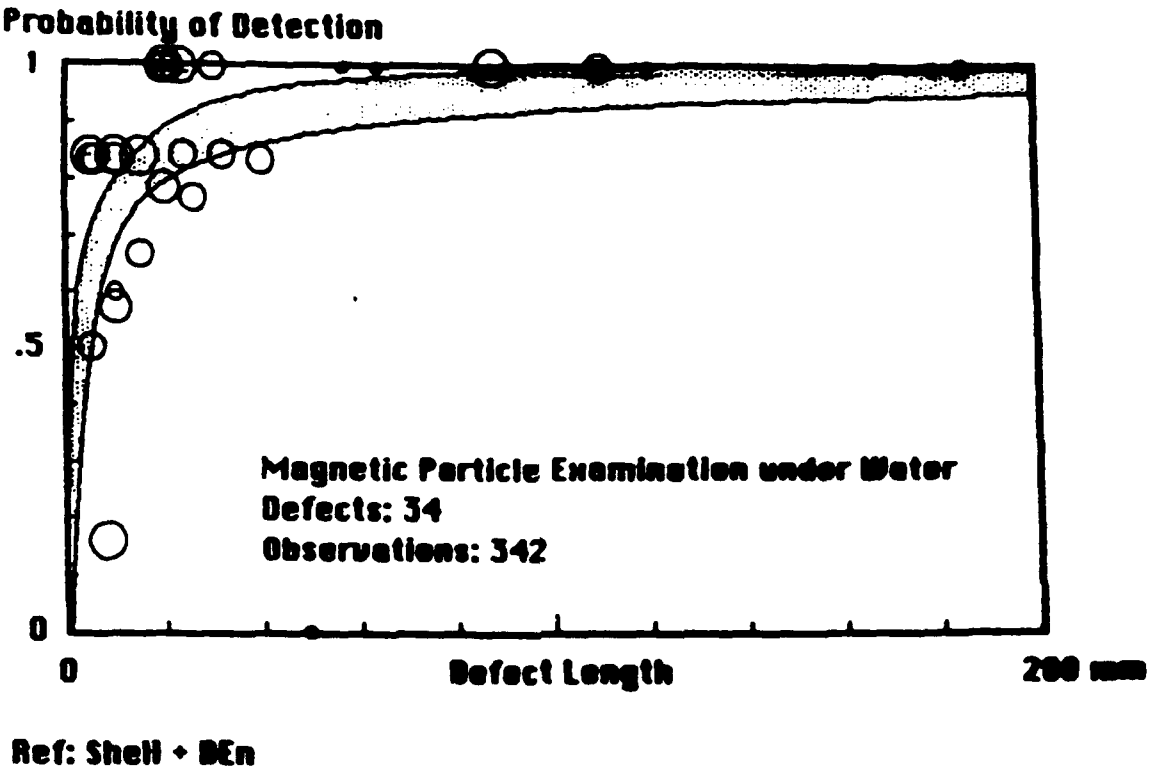

Fig. 2.4 Reliability of Magnetic Particle Examination Applied Under Water for Detection of Fatigue Cracks and Artificial Defects. Observation Points are Given with an Area Proportional to the Number of Individual Observations Contained in Each Point.

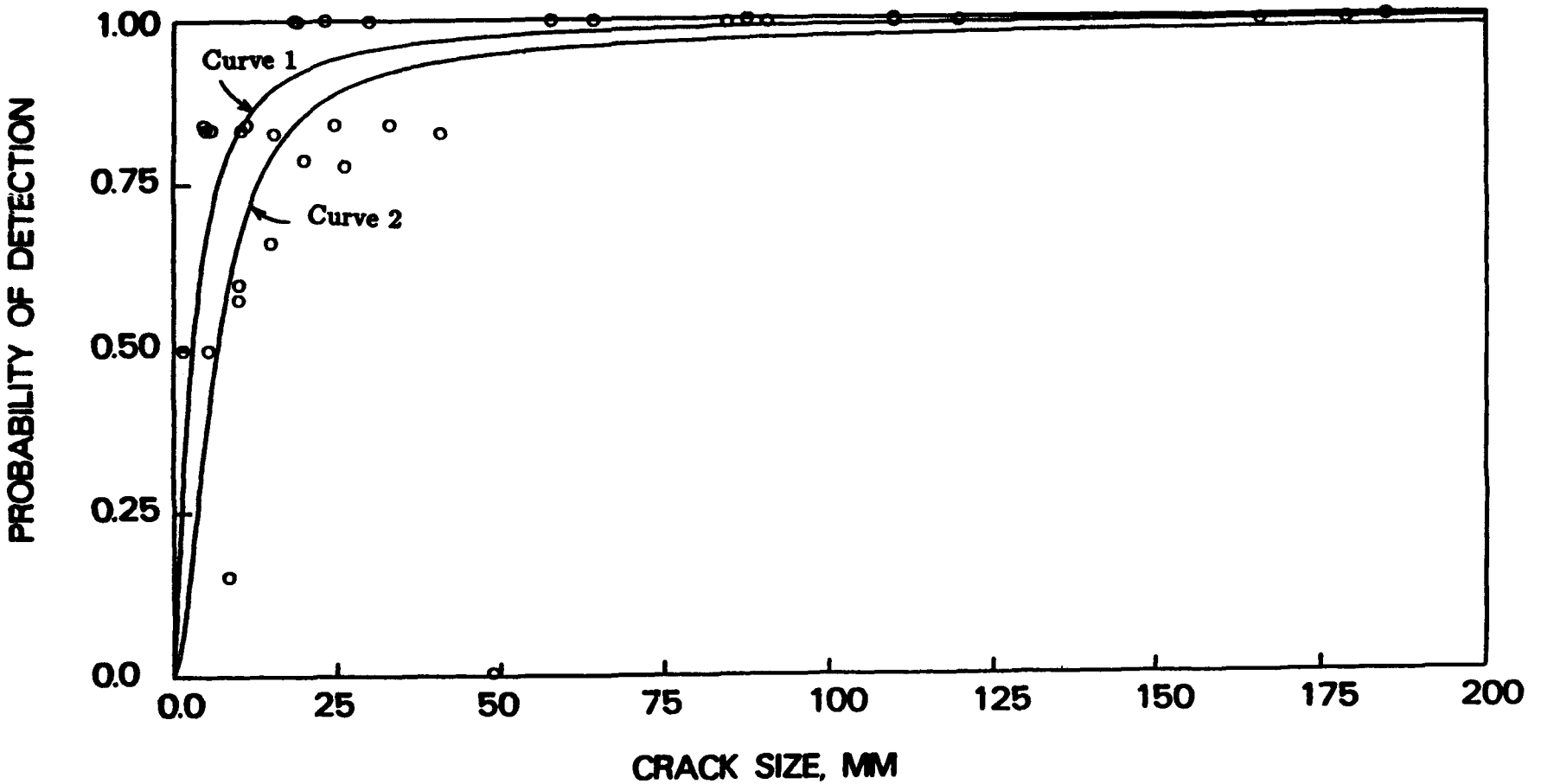

Fig. 2.5 Regression Estimate of POD Function for Pass/Fail Data with Multiple Inspections.

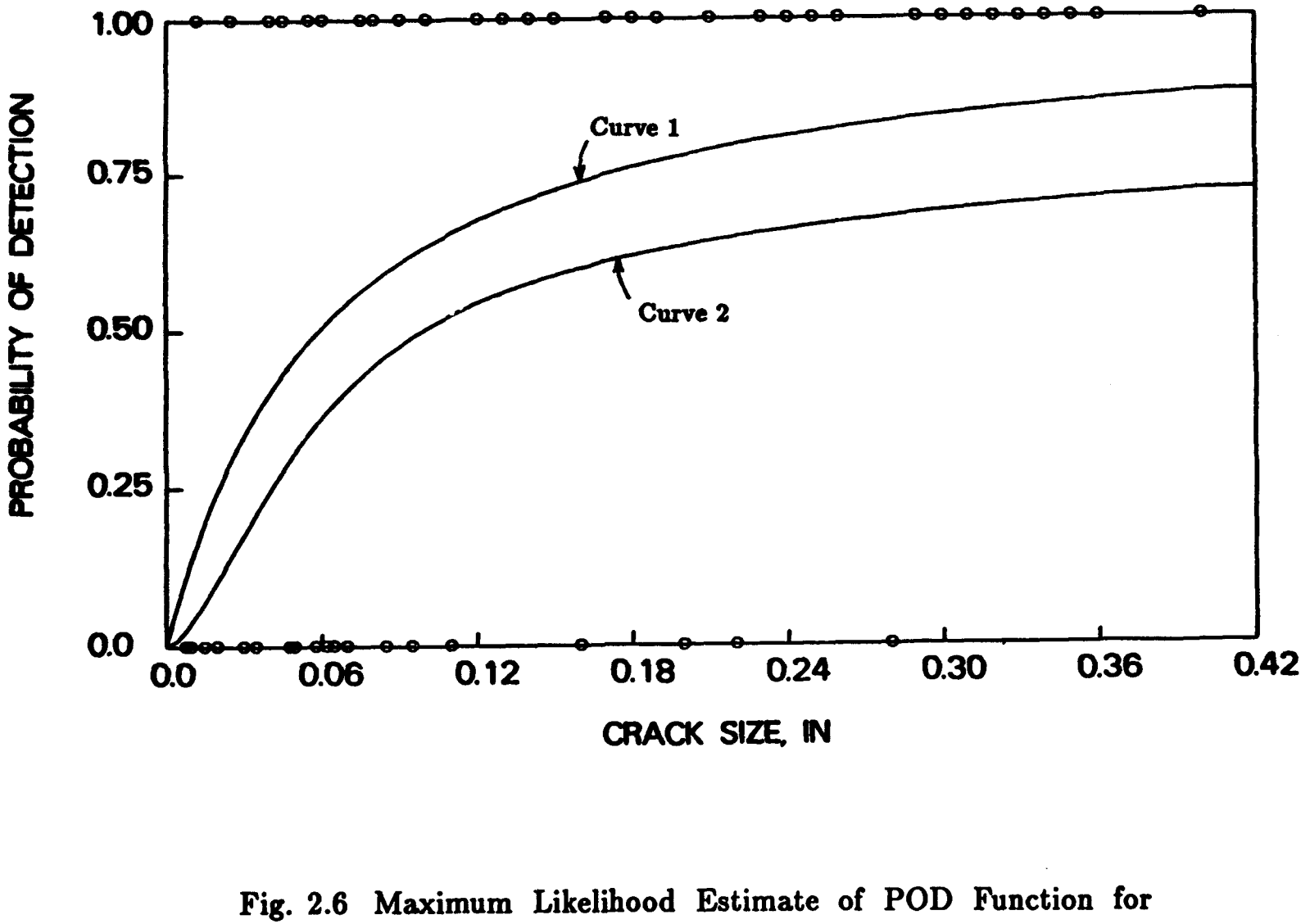

Fig. 2.6 Maximum Likelihood Estimate of POD Function for Pass/Fail Data with a Single Inspection.

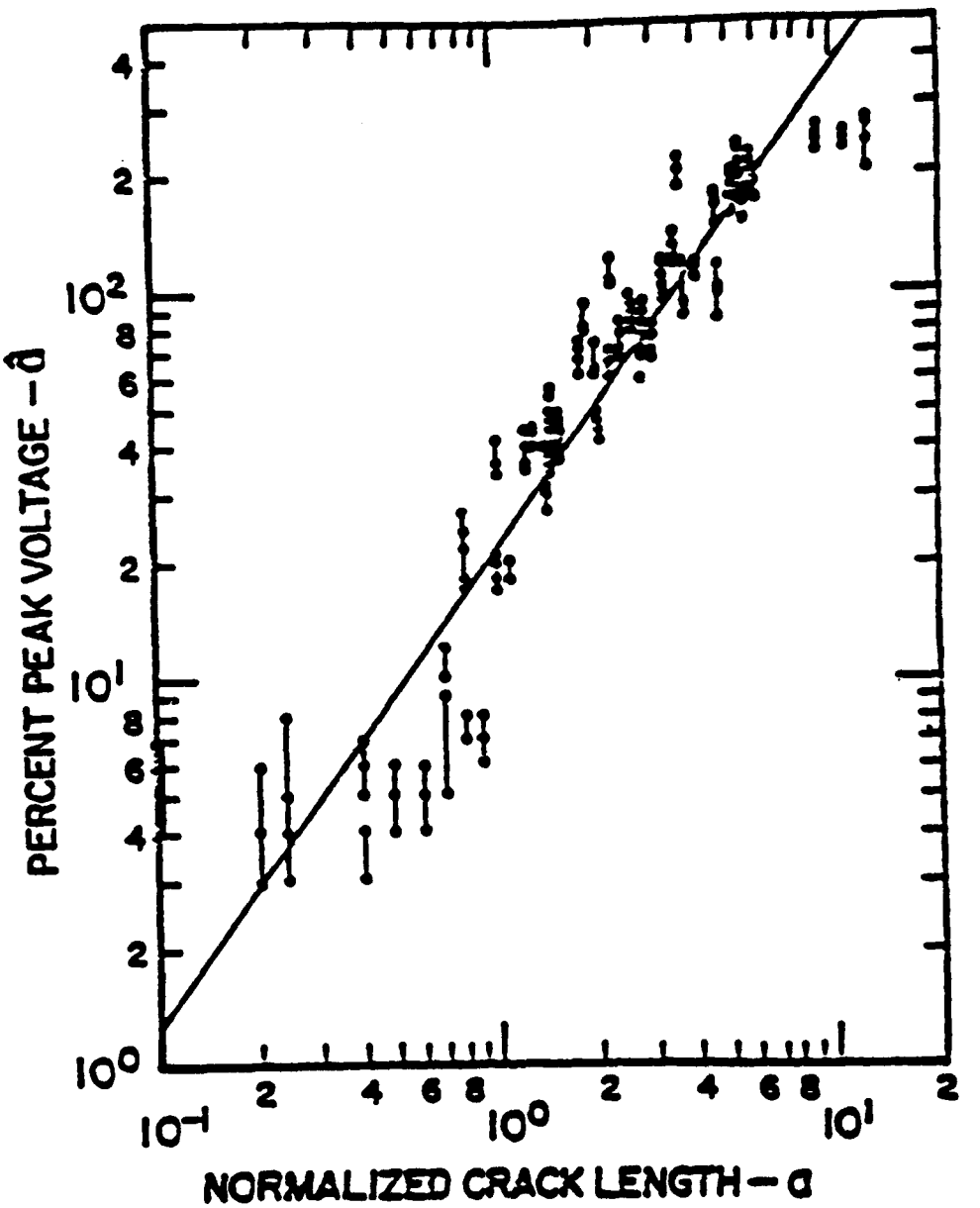

Fig. 2.7 Observed Peak Eddy Current Response Voltages From Two Measurements on Eack Crack.

III. STRUCTURAL RELIABILITY UNDER BAYESIAN INSPECTION

3.1 Introduction

After the first two introductory chapters, the third chapter constitutes the main part of this work whose basic objective is to develop a non-periodic inspection procedure for marine structures so as to maintain their reliability at a prespecified design level throughout their lifetime. In this work, the main cause of a structure's reliability decline between inspections is considered to be the formation and propagation of fatigue cracks. Fatigue is actually one of the most important problems of offshore structures located in harsh environments such as the North Sea. The problem of fatigue is further complicated by the random nature of the loading to which these structures are subjected.

Fatigue damage is considered to be initiated in a structure when the smallest size measurable crack develops, whether or not it is detected. The fatigue process in a structural member consists of crack initiation, followed by crack propagation and the resulting member strength degradation (see Fig. 3.1). Periodic inspections of fatigue-sensitive structures have been common practice in order to maintain the reliability of the structures at the desired prespecified level; if a fatigue crack is detected by inspection, the cracked component is repaired or replaced with a new member so that both the residual strength and fatigue characteristics of this component are renewed, thus increasing the overall reliability of the structure. Hence, reliability analysis of fatigue-sensitive structures under random loading and periodic inspections is of practical importance and forms the primary concern of this study.

In previous studies performed, for example, by Yang and Trapp [3.3] and Paliou and Shinozuka [3.2], the effect of periodic inspections on fatigue-sensitive structures was examined with probabilistic methods. These studies paved the way for the development of reliability-based design criteria for ocean structures involving the notion of periodic or nonperiodic inspections. However, further study is needed to deal with (a) the lack of inspection data with which statistical

analyses can be performed, (b) uncertainty in the fatigue properties of structural components, (c) difficulties in estimating the stresses acting on members due to structural complexity, (d) errors during construction, and (e) uncertainty in the detection capabilities of the various inspection techniques to be used. In fact, Itagaki and Yamamoto [3.1] analyzed the effect of non-periodic inspections using Bayesian analysis and determined the inspection interval so as to maintain the reliability of the whole structure at some prespecified design level. The present study represents a further extension of this work by Itagaki and Yamamoto in order to include such new features as the detection of a crack of a certain length. Monte Carlo simulations are carried out to verify the validity of the methodology.

Section 3.2 describes the analytical models used and the various assumptions employed in this analysis, including expressions for fatigue crack initiation time, fatigue crack propagation and failure rate. In Section 3.3, analytical interpretation of inspection results involving definition of all possible outcomes of such inspections is given. According to these definitions, the probability of occurrence of each of these outcomes and related events is presented in detail. Sections 3.4 and 3.5 are concerned with the determination of appropriate inspection intervals so that the structural reliability is kept at the desired level. For this purpose, a Bayesian approach is applied to treat the various uncertainties involved. The types of uncertainty considered in this study are those appearing in the expressions for (a) fatigue crack initiation time, (b) fatigue crack propagation rate, and (c) probability of crack detection.

Assuming prior density functions for the unknown parameters, the inspection results are used in accordance with Bayes Theorem to upgrade the prior density functions. A general formulation is given for the case where a detailed record of the entire inspection history, including repair or replacement records for each and every member, is available. Numerical simulations were carried out (see Section 3.6) to verify the validity of this Bayesian approach

3.2 Basic Assumptions

The following assumptions are made for the purposes of this study:

1. In each structural member there is only one fatigue-critical location (hotspot) where a crack can initiate.
2. All structural members are inspected immediately after initiation of service and at the time of each scheduled inspection. If a member is found not to be intact, the following action is taken:
   - If a crack is detected in a member, that member is repaired and regains its initial strength characteristics.
   - If the member is found to have failed, it is replaced by a new one.
   -
3. The entire inspection history of each member is considered to be known at the time of the current inspection.
4. For fatigue crack initiation, the time to crack initiation (TTCI), denoted by t, is assumed to be a random variable with a density function following the Weibull distribution:

$$f_c(t \mid \beta) = \frac{\alpha}{\beta} \cdot \left(\frac{t}{\beta}\right)^{\alpha-1} \cdot \exp\left[-\left(\frac{t}{\beta}\right)^{\alpha}\right] \qquad t > 0 \tag{3.1}$$

   The uncertainty in the TTCI is introduced by the scale parameter β. Hence, Eq. 3.1 indicates a Weibull density conditional to a given value of β. The shape parameter α is assumed to be deterministic for the sake of simplicity. The distribution function of the TTCI is expressed by:

$$F_c(t \mid \beta) = 1 - \exp\left[\left(\frac{t}{\beta}\right)^{\alpha}\right] \qquad t > 0 \tag{3.2}$$

5. For fatigue crack propagation, fracture mechanics theory is used to determine the length of a propagating crack under random stress. It is assumed that the crack grows in accordance with the following law:

$$\frac{da}{dt} = C_1 (\Delta K)^2 = C_1 \left(\Delta\sigma \cdot \sqrt{\pi a}\right)^2 = ca \tag{3.3}$$

with

$$c = \pi C_1 \Delta\sigma^2 \tag{3.4}$$

where a is the crack length, C_1 is a material constant, ΔK is the stress-intensity-factor fluctuation and $\Delta\sigma$ is the nominal stress fluctuation. Integrating Eq. 3.3 from the initial crack length a_0 at the TTCI = t_c, up to the current crack length $a(t - t_c)$ at time t, the following result is obtained:

$$a(t - t_c \mid c) = a_0 \exp[c(t - t_c)] \tag{3.5}$$

The uncertainty in fatigue crack propagation is introduced by parameter c, and therefore the crack length indicated by Eq. 3.5 is conditional to a given value of c.

6. The probability of detecting a fatigue crack of length a at the time of inspection is given by:

$$D(a \mid d) = 1 - \exp[-d(a - a_0)] \tag{3.6}$$

The uncertainty in the probability of crack detection is introduced by parameter d. Thus, the probability of detection shown by Eq. 3.6 is conditional to a given value of d. The minimum detectable crack length is denoted by a_0.

7. If a crack is detected in a member at the time of inspection, the crack length is assumed to be accurately measured.

8. Failure of a member occurs when random stress exceeds the strength of the member for the first time. A member can fail either before or after crack initiation. With the former, the failure rate is a constant depending only on the characteristics of the stationary random process representing the stress fluctuation at the hotspot. However, with the latter, the failure rate also depends on the crack size, on which the member's residual strength depends. Therefore, the problem of evaluating the failure rate is essentially that of estimating the first-passage failure probability with a constant or variable two-sided threshold depending on whether the member fails before or after crack initiation. The failure rates before and after crack initiation at t_c take the following forms:

Before crack initiation:

$$h(t) = h_0 = \exp(r) \tag{3.7}$$

After crack initiation:

$$h(t) = \exp[q(t - t_c) + r] \tag{3.8}$$

For the sake of simplicity, parameters r and q are assumed to be deterministic.

The reliability of a member before crack initiation during the service period from T_l to t is denoted by $U(t - T_l)$ and given by:

$$U(t - T_l) = \exp\left\{-\int_{T_l}^{t} h(\tau)\,d\tau\right\} = \exp\left\{-\int_{T_l}^{t} h_0 d\tau\right\} = \exp\left\{-\int_{T_l}^{t} \exp(r)\,d\tau\right\} \tag{3.9a}$$

or

$$U(t - T_l) = \exp\{-(t - T_l) \cdot \exp(r)\} \qquad \text{for } t \le t_c \tag{3.9b}$$

where T_l is the time of service initiation for the member under consideration; this implies that the member was repaired or replaced at the time of the l—th inspection.

The reliability of a member after crack initiation during the service period from t_c to t is denoted by $V(t - t_c)$ and given by:

$$V(t - t_c) = \exp\left\{-\int_{t_c}^{t} h(\tau)\,d\tau\right\} = \exp\left\{-\int_{t_c}^{t} \exp[q(\tau - t_c) + r]\,d\tau\right\} \tag{3.10a}$$

or

$$V(t - t_c) = \exp\left\{-\frac{1}{q}[\exp\{q(t - t_c) + r\} - \exp\{r\}]\right\} \qquad \text{for } t > t_c \tag{3.10b}$$

9. The probability of detecting member failure at the time of inspection is equal to one, if such a failure indeed exists.
10. No stress redistribution is considered in the structure after the occurrence of member failure or during crack propagation.

3.3 Possible Events at Time of Inspection

3.3.1 Definitions

At the time of the $j-$th inspection, T_j, of a certain member (with the knowledge that this member was repaired or replaced immediately as a result of the $l-$th inspection performed at time T_l $(l \leq j-1)$ or that this member initiated service at time T_l denoting the beginning of service for the structure), one of the following three events may occur:

1. $\{A : j, l\}$ = event that the member is found to have failed at the time of the $j-$th inspection T_j or equivalently, the event that failure of the member occurs during the time interval $[T_{j-1}, T_j]$.

   This event consists of the following two mutually exclusive events:

   $E_{1,j}$ = event that the member fails before crack initiation, sometime during the time interval between the two consecutive inspections at T_{j-1} and T_j.

   $E_{2,j}$ = event that the member fails after crack initiation, sometime during the time interval between the two consecutive inspections at T_{j-1} and T_j.

   It is assumed that although member failure is always detectable at the time of inspection if such a failure indeed exists, it is impossible to determine to which of these two events, $E_{1,j}$ and $E_{2,j}$, the failure belongs.

2. $\{B_1(a_j) : j, l\}$ = event that the member is found not to have failed at the time of the $j-$th inspection T_j and a crack of length between a_j and $a_j + da_j$ is detected in the member.

   Event $\{B_1(a_j) : j, l\}$ is alternatively denoted by $E_{3,j}$.

3. $\{B_2 : j, l\}$ = event that the member is found not to have failed at the time of the $j-$th inspection T_j and no crack is detected in the member.

   This event consists of the following two mutually exclusive events:

   $E_{4,j}$ = event that the member does not fail in the time interval $[T_{j-1}, T_j]$ and no crack exists in the member at the time of inspection T_j.

$E_{5,j}$ = event that the member does not fail in the time interval $[T_{j-1}, T_j]$ and a crack exists in the member which is not detected at the time of inspection T_j.

In the following, the probabilities of these events for a particular member will be evaluated in terms of the probability density and distribution functions $f_c(t \mid \beta)$ and $F_c(t \mid \beta)$ of the TTCI, reliability functions $U(t)$ and $V(t)$ and probability of crack detection $D(a \mid d \mid c)$, with the knowledge that this member was repaired or replaced as a result of the l–th inspection performed at $T_l\,(l \leq j-1)$ or that this member initiated service at time T_l denoting the beginning of service for the structure.

3.3.2 Evaluation of Probabilities of Various Events

3.3.2.1 Event $E_{1,j}$

Event $E_{1,j}$ consists of two mutually exclusive events, $E^a_{1,j}$ and $E^b_{1,j}$, which are defined as follows:

1. $E^a_{1,j}$ = event that a crack initiates after T_j, and the member fails before crack initiation sometime during the time interval $[T_{j-1}, T_j]$. The probability $P^a_{1,j}$ of event $E^a_{1,j}$ is given by:

$$P^a_{1,j} = \{1 - F_c(T_j - T_l \mid \beta)\} \cdot \{U(T_{j-1} - T_l) - U(T_j - T_l)\} \tag{3.11}$$

where $\{1 - F_c(T_j - T_l \mid \beta)\}$ denotes the probability that the crack will initiate after T_j and $\{U(T_{j-1} - T_l) - U(T_j - T_l)\}$ denotes the probability that the member will fail sometime during the time interval $[T_{j-1}, T_j]$. The latter is the conditional probability given that a crack initiates after T_j, and is found from $\{1 - U(T_j - T_l) - [1 - U(T_{j-1} - T_l)]\}$ (see Fig. 3.2a).

2. $E^b_{1,j}$ = event that a crack initiates at some time instant t in the time interval $[T_{j-1}, T_j]$ and the member fails before crack initiation sometime during the interval $[T_{j-1}, t]$.

The probability $P^b_{1,j}$ of event $E^b_{1,j}$ is given by:

$$P^b_{1,j} = \int_{T_{j-1}}^{T_j} f_c(t - T_l \mid \beta) \cdot \{U(T_{j-1} - T_l) - U(t - T_l)\}\, dt \tag{3.12}$$

where $f_c(t - T_l \mid \beta)\,dt$ denotes the probability that a crack will initiate during the time interval $[t, t + dt]$ and $\{U(T_{j-1} - T_l) - U(t - T_l)\}$ denotes the probability that the member will fail during the time interval $[T_{j-1}, t]$ (see Fig. 3.2b).

Finally, the probability $P_{1,j}$ of event $E_{1,j}$ is given by:

$$\begin{aligned} P_{1,j} &= P^a_{1,j} + P^b_{1,j} = \\ &= \{1 - F_c(T_j - T_l \mid \beta)\} \cdot \{U(T_{j-1} - T_l) - U(T_j - T_l)\} \\ &+ \int_{T_{j-1}}^{T_j} f_c(t - T_l \mid \beta) \cdot \{U(T_{j-1} - T_l) - U(t - T_l)\}\,dt \end{aligned} \tag{3.13}$$

3.3.2.2 Event $E_{2,j}$

1. Event $E_{2,j}$ consists of two mutually exclusive events, $E^a_{2,j}$ and $E^b_{2,j}$, defined in the following:

   $E^a_{2,j}$ = event that a crack initiates at some time instant t in the time interval $[T_i, T_{i+1}]$ $(i = l, ..., j-2)$ and the crack is not detected during all the subsequent inspections (from inspection at time T_{i+1} up to inspection at time T_{j-1} inclusive) and the member fails sometime during the time interval $[T_{j-1}, T_j]$.

   The probability $P^a_{2,j}$ of event $E^a_{2,j}$ is given by:

$$\begin{aligned} P^a_{2,j} = \sum_{i=l}^{j-2} \Bigg\{ &\int_{T_i}^{T_{i+1}} f_c(t - T_l \mid \beta) \cdot U(t - T_l) \cdot [V(T_{j-1} - t) - V(T_j - t)] \\ &\cdot \left[\prod_{k=i+1}^{j-1} \{1 - D(a(T_k - t \mid c) \mid d)\} \right] dt \Bigg\} \end{aligned} \tag{3.14}$$

   where $f_c(t - T_l \mid \beta)\,dt$ denotes the probability that a crack will initiate during the time interval $[t, t + dt]$, $U(t - T_l)$ denotes the probability that the member will survive during the time interval $[T_l, t]$, $\{V(T_{j-1} - t) - V(T_j - t)\}$ denotes the probability that the member will fail sometime during the time interval $[T_{j-1}, T_j]$ and

$\{1 - D(a(T_k - t \mid c) \mid d)\}$ denotes the probability that a crack will not be detected at inspection T_k (see Fig. 3.2c).

2. $E^b_{2,j}$ = event that a crack initiates at some time instant t in the time interval $[T_{j-1}, T_j]$ and the member fails sometime during the time interval $[t, T_j]$.

   The probability $P^b_{2,j}$ of event $E^b_{2,j}$ is given by:

$$P^b_{2,j} = \int_{T_{j-1}}^{T_j} f_c(t - T_l \mid \beta) \cdot U(t - T_l) \cdot [1 - V(T_j - t)]\, dt \tag{3.15}$$

   where $f_c(t - T_l \mid \beta)\, dt$ denotes the probability that a crack will initiate during the time interval $[t, t + dt]$, $U(t - T_l)$ denotes the probability that the member will survive during the time interval $[T_l, t]$ and $[1 - V(T_j - t)]$ denotes the probability that the member will fail sometime during the time interval $[t, T_j]$ (see Fig. 3.2d).

Finally, the probability $P_{2,j}$ of event $E_{2,j}$ is given by

$$\begin{aligned} P_{2,j} &= P^a_{2,j} + P^b_{2,j} = \\ &= \sum_{i=1}^{j-2} \left\{ \int_{T_i}^{T_{i+1}} f_c(t - T_l \mid \beta) \cdot U(t - T_l) \cdot [V(T_{j-1} - t) - V(T_j - t)] \right. \\ &\quad \left. \left[\prod_{k=i+1}^{j-1} \{1 - D(a(T_k - t \mid c) \mid d)\} \right] dt \right\} \\ &\quad + \int_{T_{j-1}}^{T_j} f_c(t - T_l \mid \beta) \cdot U(t - T_l) \cdot [1 - V(T_j - t)]\, dt \end{aligned} \tag{3.16}$$

3.3.2.3 Event $E_{3,j}$

Event $E_{3,j}$ is defined as follows:

$E_{3,j}$ = event that the member does not fail, but a crack of length between a_j and $a_j + da_j$ is detected at the time of the j–th inspection, T_j. Since a crack with length between

a_j and $a_j + da_j$ is found at the time of the $j-$th inspection, the time t_c of initiation of this crack can be computed from

$$a(T_j - t_c \mid c) = a_j = a_0 \cdot \exp[c(T_j - t_c)] \tag{3.17}$$

as

$$t_c = T_j - \frac{1}{c} \ln\left(\frac{a_j}{a_0}\right) \tag{3.18}$$

Then, the probability $p_{3,j}da_j$ of event $E_{3,j}$ is given by:

$$p_{3,j}da_j = p_{3,j}(a_j)\,da_j = f_c(t_c - T_l \mid \beta)\,dt_c \cdot U(t_c - T_l) \cdot V(T_j - t_c) \cdot \left[\prod_{k=l+1}^{j-1} \{1 - \delta \cdot D(a(T_k - t_c \mid c) \mid d)\}\right] \cdot D(a_j \mid c \mid d) \tag{3.19}$$

On the right-hand side of Eq. 3.19, t_c is to be replaced by the expression shown in Eq. 3.18. Similarly, on the right-hand side of Eq. 3.19, $dt_c = |dt_c/da_j|\,da_j = da_j/(ca_j)$. In this way, the right-hand side of Eq. 3.19 is given completely as a function of a_j. In Eq. 3.19, δ is given by

$$\delta = \left\{\begin{array}{l} 1 \text{ for } T_k > t_c \\ 0 \text{ for } T_k < t_c \end{array}\right\} \tag{3.20}$$

and $f_c(t_c - T_l \mid \beta)\,dt_c$ denotes the probability that a crack will initiate during the time interval $[t_c, t_c + dt_c]$, $U(t_c - T_l)$ denotes the probability that a member will survive during the time interval $[T_l, t_c]$, $V(T_j - t_c)$ denotes the probability that a member will survive during the time interval $[t_c, T_j]$, $\{1 - \delta \cdot D(a(T_k - t_c \mid c) \mid d)\}$ denotes the probability that a crack will not be detected at inspection T_k and $D(a_j \mid c \mid d)$ denotes the probability that a crack will be detected at inspection T_j (see Fig. 3.2e).

3.3.2.4 Event $E_{4,j}$

Event $E_{4,j}$ is defined as follows:

$E_{4,j}$ = event that member does not fail and no crack exists in member at time of inspection T_j.

The probability $P_{4,j}$ of event $E_{4,j}$ is given by:

$$P_{4,j} = \{1 - F_c(T_j - T_l \mid \beta)\} \cdot U(T_j - T_l) \tag{3.21}$$

where $\{1 - F_c(T_j - T_l \mid \beta)\}$ denotes the probability that a crack will initiate after T_j and $U(T_j - T_l)$ denotes the probability that a member will survive the time interval $[T_l, T_j]$.

3.3.2.5 Event $E_{5,j}$

Event $E_{5,j}$ is defined as follows:

$E_{5,j}$ = event that member does not fail, and a crack exists in the member which is not detected at the time of inspection T_j.

The probability $P_{5,j}$ of event $E_{5,j}$ is given by:

$$P_{5,j} = \sum_{i=l}^{j-1} \left\{ \int_{T_i}^{T_{i+1}} f_c(t - T_l \mid \beta) \cdot U(t - T_l) \cdot V(T_j - t) \cdot \left[\prod_{k=i+1}^{j} \{1 - D(a(T_k - t \mid c) \mid d)\} \right] dt \right\} \tag{3.22}$$

where $f_c(t - T_l \mid \beta)\,dt$ denotes the probability that a crack will initiate during time interval $[t, t + dt]$, $U(t - T_l)$ denotes the probability that a member will survive during time interval $[T_l, t]$, $V(T_j - t)$ denotes the probability that a member will survive during time interval $[t, T_j]$, and $\{1 - D(a(T_k - t \mid c) \mid d)\}$ denotes the probability that a crack will not be detected at inspection T_k (see Fig. 3.2f).

Finally, the probabilities of events $\{A : j, l\}$, $\{B_1(a_j) : j, l\}$ and $\{B_2 : j, l\}$ are given by

$$\begin{aligned} P\{A : j, l\} &= P_{1,j} + P_{2,j} \\ P\{B_1(a_j) : j, l\} &= p_{3,j}\,da_j \\ P\{B_2 : j, l\} &= P_{4,j} + P_{5,j} \end{aligned} \tag{3.23}$$

At this point, is should be noted that $P_m\{A:j,l\}$, $P_m\{B_1(a_j):j,l\}$ and $P_m\{B_2:j,l\}$ are written for $P\{A:j,l\}$, $P\{B_1(a_j):j,l\}$ and $P\{B_2:j,l\}$, respectively, in order to identify member number m.

3.4 Reliability of Member at Time Instant t* After j-th Inspection

We distinguish between the reliability of two types of members at time instant t^* after the $j-$th inspection but before the $(j+1)-$th inspection $(T_j < t^* < T_{j+1})$.

3.4.1 Members Repaired at j-th Inspection

It is known that members are replaced or repaired at the $j-$th inspection in the case of event $\{A:j,l\}$ or event $\{B_1(a_j):j,l\}$. Writing $R(t^*;\text{Repair})$ instead of $R(t^*;\text{Replacement or Repair})$ for brevity, the reliability $R(t^*;\text{Repair})$ of a member of this type is given by the sum of the following two probabilities: (a) the probability that a member will not fail during time interval $[T_j,t^*]$ and a crack will initiate after t^*; and (b) the probability that a crack will initiate during time interval $[T_j,t^*]$, but the member will not fail during the same time interval. $R(t^*:\text{Repair})$ is calculated as follows:

$$R(t^*:\text{Repair}) = \{1-F_c(t^*-T_j\mid\beta)\}\cdot U(t^*-T_j) + \int_{T_j}^{t^*} f_c(t-T_j\mid\beta)\cdot U(t-T_j)\cdot V(t^*-t)\,dt \tag{3.24}$$

where $\{1-F_c(t^*-T_j\mid\beta)\}$ denotes the probability that a crack will initiate after t^*, $U\{t^*-T_j\}$ denotes the probability that a member will survive time interval $[T_j,t^*]$, $f_c(t-T_j\mid\beta)\,dt$ denotes the probability that a crack will initiate during time interval $[t,t+dt]$, $U(t-T_j)$ denotes the probability that a member will survive time interval $[T_j,t]$ and $V(t^*-t)$ denotes the probability that a member will survive during time interval $[t,t^*]$.

3.4.2 Members Not Repaired at j-th Inspection

It is known that members are not repaired at the $j-$th inspection in the case of event $\{B_2:j,l\}$.

The reliability $R(t^*: \text{No repair})$ of a member of this type is given by the sum of the following three probabilities (written as Z) divided by $(P_{4,j} + P_{5,j})$ which represents the probability of event $\{B_2 : j, l\}$:

a. Probability that member will not fail during time interval $[T_l, t^*]$ and crack will initiate after t^*.

b. Probability that a crack will initiate during time interval $[T_j, t^*]$, but member will not fail during time interval $[T_l, t^*]$.

c. Probability that crack initiates at some time instant t during time interval $[T_i, T_{i+1}]$ $(i = l, ..., j-1)$ and this crack is not detected during all subsequent inspections (from inspection at time T_{i+1} to inspection at time T_j inclusive) and member will not fail during time interval $[T_l, t^*]$.

Hence,

$$R(t^*: \text{No repair}) = \frac{Z}{P_{4,j} + P_{5,j}} \tag{3.25}$$

In Eq. 3.25,

$$\begin{aligned} Z = {} & \{1 - F_c(t^* - T_l \mid \beta)\} \cdot U(t^* - T_l) \\ & + \int_{T_j}^{t^*} f_c(t - T_l \mid \beta) \cdot U(t - T_l) \cdot V(t^* - t)\, dt \\ & + \sum_{i=l}^{j-1} \left\{ \int_{T_i}^{T_{i+1}} f_c(t - T_l \mid \beta) \cdot U(t - T_l) \cdot V(t^* - t) \left[\prod_{k=i+1}^{j} \{1 - D(a(T_k - t \mid c) \mid d)\} \right] dt \right\} \end{aligned} \tag{3.26}$$

where $\{1 - F_c(t^* - T_l \mid \beta)\}$ denotes the probability that a crack will initiate after t^*, $U(t^* - T_l)$ denotes the probability that a member will survive time interval $[T_l, t^*]$, $f_c(t - T_l \mid \beta)\, dt$ denotes the probability that a crack will initiate during time interval $[t, t + dt]$, $U(t - T_l)$ denotes the probability that a member will survive time interval $[T_l, t]$, $V(t^* - t)$ denotes the probability that a member will survive time interval $[t, t^*]$ and $\{1 - D(a(T_k - t \mid c) \mid d)\}$ denotes the probability that a crack will not be detected at inspection T_k. Note that $R(t^*; \text{No Repair})$

indicates the probability of event A that a member survives time interval $[T_j, t^*]$ given event B that it has not been replaced or repaired at the j–th inspection. Therefore, $P\{A \cap B\} = P\{A\} \cdot P\{B \mid A\}$ where $P\{A \cap B\} = Z$, $P\{A\} = P_{4,j} + P_{5,j}$ and $P\{B \mid A\} = R(t^*; \text{No Repair})$. Equation 3.25 immediately follows from this.

3.5 Bayesian Analysis

3.5.1 Uncertain Parameters and Their Prior Density Function

In the present study, β, d and c are considered as possible sources of the uncertainty. Initially, a uniform distribution is assumed for the three uncertain parameters having the following jointly uniform density function:

$$f^0(\beta, d, c) = \frac{1}{(\beta_{\max} - \beta_{\min})(d_{\max} - d_{\min})(c_{\max} - c_{\min})} = \text{constant} \qquad (3.27)$$

where:

$$\beta_{\min} \le \beta \le \beta_{\max}$$
$$d_{\min} \le d \le d_{\max} \qquad (3.28)$$
$$c_{\min} \le c \le c_{\max}$$

3.5.2 Likelihood Function as Result of j-th Inspection

The likelihood function LF_j for the entire structure as a result of the j–th inspection is expressed as follows:

$$LF_j = \prod_{m=1}^{M} LF_j^{(m)} \qquad (3.29)$$

where $LF_j^{(m)}$ is the likelihood function as a result of the j–th inspection for member m and M is the total number of members in the structure.

For a typical member m, assume that replacement due to failure or repair due to a detected crack occurred at the time of inspections $T_{l_1}, T_{l_2}, \ldots, T_{l_r}$ where r indicates the number of times the member has been repaired or replaced before the j–th inspection, and:

$$l_1 < l_2 < \ldots < l_r < j \qquad (3.30)$$

It is pointed out that $l_1, l_2, ..., l_r$ are all known at the time of the $j-$th inspection since the whole inspection history of each member is considered to be known. Note also that:

$$l_r \leq j-1 \tag{3.31}$$

Then, the likelihood function as a result of the $j-$th inspection for member m is given by:

$$LF_j^{(m)} = P_m\{X : j, l_r\} \cdot \prod_{k=1}^{r} P_m\{Y : l_k, l_{k-1}\} \tag{3.32}$$

It is noted that $l_1, l_2, ..., l_r$ as well as r usually take certain values unique to each member.

In Eq. 3.32, X stands for either A or $B_1(a_j)$ or B_2 depending on the result of the $j-$th inspection for member m. Specifically, if at the time of the $j-$th inspection, member m is found to have failed, then X stands for A; if member m is found to have a crack of length between a_j and $a_j + da_j$, then X stands for $B_1(a_j)$ and if member m is found intact, then Xstands for B_2. Also in Eq. 3.32, Y stands for either A or $B_1(a_{l_k})$ depending on the result of the l_k—th inspection for member m. Specifically, if at the time of the l_k—th inspection, member m is found to have failed, then Y stands for A and if member m is found to have a crack of length between a_{l_k} and $a_{l_k} + da_{l_k}$, then Y stands for $B_1(a_{l_k})$. Finally, for the case where member m is found intact at all inspections prior to the $j-$th, the product appearing in Eq. 3.32 is set equal to 1 and Eq. 3.32 takes the form:

$$LF_j^{(m)} = P_m\{X : j, l_0\} \tag{3.33}$$

Note that l_0 denotes the time of initiation of service for the structure.

3.5.3 Posterior Joint Density Function of Uncertain Parameters

The posterior joint density function of the three uncertain parameters immediately after the $j-$th inspection is given by:

$$f^j(\beta, d, c) = \frac{LF_j f^0(\beta, d, c)}{\int_{\beta_{\min}}^{\beta_{\max}} \int_{d_{\min}}^{d_{\max}} \int_{c_{\min}}^{c_{\max}} (\text{Numerator})\, d\beta d(d)\, dc} \tag{3.34}$$

3.5.4 Reliability of Entire Structure at Time t*

The reliability of the entire structure consisting of M members at time t^* after the $j-$th inspection is denoted by $\overline{R_M}(t^*)$ and is given by:

$$\overline{R_M}(t^*) = \int_{\beta_{\min}}^{\beta_{\max}} \int_{d_{\min}}^{d_{\max}} \int_{c_{\min}}^{c_{\max}} R_M(t^* \mid \beta, c, d)\, f^j(\beta, c, d)\, d\beta d(d)\, dc \tag{3.35}$$

where:

$$R_M(t^* \mid \beta, c, d) = \left\{ \prod_{m=1}^{M_1} R_m(t^* : \text{Repair}) \right\} \left\{ \prod_{m=1}^{M_2} R_m(t^* : \text{No repair}) \right\} \tag{3.36}$$

where M_1 = number of members being repaired or replaced at the $j-$th inspection, M_2 = number of members found intact at the $j-$th inspection, and $M_1 + M_2 = M$. In Eq. 3.36, $R_m(t^* : \text{Repair})$ and $R_m(t^* : \text{No Repair})$ are identical with the reliabilities $R(t^* : \text{Repair})$ and $R(t^* : \text{No Repair})$ defined in Eqs. 3.24 and 3.25, respectively. The subscript m is used to indicate that these reliabilities are associated with member m. Furthermore, the dependence of $R_m(t^* : \text{Repair})$ and $R_m(t^* : \text{No Repair})$ as implied in Eqs. 3.24 and 3.26 has not been explicitly shown for the sake of brevity.

3.5.5 Time T_{j+1} for (j+1)-th Inspection

If the reliability of the entire structure is specified to be not less than a value R_{design}, find t^* such that:

$$\overline{R_M}(t^*) \geq R_{\text{design}} \tag{3.37}$$

Then the time T_{j+1} of the $(j+1)-$th inspection is found as the minimum value of t^* which satisfies the above equation.

3.6 Numerical Example

Numerical simulations have been carried out in order to verify the validity and effectiveness of Bayesian analysis to determine appropriate inspection intervals and true values of uncertain parameters. The structure used in this study is assumed to have 100 members (M = 100). Its

design service life is 25 years and the desired minimum reliability level of the entire structure throughout its service life is set equal to 0.80 ($R_{\text{design}} = 0.80$). In general, three uncertain parameters have been considered: β, d and c. Four cases have been worked out according to the number of uncertain parameters involved in each one: three cases involving two uncertain parameters each (Case 1: β and d are uncertain, Case 2: β and c are uncertain and Case 3: d and c are uncertain) and one case involving all three uncertain parameters (Case 4: β, d and c are uncertain). The true values of the uncertain parameters as well as their assumed ranges are shown in Table 3.1, along with the values of the deterministic parameters appearing in the problem. According to these values, the probability density function of the TTCI is plotted in Fig. 3.3, the law of crack propagation in Fig. 3.4, the probability of crack detection in Fig. 3.5 and the failure rate and reliability curves before and after crack initiation in Fig. 3.6. As an example of POD curves obtained from actual data, Fig. 3.7 displays the 50% (upper curve) and 95% (lower curve) confidence level curves fitted to data obtained from magnetic particle examination under water for detection of fatigue cracks and artificial defects (compare to Fig. 3.5). Figure 3.8 shows the failure rate after crack initiation according to Ref. 3.2 (compare to Fig. 3.6).

Before dealing with the above-mentioned four cases involving uncertain parameters, the particular case where all three uncertain parameters (β, d and c) assume their true values is examined. The inspection schedule resulting from one simulation is displayed in Table 3.2 while the corresponding structural reliability for the entire structure is plotted in Fig. 3.9. The results shown in Table 3.2 and Fig. 3.9 are obtained in the following way. Equations 3.24 and 3.25 are used to calculate $R_M(t^* \mid \beta, c, d)$ given by Eq. 3.36. In this case, since all three uncertain parameters assume their true values, no Bayesian upgrading is needed. Then, the time T_{j+1} for the $(j+1)$-th inspection is calculated by replacing $\overline{R_M}(t^*)$ appearing in Eq. 3.37 with $R_M(t^* \mid \beta, c, d)$. Parameters β, c and d appearing in the expression for $R_M(t^* \mid \beta, c, d)$ are set equal to their true values shown in Table 3.1.

Fifty simulations are performed for each of the four cases involving uncertain parameters. The results of one simulation for each case are displayed in Tables 3.3–3.6. These results include

the inspection schedule, number of failed members and number and length of detected cracks. The corresponding structural reliabilities for the entire structure are plotted in Figs. 3.10–3.13. The results shown in Tables 3.3–3.6 and Figs. 3.10–3.13 are obtained in the following way. Equations 3.24 and 3.25 are used again to calculate $R_M(t^* \mid \beta, c, d)$ given by Eq. 3.36. In this case, since uncertain parameters are considered, Bayesian upgrading is needed. This upgrading is carried out by using Eq. 3.34 to compute $f^j(\beta, c, d)$ in Eq. 3.35. After having calculated $\overline{R_M}(t^*)$ according to Eq. 3.35, the time T_{j+1} for the $(j+1)$-th inspection is calculated using Eq. 3.37. Finally, the corresponding posterior joint density functions of the uncertain parameters after the fifth and tenth inspections are plotted in Figs. 3.14–3.16 for cases 1, 2 and 3 respectively. In these figures, it can be easily seen that for the specific simulations considered, the modal values of the posterior joint density functions coincide with the true values of the uncertain parameters after ten inspections. Unfortunately, such a plot cannot be given for case 4, since it involves three uncertain parameters.

The statistics of the modal values of the posterior joint density functions after five and ten inspections are shown in Table 3.7 for the four cases examined. Finally, the average inspection frequency during the twenty-five years of design service life is displayed in Table 3.8 for the four cases examined. It should be noted that the statistics appearing in Tables 3.7 and 3.8 are calculated from the results of the fifty simulations performed.

3.7 Structures With Members Subjected To Different Stress Levels

3.7.1 Introduction

The structures considered in Sections 3.2–3.6 consisted of structural components subjected to the same level of stress intensity. In this chapter, however, the structures are assumed to consist of three classes of components: class A components subjected to the highest stress level A, class B components subjected to stress level B and class C components subjected to stress level C where $A > B > C$.

3.7.2 Bayesian Analysis

The reliability of the group of structural components subjected to stress intensity level J at time t^* after the $j-$th inspection is denoted by $\overline{R_{M,J}}(t^*)$ and is given by:

$$\overline{R_{M,J}}(t^*) = \int_{\beta_{Jmin}}^{\beta_{Jmax}} \int_{d_{min}}^{d_{max}} \int_{c_{Jmin}}^{c_{Jmax}} R_{M,J}(t^* \mid \beta_J, d, c_J) \cdot f_J^j(\beta_J, d, c_J)\, d\beta_J d(d)\, dc_J \tag{3.38}$$

where $J = A, B, C$ and:

$$R_{M,J}(t^* \mid \beta_J, d, c_J) = \left\{ \prod_{m=1}^{M_{1J}} R_{mJ}(t^*\text{:Repair}) \right\} \left\{ \prod_{m=1}^{M_{2J}} R_{mJ}(t^*\text{:No Repair}) \right\} \tag{3.39}$$

where M_{1J} = number of members of group J being replaced or repaired at the $j-$th inspection, M_{2J} = number of members of group J found intact at the $j-$th inspection, and $M_{1J}+M_{2J} = M_J$ = number of members in group J. The posterior joint density function of the three uncertain parameters of group J immediately after the $j-$th inspection is given by:

$$f_J^j(\beta_J, d, c_J) = \frac{LF_{jJ} \times f_J^0(\beta_J, d, c_J)}{\int_{D_J} \int \int (\text{Numerator})\, d\beta_J d(d)\, dc_J} \tag{3.40}$$

Therefore, the structural reliability of the entire structure can be estimated as:

$$\overline{R_M}(t^*) = \prod_{J=A,B,C} \overline{R_{M,J}}(t^*) \tag{3.41}$$

Time T_{j+1} of the $(j+1)$–th inspection can then be estimated with the aid of Eq. 3.37.

3.7.3 Parameter Values

The numerical values of the various parameters appearing in the analytical model are assumed to be the same as those chosen in the previous chapter, with the obvious exception of parameters that depend on the stress intensity level.

In the numerical analysis that follows, it is assumed that the stress intensity characteristics of the three groups of structural components are given by:

Stress intensity level	A	B	C
Stress	S	0.9S	0.8S
Stress range	$\Delta\sigma$	$0.9\Delta\sigma$	$0.8\Delta\sigma$

On the basis of the above table, the following assumptions are made for those parameter values that depend on the stress intensity level:

a. Scale Parameter β in TTCI Distribution:

If $\beta = 30$ years under a cyclic load with amplitude $\Delta\sigma$, the values of β for cyclic loads with amplitudes $0.9\Delta\sigma$ and $0.8\Delta\sigma$ are estimated to be 45 years and 65 years respectively:

Stress intensity level	A	B	C
β (years)	30	45	65

b. Coefficient c in Crack Propagation Law:

According to Eq. 3.3,

$$\frac{da}{dt} = C_1 (\Delta K)^b = C_1 \left(\Delta\sigma\sqrt{\pi a}\right)^b = c \cdot a \tag{3.42}$$

where $b = 2$ and $c = \pi C_1 (\Delta\sigma)^2$. Therefore, c is proportional to $(\Delta\sigma)^2$ and hence,

Stress intensity level	A	B	C
c	0.6	$0.486 = 0.9^2 \times 0.6$	$0.384 = 0.8^2 \times 0.6$

c. Parameters r and q in Failure Rate Expressions:

To be rigorous, the values of parameters r and q for different stress levels must be obtained by evaluating the crossing rate of appropriate threshold values of the response stress process. Since in the present study no specific dynamic system is considered for a response analysis and since emphasis is placed on the development of a Bayesian method for nondestructive inspection procedures, the values shown in the following table are assumed for r and q. Note that r is proportional to the stress intensity level and q is proportional to its square.

Stress intensity level	A	B	C
r	- 7.5	$-8.25 = 1.1 \times (-7.5)$	$-9.0 = 1.2 \times (-7.5)$
q	0.9	$0.729 = 0.9^2 \times 0.9$	$0.576 = 0.8^2 \times 0.9$

The parameter values for β, c, r, and q shown in the previous three tables will be used for Monte Carlo simulation study.

3.7.4 Numerical Example

Numerical simulations have been carried out in order to verify the validity and effectiveness of Bayesian analysis to determine inspection intervals and true values of uncertain parameters. The structure used in this study is assumed to have 100 members (M_T = 100). Of the total number of 100 members, 20 are subjected to stress intensity level A, 30 to stress intensity level B and 50 to stress intensity level C.

The design service life is 25 years and the desired minimum reliability level of the entire structure throughout its service life is set equal to 0.80 (R_{design} = 0.80).

Only one case involving two uncertain parameters (specifically β and c) is examined now. The true values of the uncertain parameters as well as their assumed ranges are shown in Table 3.9, along with the values of the deterministic parameters appearing in the problem.

Before dealing with the above-mentioned case involving two uncertain parameters, the particular case where both uncertain parameters (β and c) assume their true values is examined. The inspection schedule resulting from one simulation is displayed in Table 3.10, while the corresponding structural reliability for the entire structure and for the three stress intensity level groups is plotted in Fig. 3.17.

Fifty simulations are now performed for the case involving the two uncertain parameters β and c. The results of one of these simulations are displayed in Table 3.11. These results include the inspection schedule, number of failed members in each stress intensity level group, and number and length of detected cracks in each stress intensity level group. The corresponding

structural reliabilities for the entire structure and for the three stress intensity level groups are plotted in Fig. 3.18. Finally, the corresponding posterior joint density functions of the two uncertain parameters after the third and sixth inspection are plotted in Fig. 3.19 for the three stress intensity level groups, A, B, and C. The estimation of the true values of uncertain parameters β and c immediately after the sixth inspection for structural components under stress intensity level A is accomplished reasonably well. This is due primarily to the fact that 8 cracks were found during the first six inspections. It should be noted that the estimation is considered reasonable in the sense that a distinct mode emerges at a location close to the true values of β and c. On the other hand, the same did not apply to structural components under stress intensity levels B and C for which only 7 and 3 cracks were respectively found. In all cases, however, the posterior probability density function after the sixth inspection indicates a mode located closer to the true location than after the third inspection.

The statistics of the modal values of the posterior joint density functions after three, six and seven inspections are shown in Table 3.12. These statistics are based on Monte Carlo simulations with a sample size equal to 50. Finally, the average number of inspections required to maintain the specified reliability level for 25 years is equal to 6.8, based on Monte Carlo simulations with a sample size equal to 50. This value of 6.8 should be compared with 6.0 which is the number of inspections required when the true values of β and c are known (see Table 3.13).

3.8 Future Work

The following five areas require further study:

a. In this work, the three uncertain parameters β, c, and d were considered to be uncorrelated. However, there is strong evidence that β, c, and d are in reality correlated to each other. Therefore, the statistical correlation among β, c, and d and the influence of this correlation on the obtained results require further study. Another part of future work concerning parameters β, c, and d is to examine their sensitivity to the obtained results;

b. The effect of the form of certain POD curves on the reliability of marine structures throughout their service life requires further study. A comparison has to be made among several established POD curves in the aerospace industry, in order to assess their relative influence on the reliability of marine structures subjected to non-periodic inspections. In this way, more reliable POD curves can be established for marine structures;

c. The cost-effectiveness of the proposed method of non-periodic inspections based on Bayesian analysis requires further study. Specifically, a cost-benefit analysis can be performed taking into consideration the cost of the non-periodic inspection procedure and the increased level of reliability for the structure. These results have to be compared with the results of cost-benefit analysis associated with the standard periodic inspection procedure;

d. Verification of the proposed methodology using actual data from inspections of marine structures is one of the most important tasks of future work. This task can be accomplished by taking advantage of already completed inspections in marine structures to determine whether these structures actually maintained a prespecified reliability level throughout their life;

e. The failure rate expression after crack initiation should at least be validated by Monte Carlo simulation utilizing the crack propagation law and uncontrolled crack growth condition based on fracture mechanics theory under various random stress histories consistent with the stress intensity factor fluctuation considered.

REFERENCES

3.1 Itagaki, H. and Yamamoto, N. (1985), *Bayesian Analysis of Inspection on Ship Structural Members*, Proceedings of ICOSSAR '85, pp. III-533 — III-542.

3.2 Paliou, C., Shinozuka, M. and Chen, Y.N., (1987), *Reliability and Durability of Marine Structures*, Journal of Structural Engineering, ASCE, Vol. 113, No. 6, pp. 1297–1314.

3.3 Yang, J-N. and Trapp, W.J. (1974), *Reliability Analysis of Aircraft Structures Under Random Loading and Periodic Inspections*, AIAA Journal, Vol. 12, No. 12, pp. 1623–1630.

Table 3.1 Parameter Values of Numerical Example.

Item		True value	Assumed range
Design life		25 years	---
Minimum structural reliability required	R_{design}	0.8	---
Total number of structural members	M	100	---
Parameters in PDF of TTCI	α	2.0	---
	β	30 years	20 - 40
Parameter in crack propagation	c	0.6	0.4 - 0.6
Initial crack length	a_0	10 mm (0.4 in)	---
Parameter in POD	d	0.01	0.002 - 0.018
Parameters in failure rate	r	-7.5	---
	q	0.9	---

Table 3.2 **Inspection Schedule for the Case Where All Uncertain Parameters Assume Their True Values ($\beta = 30$, $d = 0.01$ and $c = 0.6$).**

Inspection No.	Inspection time : T (years)
1	4.9
2	7.9
3	10.1
4	12.1
5	13.9
6	15.7
7	17.4
8	19.0
9	20.6
10	22.1
11	23.6

Table 3.3 **Results for Case 1 (Uncertain Parameters : β and d).**

Inspection No.	Inspection time : T (years)	No. of failed members	No. of detected cracks	Detected crack length (mm)
1	5.0	1(b)	1	22
2	7.9	0	1	42
3	10.1	0	4	189,189,124, 23
4	12.1	0	1	1215,
5	13.5	0	3	117, 29, 25
6	15.2	0	4	110,110, 54, 98
7	17.0	0	7	16,241, 29, 13,465, 98, 21
8	18.7	1(a)	6	64,178,168,104, 42,117
9	20.3	0	4	68,124,241, 45
10	21.9	0	3	149,140,124
11	23.5	0	4	628,189,227,158
12	24.9	0	6	168, 98, 64, 57, 42,306

(a) : Failure after crack initiation
(b) : Failure before crack initiation

1 in = 25.4 mm

Table 3.4 Results for Case 2 (Uncertain Parameters : β and c).

Inspection No.	Inspection time : T (years)	No. of failed members	No. of detected cracks	Detected crack length (mm)
1	5.0	1(b)	1	22
2	7.8	0	1	40
3	9.6	0	3	140,140, 92
4	11.2	0	1	708
5	13.4	0	3	33,168, 11
6	15.3	0	4	117,345, 87, 87
7	17.2	0	8	366,178, 72, 33, 14,227,525, 23
8	19.0	1(a)	7	42,201,124,110, 51, 21,140
9	20.5	0	5	189,140, 26, 61, 54
10	22.0	0	3	189, 29, 54
11	23.5	0	4	798,189,227,389

(a) : Failure after crack initiation
(b) : Failure before crack initiation

1 in = 25.4 mm

Table 3.5 Results for Case 3 (Uncertain Parameters : d and c).

Inspection No.	Inspection time : T (years)	No. of failed members	No. of detected cracks	Detected crack length (mm)
1	4.9	1(b)	1	21
2	7.9	0	1	42
3	9.8	0	3	158,158,104
4	11.6	0	1	900
5	13.2	0	3	21,149, 48
6	15.0	0	4	288, 98, 48, 87
7	16.8	0	5	288,213,213, 26, 87
8	18.6	1(a)	8	61,168,158, 98, 87, 40, 16,110
9	20.4	0	5	98,132, 98, 57,158
10	22.2	0	6	213,366, 87,178, 72,158
11	23.9	0	3	54,288,168

(a) : Failure after crack initiation
(b) : Failure before crack initiation

1 in = 25.4 mm

Table 3.6 Results for Case 4 (Uncertain Parameters : β, d and c).

Inspection No.	Inspection time : T (years)	No. of failed members	No. of detected cracks	Detected crack length (mm)
1	5.0	1(b)	1	22
2	7.8	0	1	40
3	9.6	0	3	140,140, 92
4	11.2	0	1	708
5	12.9	0	1	124
6	14.7	0	5	82,241, 82, 61, 61
7	16.6	0	8	124, 51,227,158,366, 77, 12, 33
8	18.4	1(a)	4	37,140, 87, 48
9	20.1	0	6	82,149,110,213, 82, 42
10	21.8	0	6	168, 26, 68, 82,525,110
11	23.5	0	5	42,389,158,132,366

(a) : Failure after crack initiation
(b) : Failure before crack initiation

1 in = 25.4 mm

Table 3.7 Statistics of Modal Values of the Posterior Joint Density Functions of Uncertain Parameters (True Values : $\beta = 30$, $d = 0.01$ and $c = 0.6$; Number of Simulations = 50)

1. The Fifth Inspection

Mean

Case	β	d	c
1	31.6	0.0112	---
2	32.1	---	0.622
3	---	0.0109	0.616
4	32.2	0.0121	0.617

Standard deviation

Case	β	d	c
1	4.23	0.000354	---
2	4.10	---	0.0884
3	---	0.000361	0.0924
4	4.47	0.000382	0.0976

COV

Case	β	d	c
1	0.134	0.292	---
2	0.128	---	0.142
3	---	0.331	0.150
4	0.139	0.316	0.158

2. The Tenth Inspection

Mean

Case	β	d	c
1	31.4	0.0114	---
2	31.1	---	0.606
3	---	0.0116	0.635
4	31.5	0.0122	0.636

Standard deviation

Case	β	d	c
1	2.83	0.000238	---
2	2.84	---	0.0646
3	---	0.000280	0.0801
4	2.92	0.000303	0.0845

COV

Case	β	d	c
1	0.0902	0.209	---
2	0.0913	---	0.107
3	---	0.241	0.126
4	0.0926	0.248	0.133

Table 3.8 Average Inspection Frequency During 25 years (Number of Simulations = 50)

Case	Frequency
1	11.4
2	11.6
3	11.6
4	11.4
True value	11

Item		Model value		
Design life (years)		25		
Minimum structural reliability Required	R_{design}	0.8		
Stress intensity level		A	B	C
Stress		S	0.9S	0.8S
Stress range		$\Delta\sigma$	$0.9\Delta\sigma$	$0.8\Delta\sigma$
Number of structural members (Total : $M_T = 100$)	M	20	30	50
Parameters in PDF of TTCI				
α		2.0	2.0	2.0
β (years)	True value	30	45	65
	Assumed range	(20-40)	(35-55)	(55-75)
Parameter in crack propagation				
b		2.0	2.0	2.0
c	True value	0.6	0.486	0.384
	Assumed range	(0.4 - 0.8)	(0.286 - 0.686)	(0.184 - 0.584)
Initial crack length	a_0 mm(in)	10 (0.4)	10 (0.4)	10 (0.4)
Parameter in POD	d	0.01	0.01	0.01
Parameter in failure rate	r	-7.5	-8.25	-9
	q	0.9	0.729	0.576

Table 3.9 Parameter Values of Numerical Example
[Case 2 Uncertain Parameters : β and c]

Inspection No.	Inspection time : T (years)
1	8.3
2	12.1
3	15.3
4	18.2
5	20.9
6	23.6

Table 3.10 Inspection Schedule for True Value

Inspection No.	Inspection time : T (years)	No. of failed members	No. of detected cracks	Detected crack length (mm)
1	8.2	0	A[1], B[1]	A[132], B[55]
2	11.6	0	A[2]	A[11,213]
3	14.2	0	A[1]	A[82]
4	16.6	0	B[3], C[1]	B[160,168,70], C[178]
5	19.1	0	A[2], B[1]	A[57,255], B[138]
6	21.5	C[1] (a)	A[2], B[2], C[2]	A[132,98], B[63,365], C[131,165]
7	23.9	0	A[3], C[1]	A[35,752,42], C[74]

Stress Intensity Level : A, B and C

1 in = 25.4 mm

(a) : Failure after crack initiation

(b) : Failure before crack initiation

Table 3.11 Inspection Schedule and Result on Failure and Detected Crack

[Case 2 Uncertain Parameters : β and c]

1. The Third Inspection

Mean

	β	c
A	30.6	0.599
B	45.4	0.484
C	65.2	0.371

Standard deviation

	β	c
A	5.65	0.112
B	6.37	0.118
C	6.62	0.121

COV

	β	c
A	0.185	0.188
B	0.140	0.244
C	0.102	0.327

No. of Simulations = 50

2. The Sixth Inspection

Mean

	β	c
A	30.5	0.602
B	45.4	0.505
C	64.8	0.411

Standard deviation

	β	c
A	4.59	0.0962
B	5.72	0.1010
C	6.34	0.0974

COV

	β	c
A	0.151	0.160
B	0.126	0.200
C	0.0979	0.237

No. of simulations = 50

3. The Seventh Inspection

Mean

	β	c
A	30.4	0.586
B	45.3	0.486
C	65.0	0.410

Standard deviation

	β	c
A	4.53	0.0948
B	5.61	0.1010
C	6.26	0.0967

COV

	β	c
A	0.149	0.162
B	0.124	0.208
C	0.0964	0.236

No. of simulations = 35

Table 3.12 Statistics of Modal Value for Posterior Joint Probability Density of Uncertain Paramaters

[Case 2 Uncertain Parameters : β and c]

True Value (β, c) = { A(30, 0.6), B(45, 0.486), C(65, 0.384) }

Case	Frequency
2	6.8
True value	6

Table 3.13 Average Inspection Frequency during 25 years

[Case 2 Uncertain Parameters : β and c
Number of Simulations = 50]

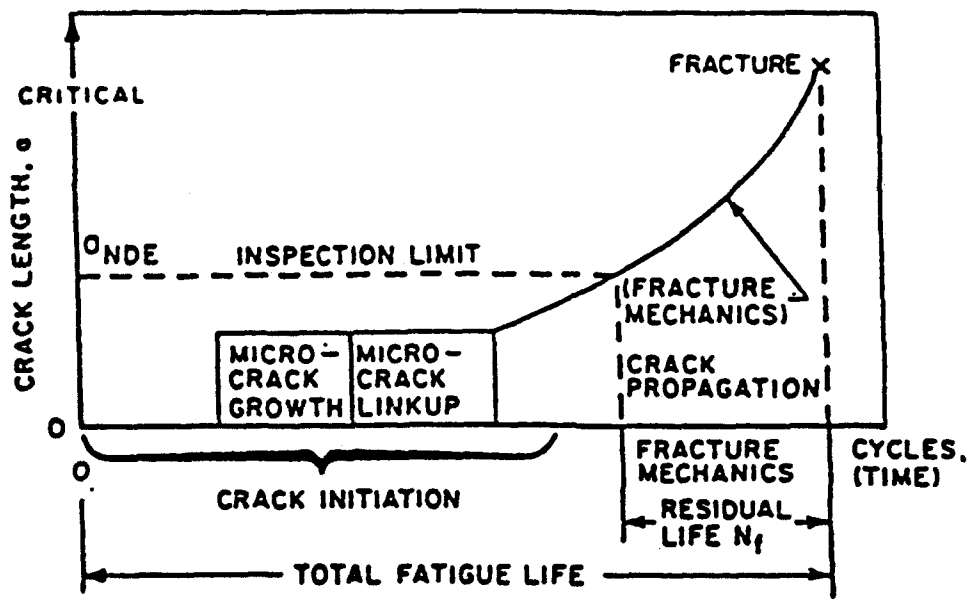

Fig. 3.1 Total Fatigue Life Consists of Crack Initiation, Subcritical Crack Propagation and Final Fracture.

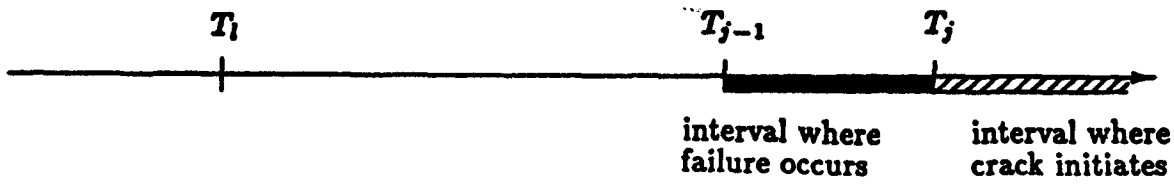

Fig. 3.2a

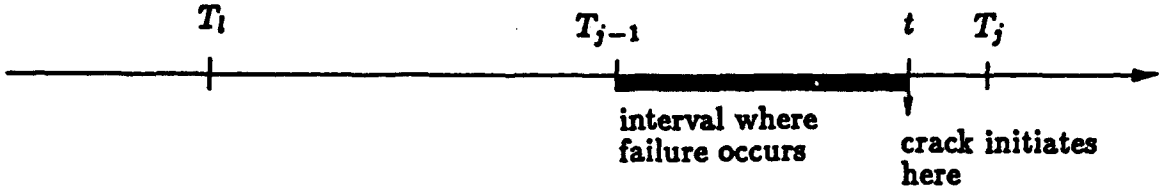

Fig. 3.2b

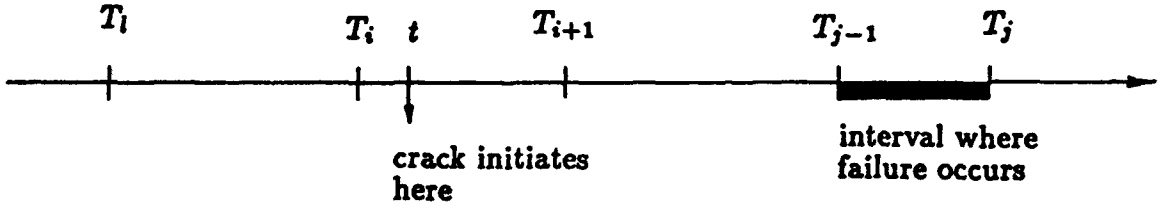

Fig. 3.2c

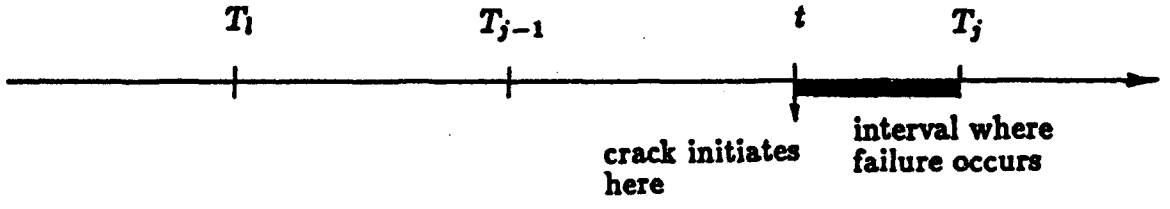

Fig. 3.2d

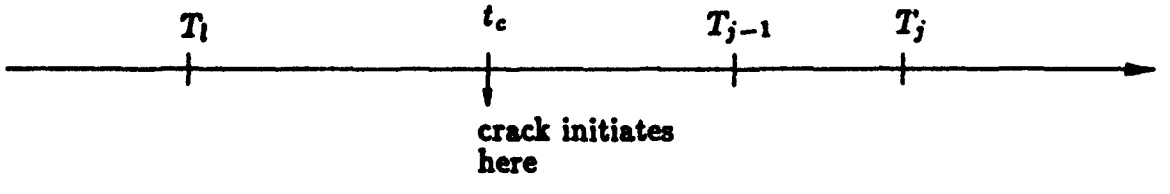

Fig. 3.2e

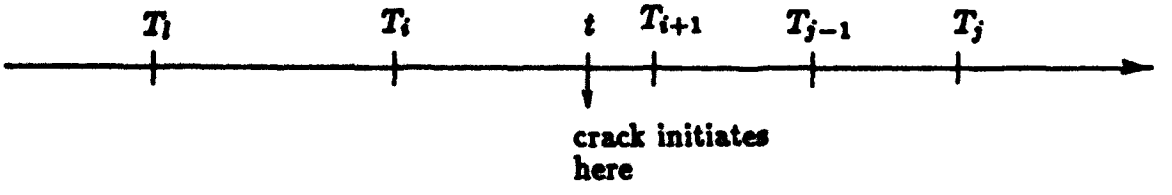

Fig. 3.2f

Fig. 3.2 Chronology of Events.

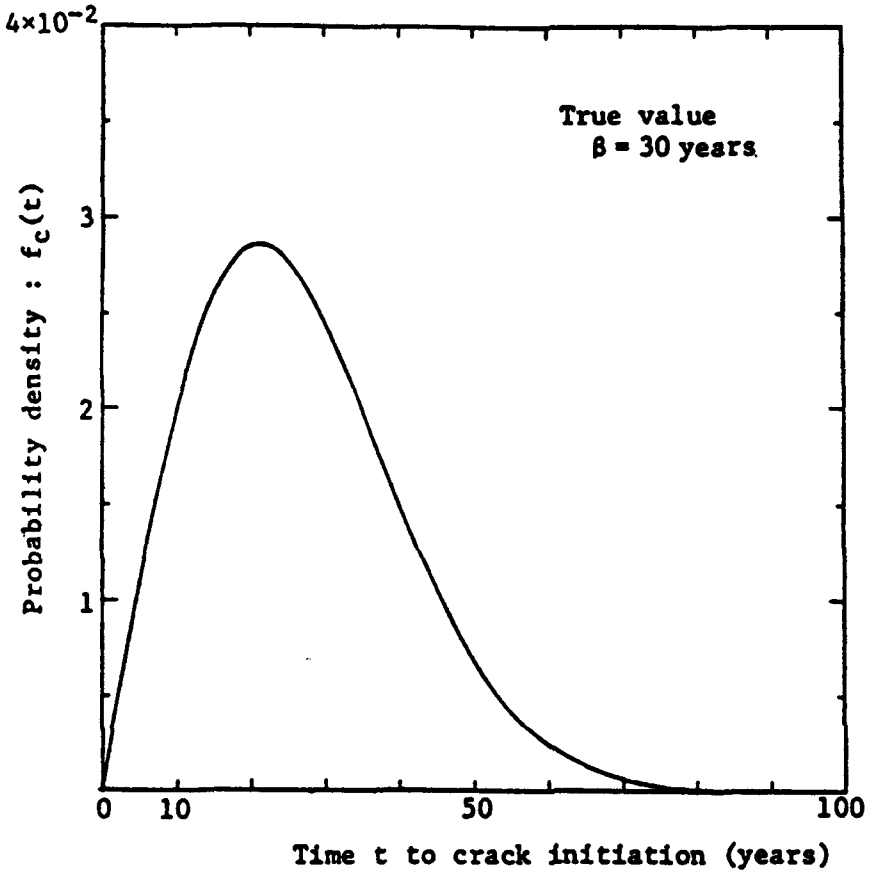

Fig. 3.3 Probability Density Function of Time to Crack Initiation.

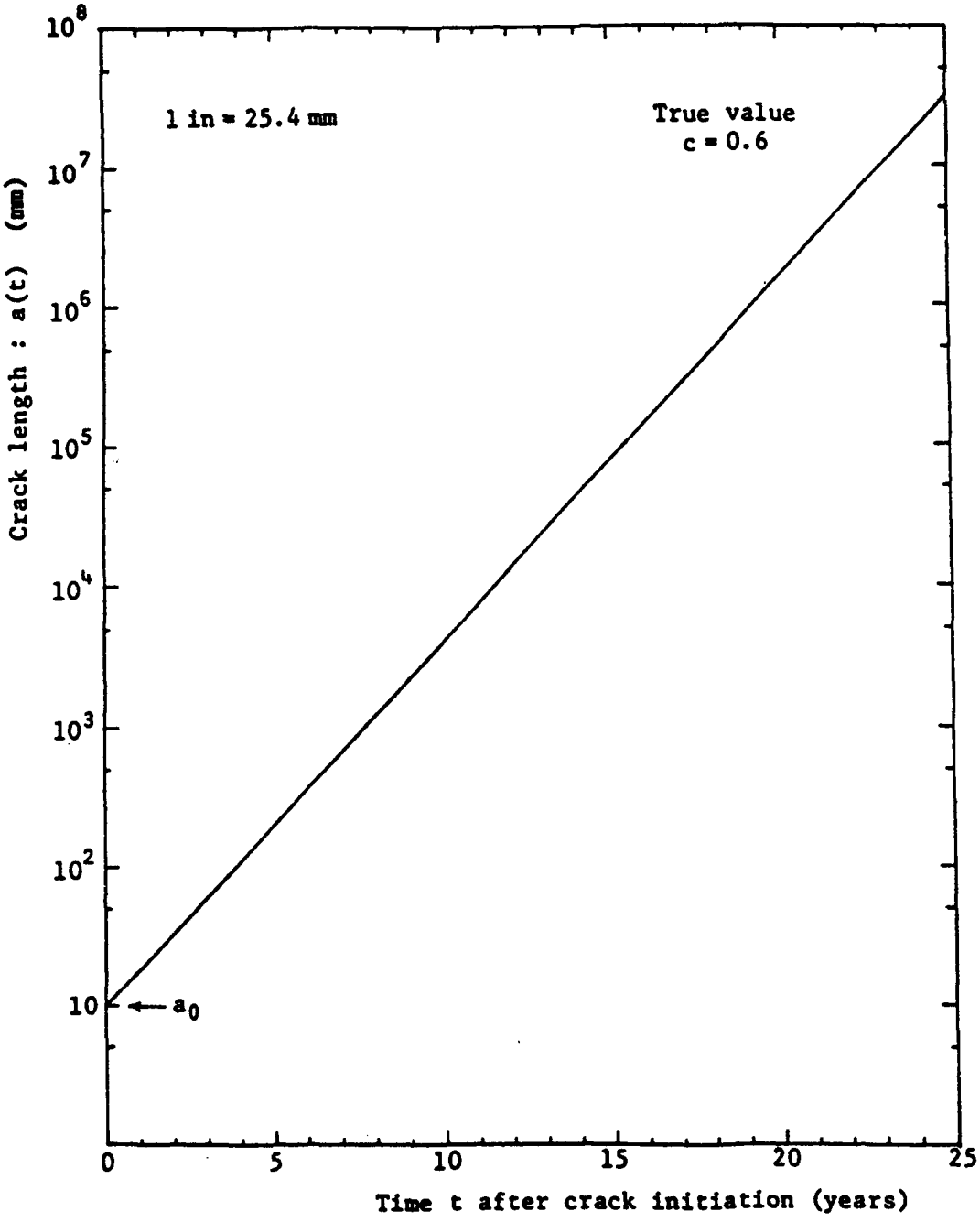

Fig. 3.4 Law of Crack Propagation.

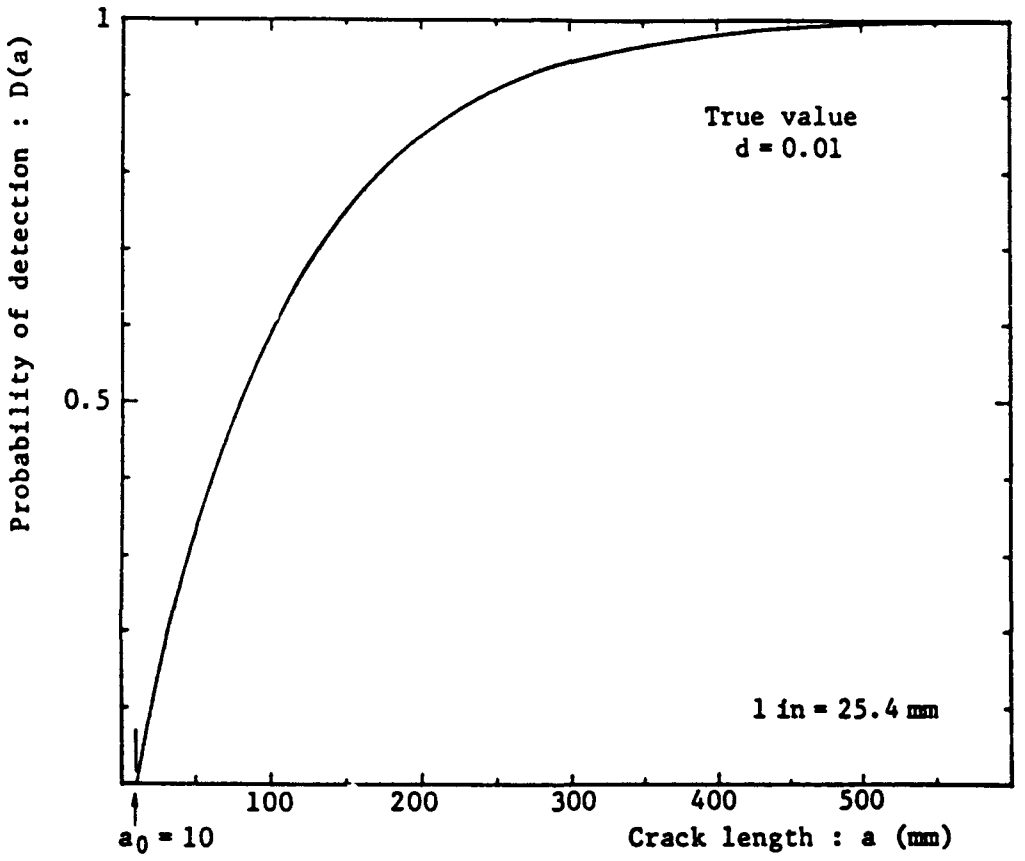

Fig. 3.5 Probability of Crack Detection.

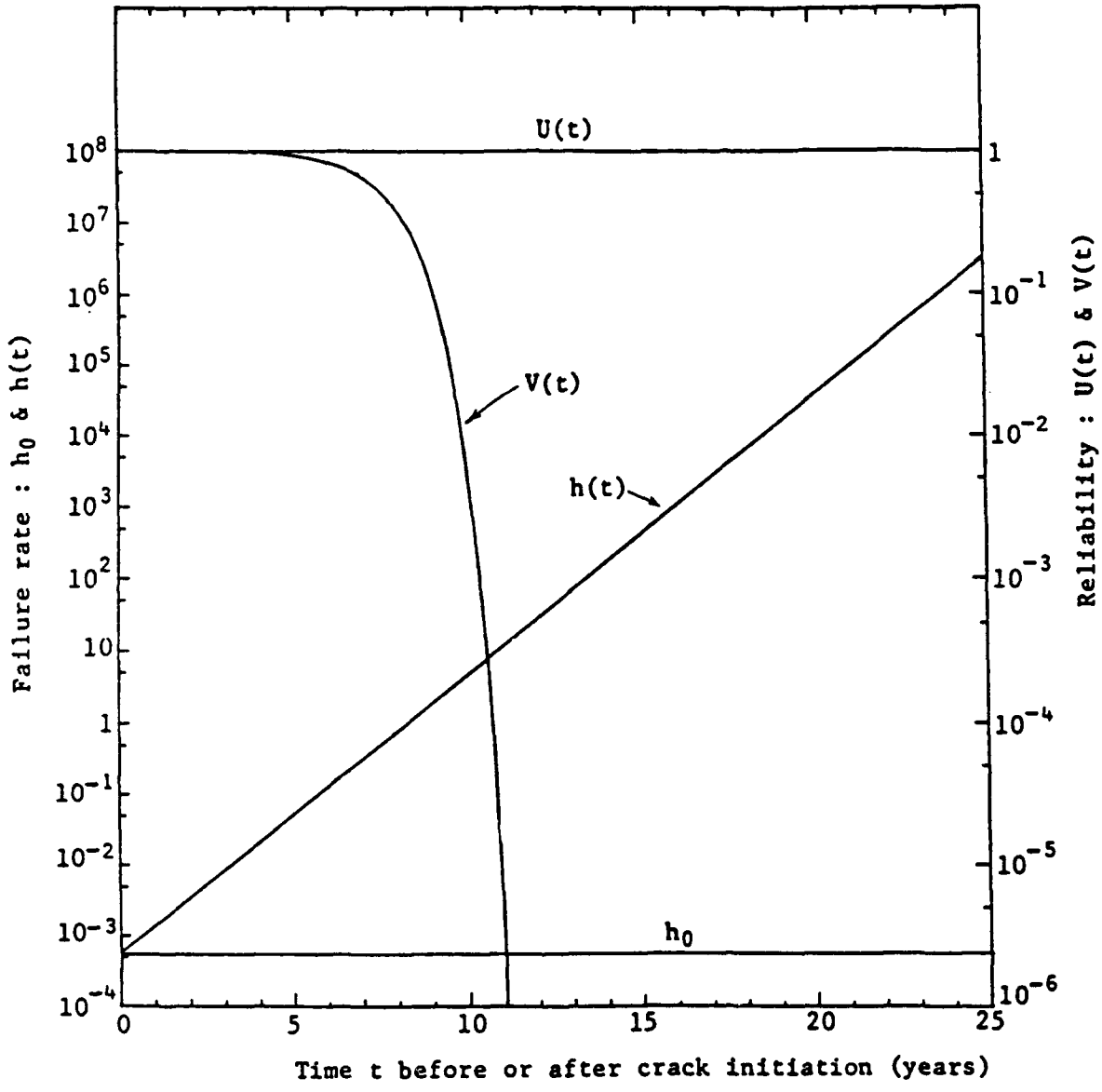

Fig. 3.6 Failure Rate and Reliability Curves Before and After Crack Initiation.

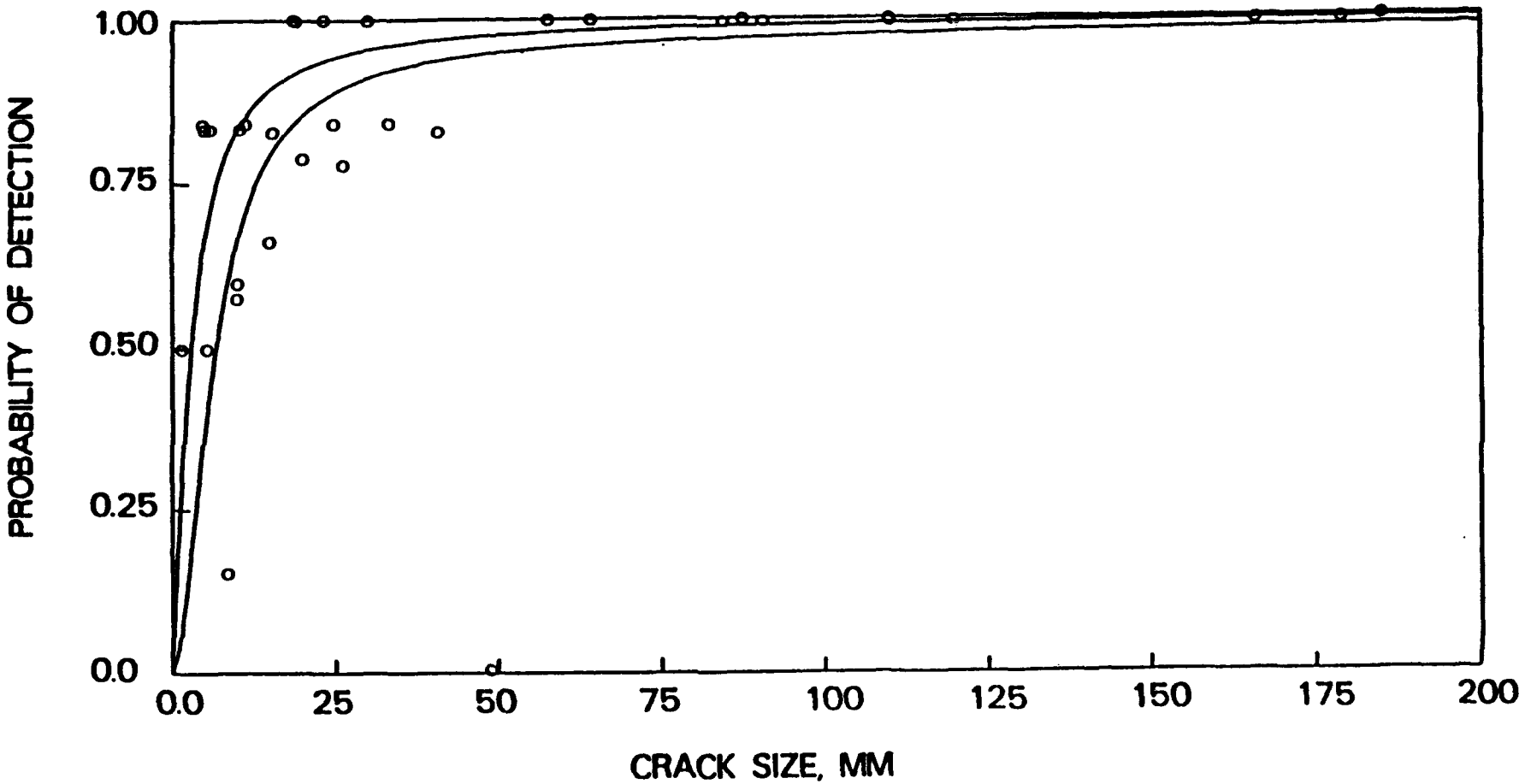

Fig. 3.7 50% (upper curve) and 95% (lower curve) Confidence Level Curves Fitted to Data Obtained from Magnetic Particle Examination Applied Under Water for Detection of Fatigue Cracks and Artificial Defects.

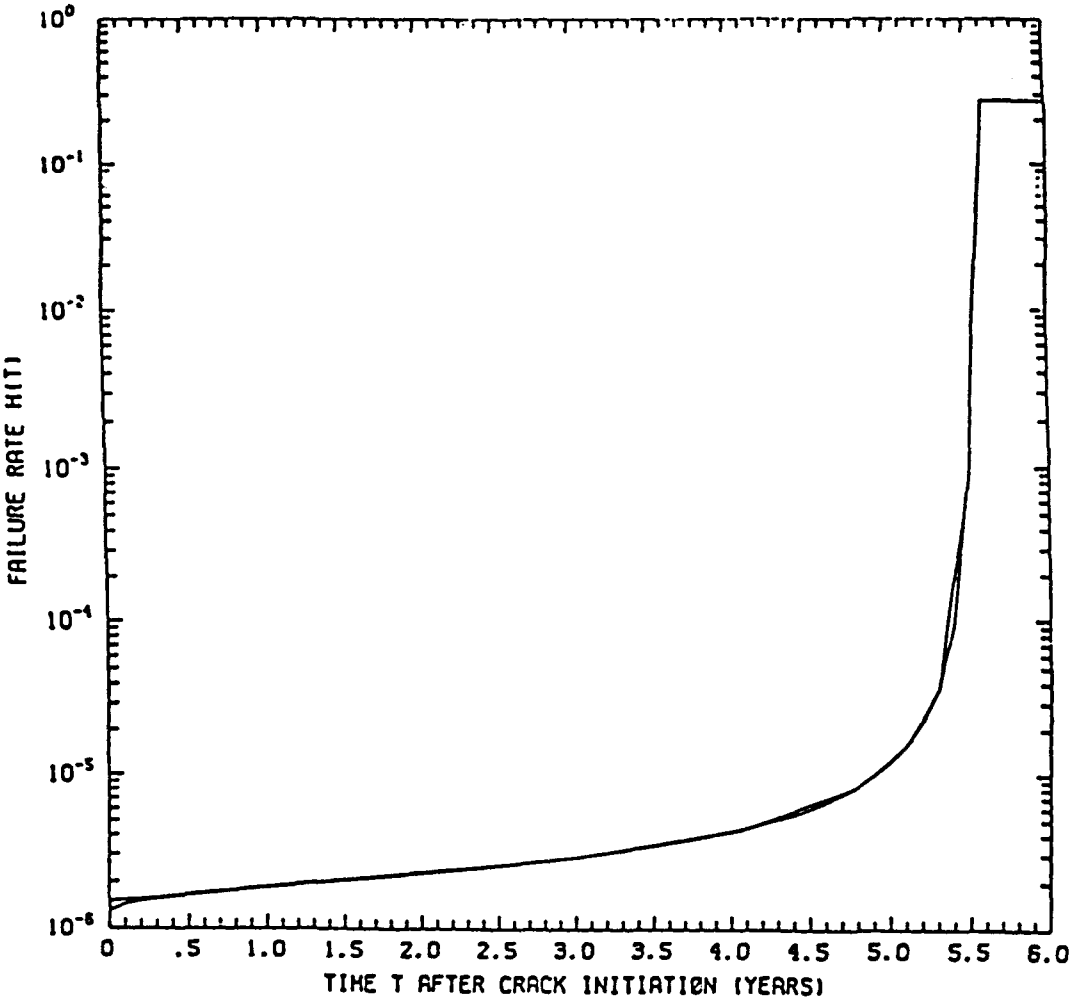

Fig. 3.8 Failure Rate After Crack Initiation According to [3.2].

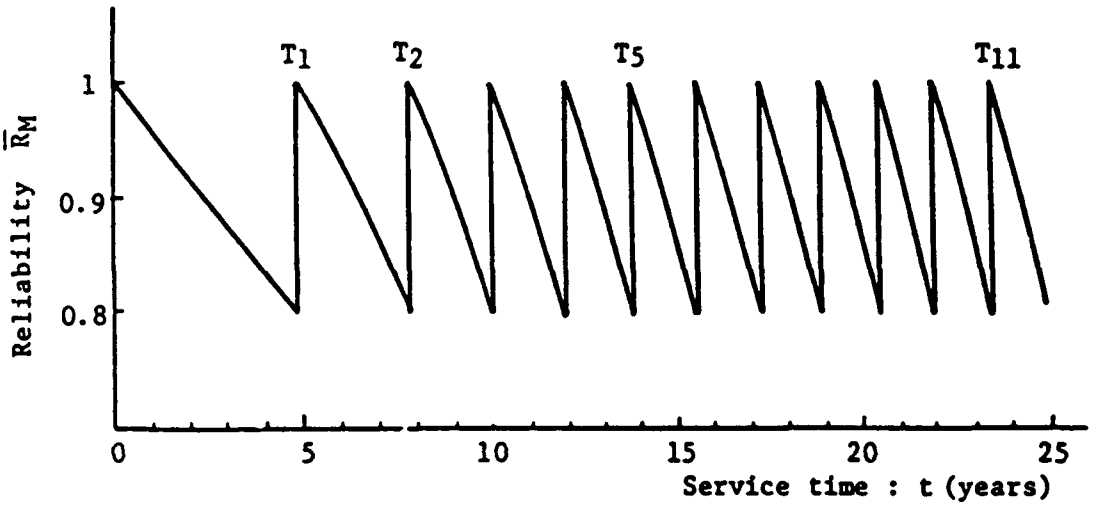

Fig. 3.9 Inspection Schedule and Structural Reliability for the Case Where All Uncertain Parameters Assume Their True Values.

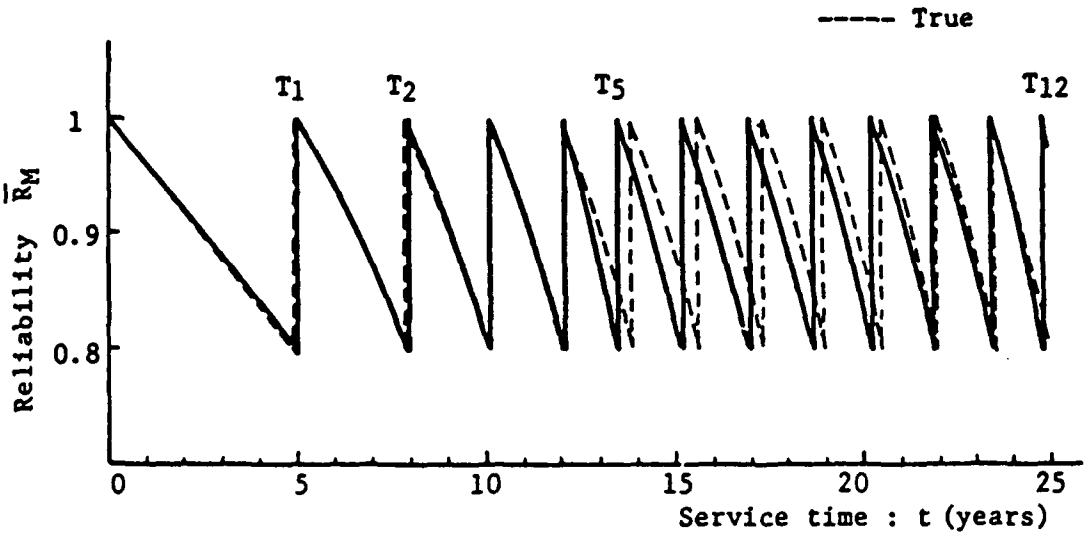

Fig. 3.10 Inspection Schedule and Structural Reliability for Case 1 (Uncertain Parameters: β and d).

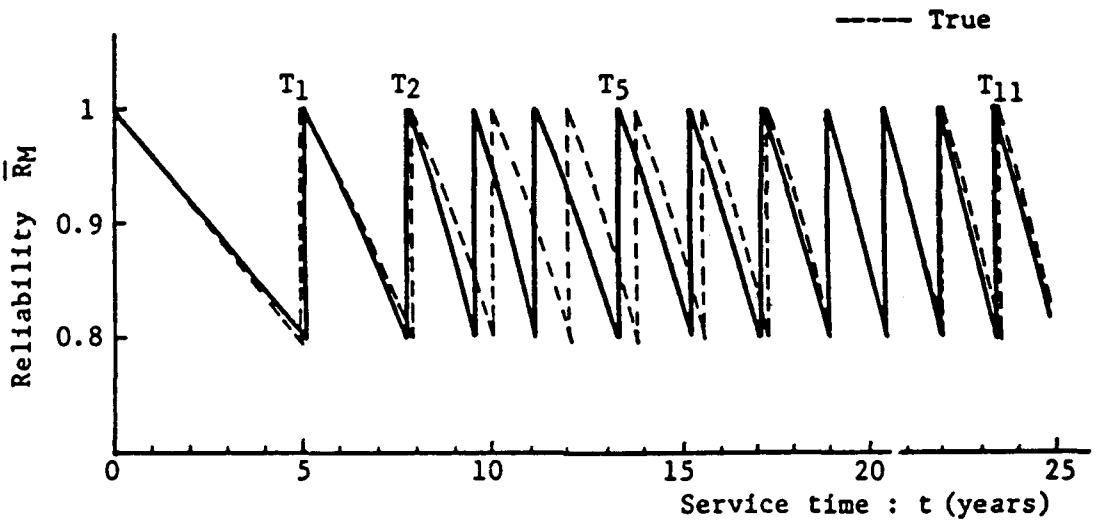

Fig. 3.11 Inspection Schedule and Structural Reliability for Case 2 (Uncertain Parameters: β and c).

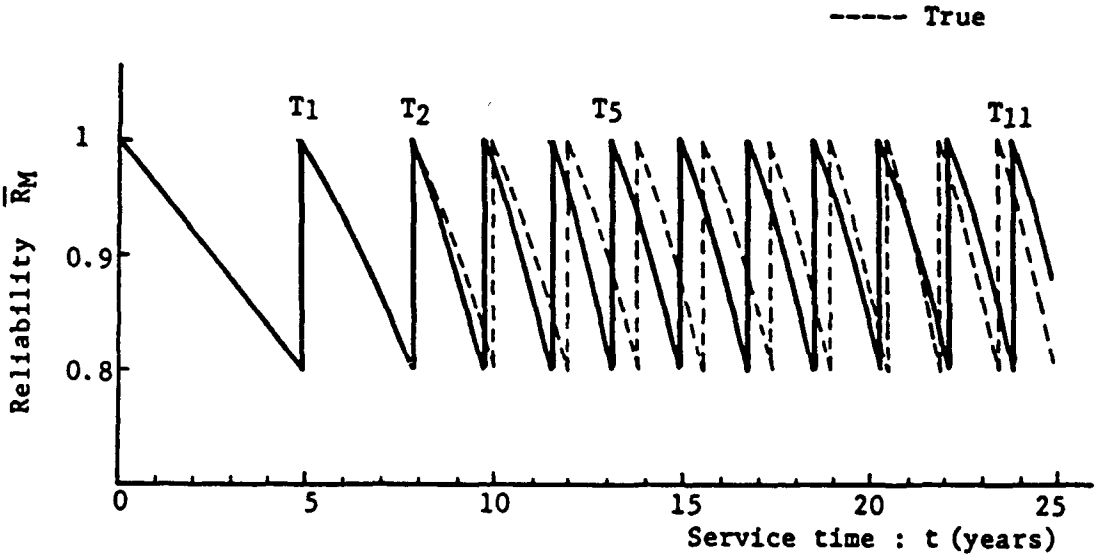

Fig. 3.12 Inspection Schedule and Structural Reliability for Case 3 (Uncertain Parameters: d and c).

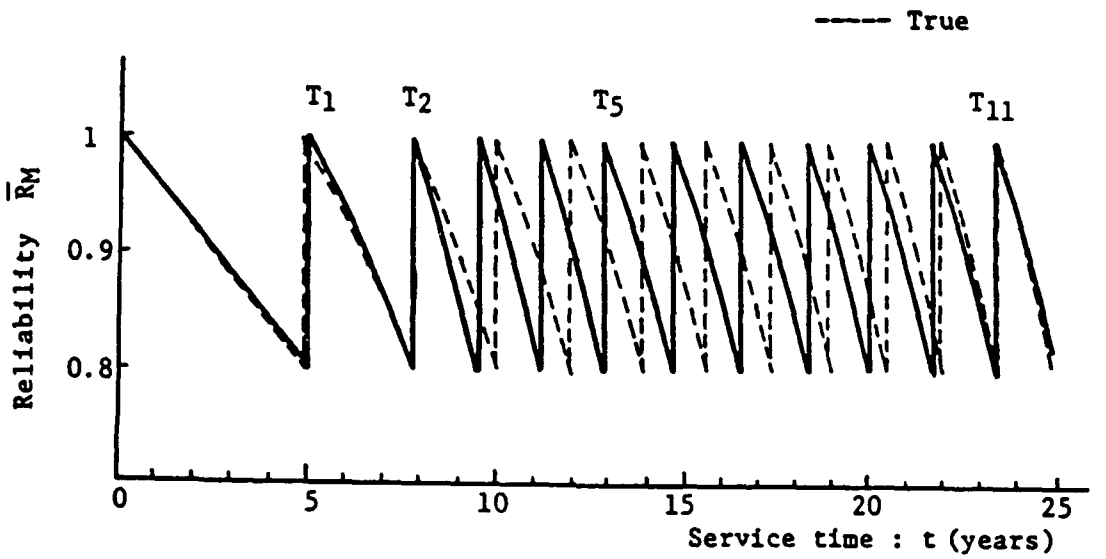

Fig. 3.13 Inspection Schedule and Structural Reliability for Case 4 (Uncertain Parameters: β, d and c).

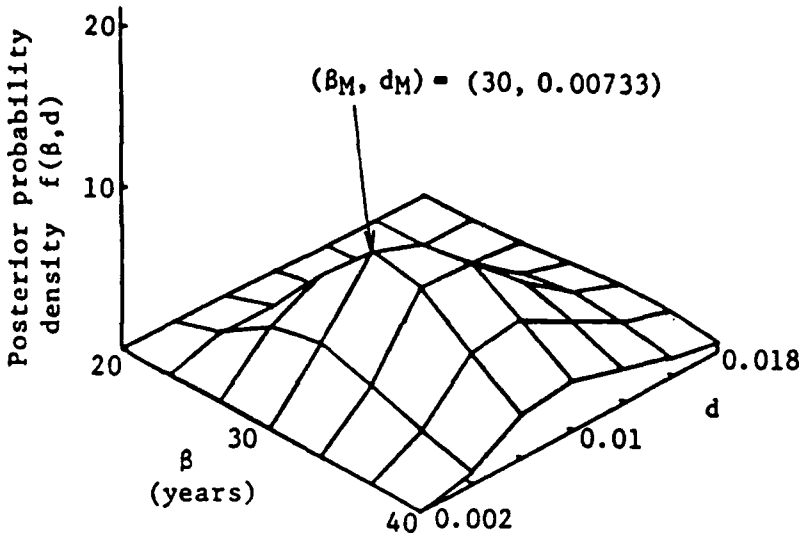

1. The Fifth Inspection

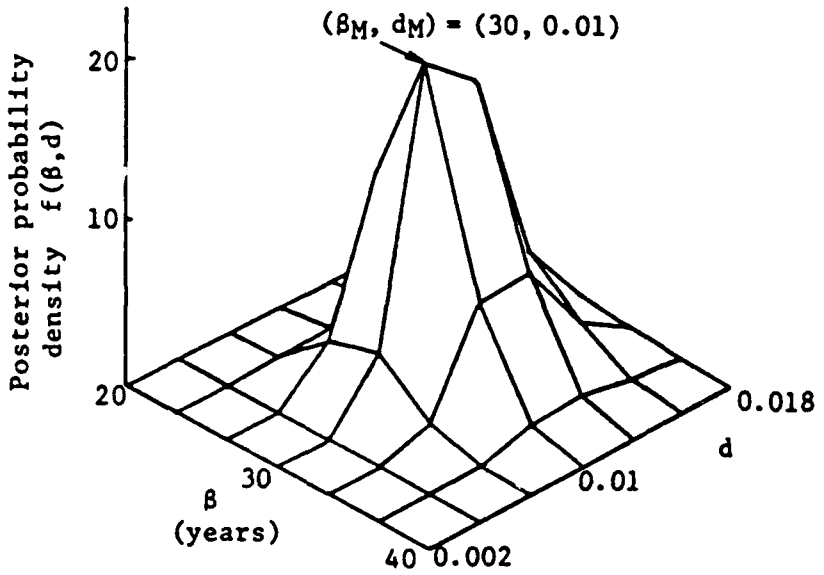

2. The Tenth Inspection

True value (β, d) = (30, 0.01)

Fig. 3.14 Posterior Joint Probability Density Function for Case 1 (Uncertain Parameters: β and d).

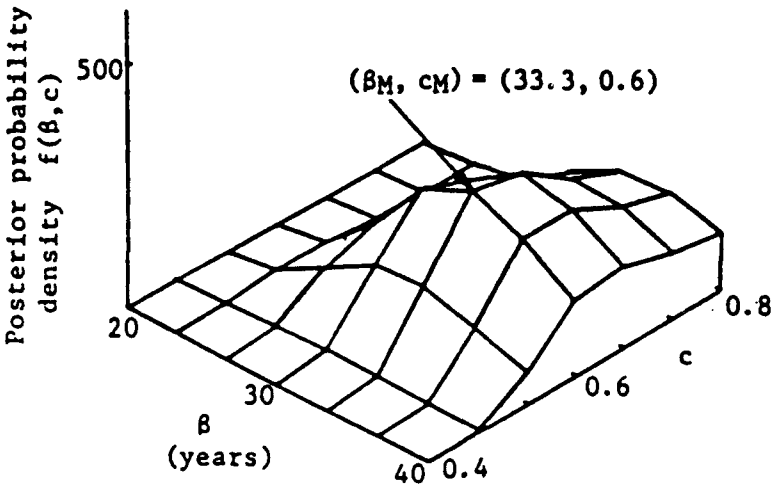

1. The Fifth Inspection

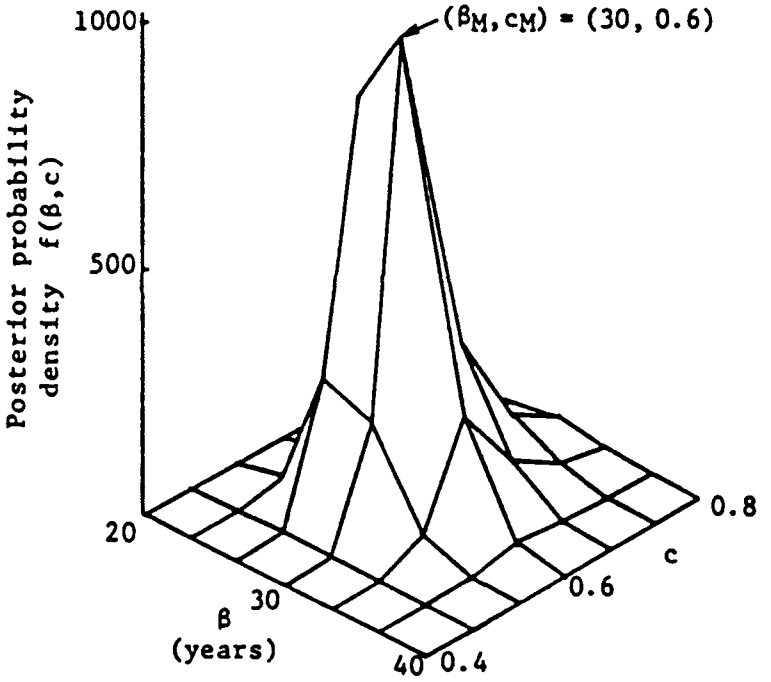

2. The Tenth Inspection

True value (β, c) = (30, 0.6)

Fig. 3.15 Posterior Joint Probability Density Function for Case 2 (Uncertain Parameters: β and c).

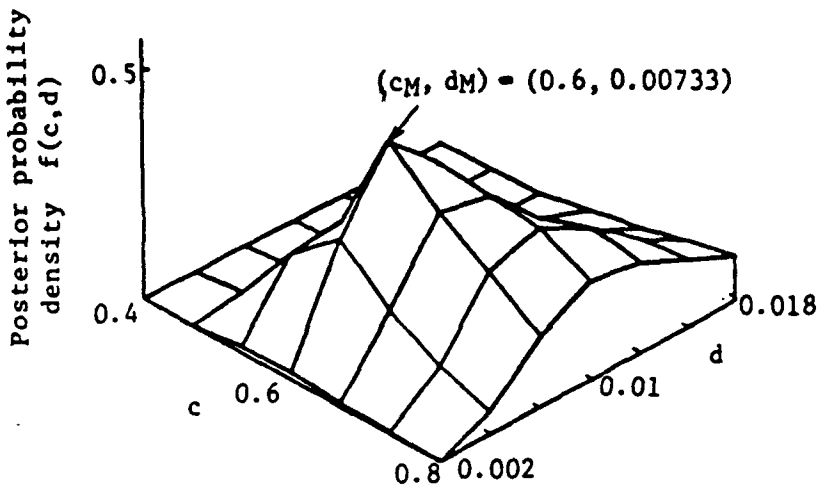

1. The Fifth Inspection

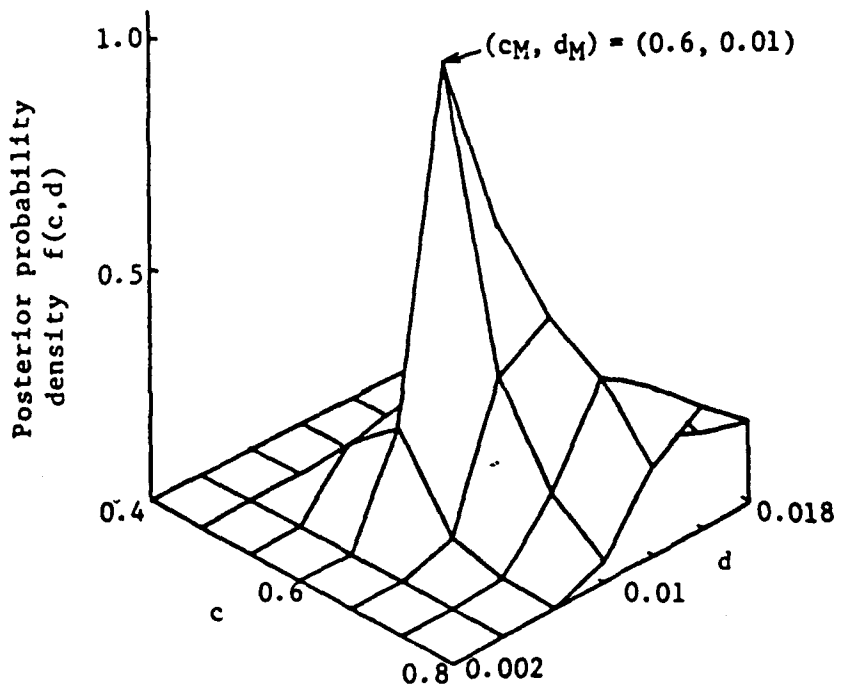

2. The Tenth Inspection

True value (c, d) = (0.6, 0.01)

Fig. 3.16 Posterior Joint Probability Density Function for Case 3 (Uncertain Parameters: *d* and *c*).

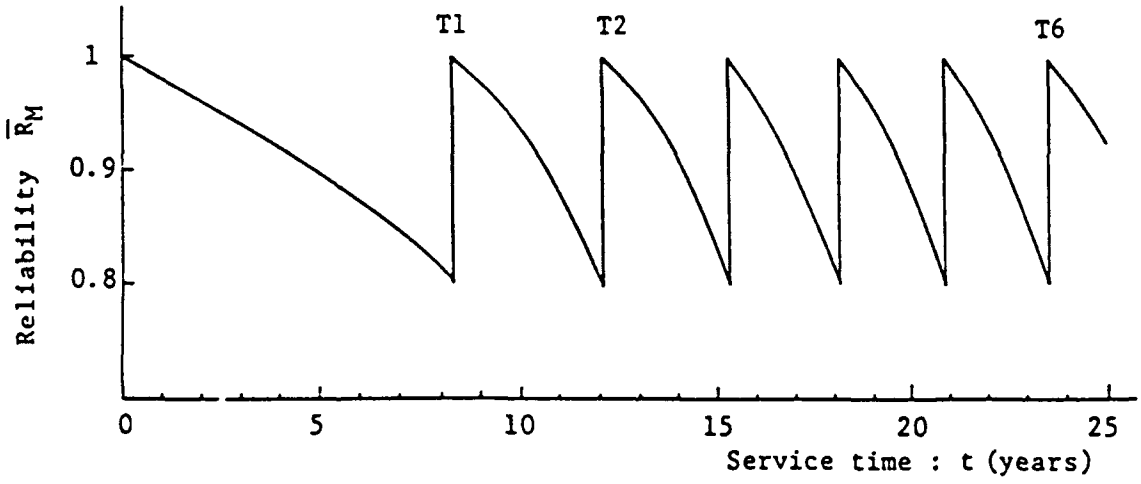

Fig. 3.17a Inspection Schedule and Structural Reliability for True Value (Whole Structure).

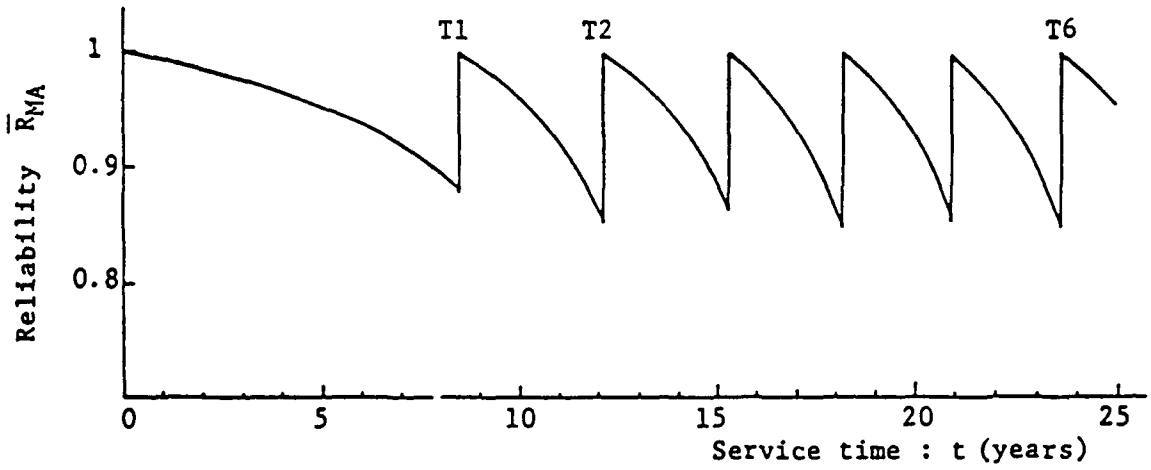

Fig. 3.17b Inspection Schedule and Structural Reliability for True Value (Stress Intensity Level A).

Fig. 3.17c Inspection Schedule and Structural Reliability for True Value (Stress Intensity Level B).

Fig. 3.17d Inspection Schedule and Structural Reliability for True Value (Stress Intensity Level C).

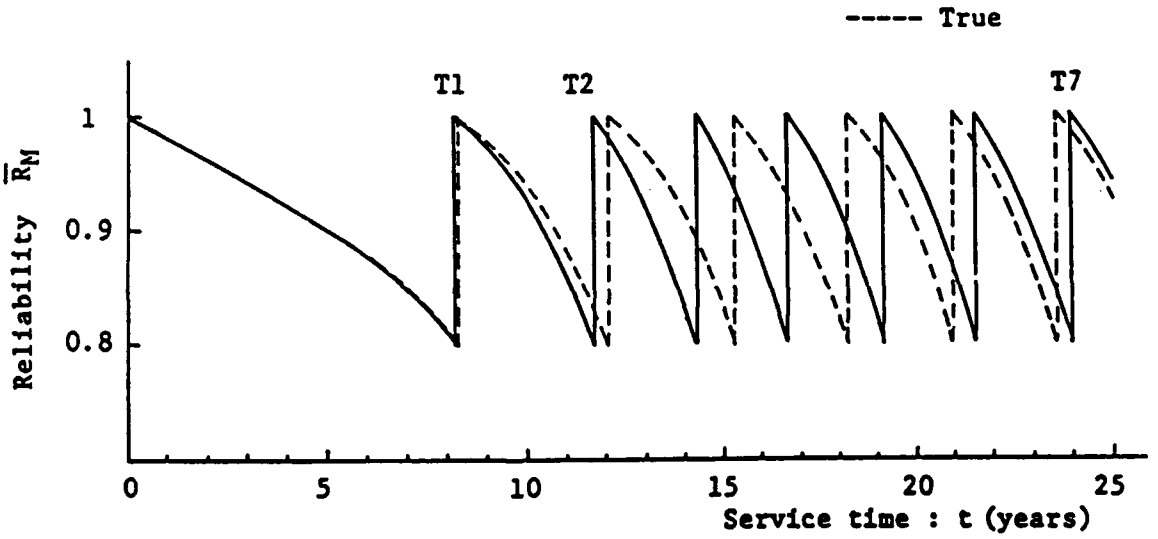

Fig. 3.18a Inspection Schedule and Structural Reliability for Case 2: Uncertain Parameters β and c (Whole Structure).

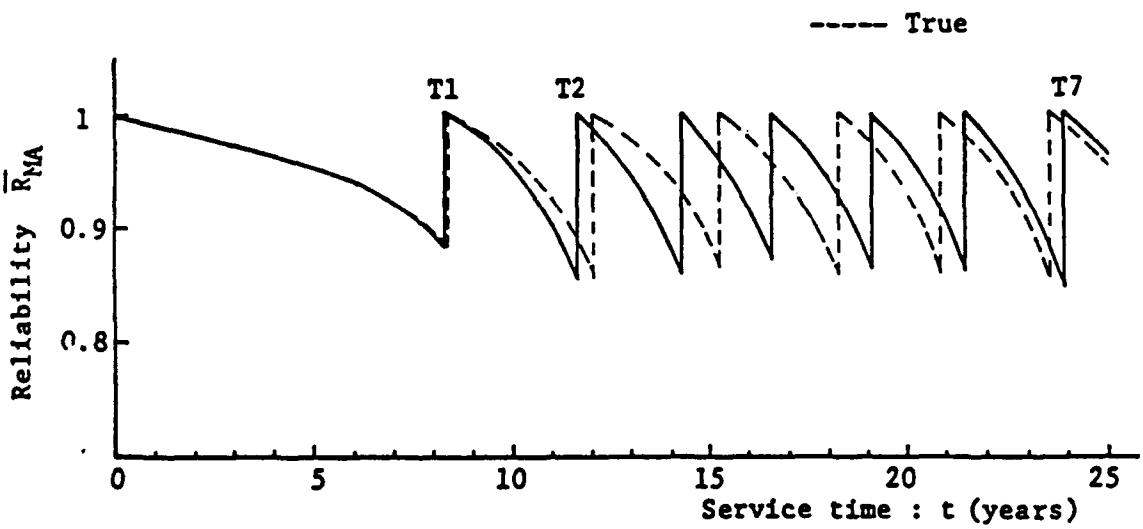

Fig. 3.18b Inspection Schedule and Structural Reliability for Case 2: Uncertain Parameters β and c (Stress Intensity Level A).

Fig. 3.18c Inspection Schedule and Structural Reliability for Case 2: Uncertain Parameters β and c (Stress Intensity Level B).

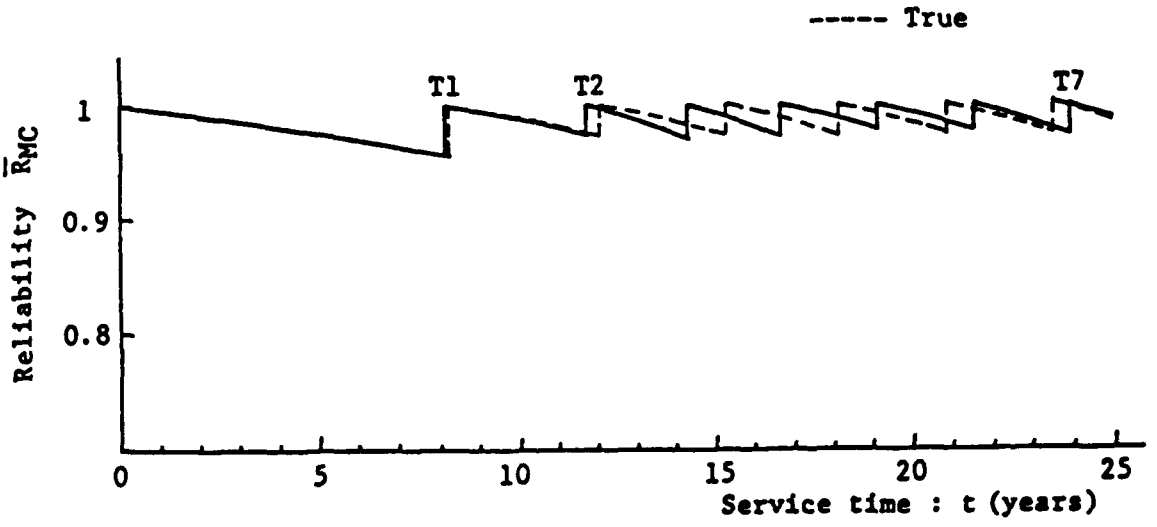

Fig. 3.18d Inspection Schedule and Structural Reliability for Case 2: Uncertain Parameters β and c (Stress Intensity Level C).

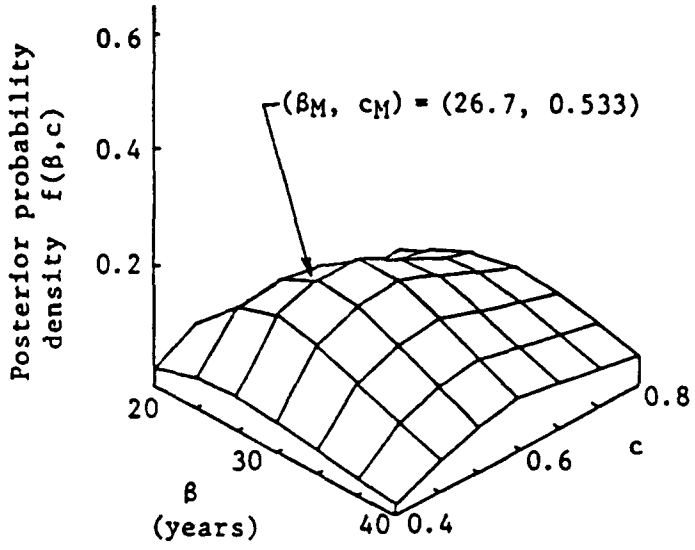

1. The Third Inspection

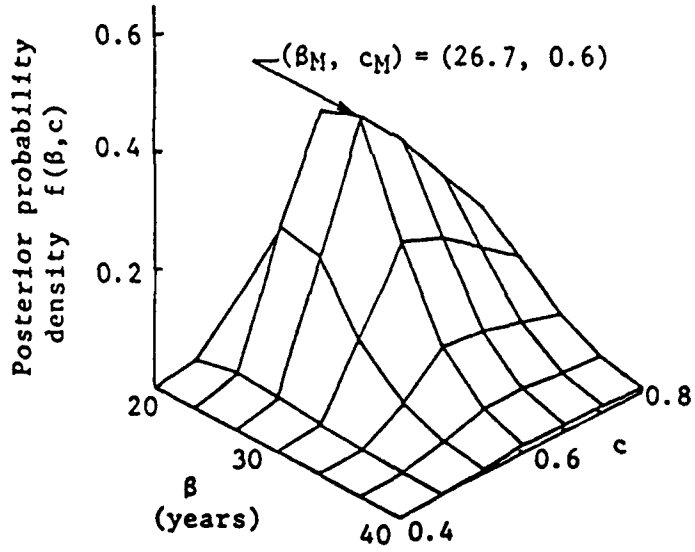

2. The Sixth Inspection

True value (β, c) = (30, 0.6)

Fig. 3.19a Posterior Joint Probability Density Function for Case 2: Uncertain Parameters β and c (Stress Intensity Level A).

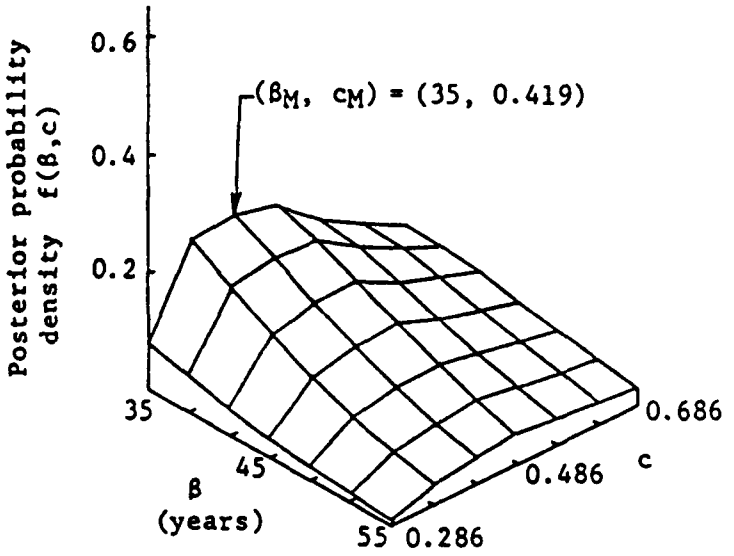

1. The Third Inspection

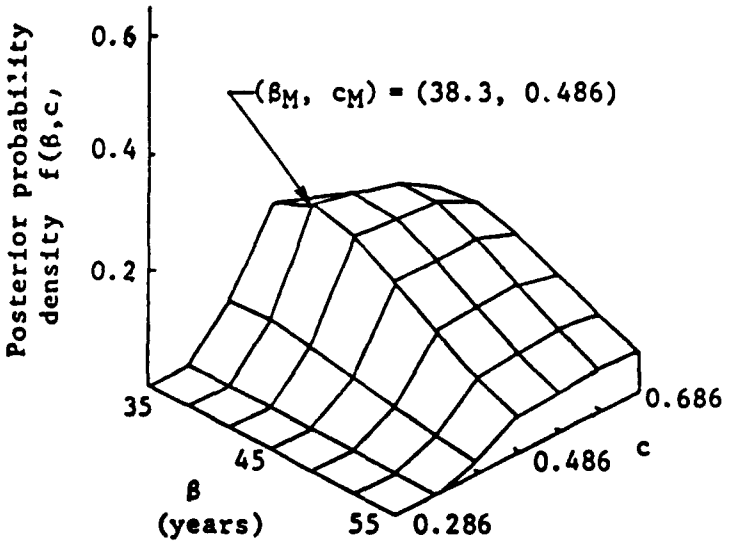

2. The Sixth Inspection

True value (β, c) = (45, 0.486)

Fig. 3.19b Posterior Joint Probability Density Function for Case 2: Uncertain Parameters β and c (Stress Intensity Level B).

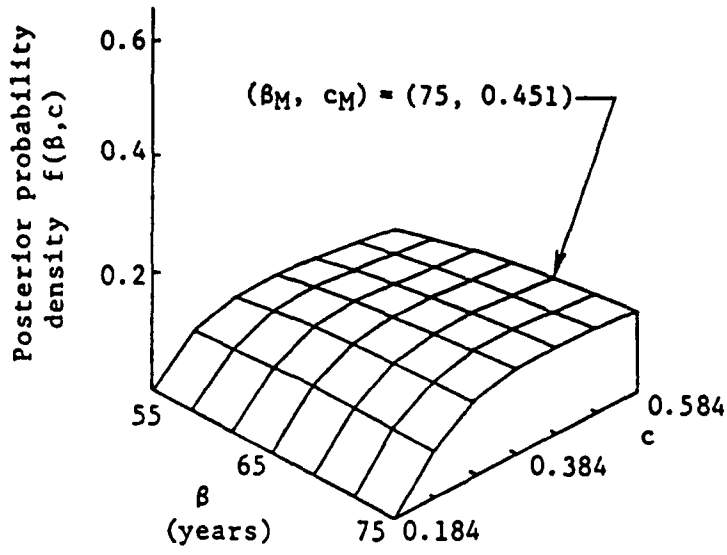

1. The Third Inspection

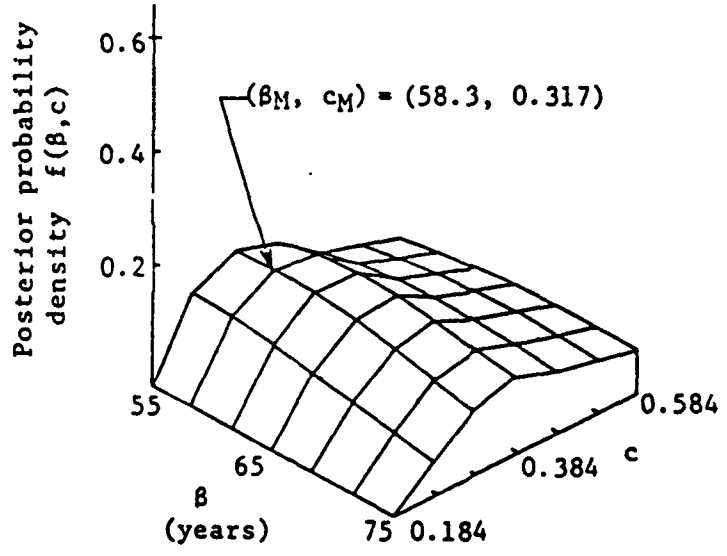

2. The Sixth Inspection

True value (β, c) = (65, 0.384)

Fig. 3.19c Posterior Joint Probability Density Function for Case 2: Uncertain Parameters β and c (Stress Intensity Level C).

★U.S. GOVERNMENT PRINTING OFFICE: 1991 - 519 - 630/21202

COMMITTEE ON MARINE STRUCTURES

Commission on Engineering and Technical Systems

National Academy of Sciences - National Research Council

The COMMITTEE ON MARINE STRUCTURES has technical cognizance over the interagency Ship Structure Committee's research program.

Stanley G. Stiansen (Chairman), Riverhead, NY
Mark Y. Berman, Amoco Production Company, Tulsa, OK
Peter A. Gale, Webb Institute of Naval Architecture, Glen Cove, NY
Rolf D. Glasfeld, General Dynamics Corporation, Groton, CT
William H. Hartt, Florida Atlantic University, Boca Raton, FL
Paul H. Wirsching, University of Arizona, Tucson, AZ
Alexander B. Stavovy, National Research Council, Washington, DC
Michael K. Parmelee, Secretary, Ship Structure Committee, Washington, DC

LOADS WORK GROUP

Paul H. Wirsching (Chairman), University of Arizona, Tucson, AZ
Subrata K. Chakrabarti, Chicago Bridge and Iron Company, Plainfield, IL
Keith D. Hjelmstad, University of Illinois, Urbana, IL
Hsien Yun Jan, Martech Incorporated, Neshanic Station, NJ
Jack Y. K. Lou, Texas A & M University, College Station, TX
Naresh Maniar, M. Rosenblatt & Son, Incorporated, New York, NY
Solomon C. S. Yim, Oregon State University, Corvallis, OR

MATERIALS WORK GROUP

William H. Hartt (Chairman), Florida Atlantic University, Boca Raton, FL
Fereshteh Ebrahimi, University of Florida, Gainesville, FL
Santiago Ibarra, Jr., Amoco Corporation, Naperville, IL
Paul A. Lagace, Massachusetts Institute of Technology, Cambridge, MA
John Landes, University of Tennessee, Knoxville, TN
Mamdouh M. Salama, Conoco Incorporated, Ponca City, OK
James M. Sawhill, Jr., Newport News Shipbuilding, Newport News, VA

SHIP STRUCTURE COMMITTEE PUBLICATIONS

SSC-337 Part 2 - Ship Fracture Mechanisms - A Non-Expert's Guide for Inspecting and Determining the Causes of Significant Ship Fractures by Karl A. Stambaugh and William A. Wood 1987

SSC-338 Fatigue Prediction Analysis Validation from SL-7 Hatch Corner Strain Data by Jen-Wen Chiou and Yung-Kuang Chen 1985

SSC-339 Ice Loads and Ship Response to Ice - A Second Season by C. Daley, J. W. St. John, R. Brown, J. Meyer, and I. Glen 1990

SSC-340 Ice Forces and Ship Response to Ice - Consolidation Report by C. Daley, J. W. St. John, R. Brown, and I. Glen 1990

SSC-341 Global Ice Forces and Ship Response to Ice by P. Minnick, J. W. St. John, B. Cowper, and M. Edgecomb 1990

SSC-342 Global Ice Forces and Ship Response to Ice - Analysis of Ice Ramming Forces by Yung-Kuang Chen, Alfred L. Tunik, and Albert P-Y Chen 1990

SSC-343 Global Ice Forces and Ship Response to Ice - A Second Season by P. Minnick and J. W. St. John 1990

SSC-344 Development of an Onboard Strain Recorder by Eric Greene and William A. Wood 1987

SSC-345 Elastic-Plastic Fracture Mechanics by T. L. Anderson 1990

SSC-346 Fatigue Characterization of Fabricated Ship Details - Phase 2 by K. K. Park and F. V. Lawrence, Jr. 1988

SSC-347 Strategies for Nonlinear Analysis of Marine Structures by Subrata K. Chakrabarti 1988

SSC-348 Corrosion Experience Data Requirements by Karl A. Stambaugh and John C. Knecht 1988

SSC-349 Development of a Generalized Onboard Response Monitoring System (Phase I) by F. W. DeBord, Jr. and B. Hennessy 1987

SSC-350 Ship Vibration Design Guide by Edward F. Noonan 1989

SSC-351 An Introduction to Structural Reliability Theory by Alaa E. Mansour 1990

None Ship Structure Committee Publications - A Special Bibliography 1983